Residential Flashover Prevention with Reduced Water Flow: Phase 2

Nicholas Dow
Daniel Madrzykowski

Fire Safety Research Institute
Underwriters Laboratories Inc
Columbia, MD 21045

This publication is available free of charge from:
https://dx.doi.org/10.54206/102376/NUZJ8120

UNDERWRITERS LABORATORIES™

Residential Flashover Prevention with Reduced Water Flow: Phase 2

Nicholas Dow
Daniel Madrzykowski

Fire Safety Research Institute
Underwriters Laboratories Inc
Columbia, MD 21045

November 9, 2021

This publication is available free of charge from:
https://dx.doi.org/10.54206/102376/NUZJ8120

UNDERWRITERS LABORATORIES™

Underwriters Laboratories Inc.
Terrence R.Brady, President
Christopher J. Cramer, Chief Research Officer

Fire Safety Research Institute
Steve Kerber, Director

In no event shall UL be responsible to anyone for whatever use or non-use is made of the information contained in this Report and in no event shall UL, its employees, or its agents incur any obligation or liability for damages including, but not limited to, consequential damage arising out of or in connection with the use or inability to use the information contained in this Report. Information conveyed by this Report applies only to the specimens actually involved in these tests. UL has not established a factory Follow-Up Service Program to determine the conformance of subsequently produced material, nor has any provision been made to apply any registered mark of UL to such material. The issuance of this Report in no way implies Listing, Classification or Recognition by UL and does not authorize the use of UL Listing, Classification or Recognition Marks or other reference to UL on or in connection with the product or system.

Contents

List of Figures

List of Tables

List of Abbreviations

DHS	U.S. Department Of Homeland Security
ESTC	Emergency Services Training Center
FSRI	Fire Safety Research Institute
gpm	gallons per minute
HRR	heat release rate
IDLH	immediately dangerous to life or health
kg	kilogram
kW	kilowatt
lpm	liters per minute
min	minute
mm	millimeter
NFPA	National Fire Protection Association
s	seconds
UL	Underwriters Laboratories
USFA	U.S. Fire Administration

Acknowledgments

The authors wish to thank the FSRI and the Delaware County ESTC teams. The FSRI team assisted with the conduct of these experiments. The authors appreciate all of the work that Keith Stakes, Matt DiDomizio, Joe Willi, Ethan Crivaro, and Brad Morrissey of UL FSRI put into this project. The time and effort that Steve Kerber and Kerry Bell of UL LLC put into the review of this study is greatly valued.

The Delaware County (PA) ESTC provided the location and logistical support for these experiments. The Delaware County team was under the direction of Kerby Kerber.

The support of the U.S. Fire Administration in advancing their mission to improve fire safety is greatly appreciated.

Abstract

The purpose of this study was to investigate the feasibility of a residential flashover prevention system with reduced water flow requirements relative to a residential sprinkler system designed to meet NFPA 13D requirements. The flashover prevention system would be designed for retrofit applications where water supplies are limited. In addition to examining the water spray's impact on fire growth, this study utilized thermal tenability criteria as defined in UL 199, Standard for Automatic Sprinklers for Fire-Protection Service. The strategy investigated was to use full cone spray nozzles that would discharge water low in the fire room and directly onto burning surfaces of the contents in the room. Where as current sprinkler design discharges water in a manner that cools the hot gas layer, wets the walls and wets the surface of the contents in the fire room.

A series of eight full-scale, compartment fire experiments with residential furnishings were conducted with low flow nozzles. While the 23 lpm (6 gpm) of water was the same between experiments, the discharge density or water flux around the area of ignition varied between 0.3 mm/min (0.008 gpm/ft^2) and 1.8 mm/min (0.044 gpm/ft^2). Three of the experiments prevented flashover. Five of the experiments resulted in the regrowth of the fire while the water was flowing. Regrowth of the fire led to untenable conditions, per UL 199 criteria, in the fire room. At approximately the same time as the untenability criteria were reached, the second sprinkler in the hallway activated. In a completed system, the activation of the second sprinkler would reduce the water flow to the fire room, which would potentially lead to flashover. The variations in the burning behavior of the sofa resulted in shielded fires which led to the loss of effectiveness of the reduced flow solid cone water sprays. As a result of these variations, a correlation between discharge density at the area of ignition and fire suppression performance could not be determined given the limited number of experiments.

An additional experiment using an NFPA 13D sprinkler system, flowing 30 lpm (8 gpm), demonstrated more effective suppression than any of the experiments with a nozzle. The success of the sprinkler compared with the unreliable suppression performance of the lower flow nozzles supports the minimum discharge density requirements of 2 mm/min (0.05 gpm/ft^2) from NFPA 13D. The low flow nozzle system tested in this study reliably delayed fire growth, but would not reliably prevent flashover.

1 Introduction

Automatic residential fire sprinkler systems, designed and installed in accordance with NFPA 13D, Standard for the Installation of Sprinkler Systems in One- and Two-Family Dwellings and Manufactured Homes [1] have been shown to save lives and property. The purpose of the standard is "...to provide a sprinkler system that aids in the detection and control of residential fires and thus provides improved protection against injury and life loss." In addition, a sprinkler system designed and installed in accordance with NFPA 13D is intended to prevent flashover in the sprinklered room of fire origin to improve the chance for occupants to escape or be evacuated [1].

According to the NFPA, the civilian death rate in homes with fire sprinklers was 81% lower than in homes without an automatic suppression system. A similar comparison was made on both civilian and firefighter injury rates, in the homes with fire sprinklers the injury rates were 27% and 67% lower respectively [2].

The U.S. Census Bureau conducted an American Housing Survey in 2011 which included questions regarding the Health and Safety Characteristics of a home. The survey contained a section on Safety Equipment. In this section the question was asked; is there a sprinkler system inside the home? NFPA tabulated the data from the American Housing Survey to show, based on occupied units, that approximately 1% of manufactured homes, 2% of single-family detached homes, and 8% of single-family attached homes had residential sprinkler systems [2].

While the life safety benefits are clear based on fire incident data, the American Housing Survey data shows that the majority of single family homes in the United States are not sprinklered. Their are many reasons for this but a key reason is that more than half of the housing stock existed prior to the adoption of the first edition of NFPA 13D in 1975 [3]. Retrofitting a sprinkler system in an existing home can be more expensive than installing a system in a new home, with costs depending on a number of factors specific to each individual home [4]. This raises the question, is there another approach to water based, residential fire suppression systems that could be used to enable retrofit in the existing housing stock? When considering a fire suppression system for residential retrofit, challenges such as the available water supply may need to be overcome.

The NFPA 13D design criteria are based on a significant body of research [5] that guided the design requirements, including the design discharge of residential sprinklers, the minimum discharge density of 2.0 mm/min (0.05 gpm/ft^2) [1], and the standardized tests included in UL 199 [6]. Fire suppression experiments demonstrated the importance of residential sprinklers delivering water high enough on the wall to cool the hot gas layer, prevent the fire from getting above the sprinkler discharge, and apply water to furnishings, such as beds or sofas, which may be located around the perimeter of the room [5].

This study is focused on the use of nozzles that would direct water into the lower half of the room as a means to cool the fuel load. This has the potential to reduce the required water flow, which could enable retrofit systems with an existing domestic supply. The effectiveness of this approach will

be examined in terms of: preventing flashover, occupant tenability based on UL 199 criteria [6], and if system activation can be limited to a single nozzle.

1.1 Summary of Phase 1

This study is the second phase of a project to investigate flashover prevention methods for residential homes with limited water supplies. The focus is on the use of low flow, 23 lpm (6 gpm), spray nozzles in place of residential sprinklers. Here the focus is on spray nozzles that offer a water discharge in a conical pattern with nearly uniform distribution on a flat surface. The intended strategy is to directly impact the burning fuel for suppression, which could be a more efficient use of a limited water supply. This is counter to the current residential sprinkler design approach of broadly distributing the water with larger droplets primarily near the edges of the spray radius.

Previous FSRI research on this project compared low flow nozzles to sprinklers in terms of water distribution patterns, gas cooling ability, and fire suppression performance for small compartment fires. One of the fire scenarios tested a discharge density or water flux at the ignition location of 1.6 mm/min (0.040 gpm/ft^2) (23 lpm (6 gpm) flow rate and 1.6 m (5.2 ft) nozzle-to-ignition distance), which extinguished the fire. Another scenario reduced the flow rate by half which provided a water flux of 1.1 mm/min (0.027 gpm/ft^2) at the ignition location. This proved insufficient to suppress the fire and conditions in the structure became untenable. A third scenario tested a water flux at the ignition location of 0.3 mm/min (0.008 gpm/ft^2) by moving the ignition location 1.0 m (3.3 ft) further away. The fire was not extinguished, but conditions in the structure remained tenable. These results showed that a low flow nozzle could suppress a fire, but the relationship between the water flux at the ignition location and suppression performance was ambiguous.

1.2 Objective

The objective of this study was to investigate flashover prevention capabilities of low flow nozzles as a proof of concept for residential retrofit fire suppression systems with limited water supplies. This study expands on the findings from Phase 1 of this project by examining a variety of fire scenarios including different sprinkler spacing, ignition locations and low flow nozzles. The experiments were compared based on the water flux at the ignition location for each scenario. In particular, what is the minimum water flux that will reliably suppress a fire started in an upholstered sofa? The answer to this question determines under what circumstances a low flow nozzle could be viable.

1.3 Technical Approach

Two series of full-scale experiments were designed. The first set of experiments measured the water spray distributions of the nozzles. The water spray measurements were made without the presence of a fire. The second set of experiments were fire experiments which examined the ability of a low flow nozzle to suppress a fire started on an upholstered sofa.

The most relevant measure of success is whether or not the water spray system prevented flashover. This measure can not be accurately applied, however, because only one water spray was active in every experiment. A residential sprinkler system can include multiple sprinklers, and a second sprinkler will activate if the first was insufficient to prevent the spread of hot gases through the structure. In this event, the flow rate through the first sprinkler will decrease as the water supply is divided among two sprinklers. The flow rate through the water spray in these experiments was constant, despite the possibility that additional water sprays would have activated. It can not be determined whether flashover would have been prevented if a second water spray activated. Therefore, other measures of success were considered.

A sprinkler was installed remote from the fire, but was not connected to the water system. This sprinkler was used to indicate whether a second water spray would have activated during the fire. Its activation did not impact the flow rate to the first water spray.

UL 199 defines limits for the conditions in a residence to be maintained by a sprinkler system such that the residence is tenable for occupants. The criteria of primary relevance to this study are listed under 55.5.1.1, and are as follows:

(a) The maximum temperature 76 mm (3 in.) from the ceiling at [the room center and/or the nearest sprinkler] shall not exceed 316 °C (600 °F).

(b) The maximum temperature 1.6 m (5.25 ft) above the floor shall not exceed 93 °C (200 °F).

(c) The temperature at the location described in (b) shall not exceed 54 °C (130 °F) for more than any continuous 2-minute period.

These criteria were used as a pass/fail metric to categorize the outcomes of the experiments. For experiments that did not maintain tenable conditions, the times until these criteria were exceeded were used to further evaluate success.

Gas concentrations of O_2, CO, and CO_2 were measured as an additional component of tenability. UL 199 does not state limits on gas concentrations for tenability. However, concentrations of CO above 0.012% and CO_2 above 4% are considered immediately dangerous to life or health (IDLH) for a 30 minute exposure [7].

2 Experimental Setup

The goal of this study was to evaluate the performance of low flow nozzles as a flashover prevention method for residential homes with limited water supplies. This study expands on previous UL FSRI research by testing additional fire scenarios and using a structure that better represents a residential home. The variable adjusted between experiments was the water flux at the ignition location. This variation was achieved by changes in room size, ignition location, and nozzle type.

Prior to the fire tests, a series of water distribution tests were conducted to evaluate a set of nozzles. The results were used to determine which nozzles to include in the fire tests. A series of eight experiments were conducted with low flow nozzles where the water flux at the ignition location varied between 0.3 mm/min (0.008 gpm/ft^2) and 1.8 mm/min (0.044 gpm/ft^2). Changes in room size and ignition location allowed for different nozzle-ignition distances, which ranged between 2.2 m (7.1 ft) and 2.6 m (8.5 ft). Two different nozzles were used, each set to flow water at 23 lpm (6 gpm). To provide a baseline for comparison, one additional experiment was conducted using a residential sprinkler. The sprinkler-ignition distance was 2.6 m (8.5 ft) and the flow rate was 30 lpm (8 gpm) – the minimum flow rate listed by the manufacturer.

The configuration of the structure was consistent between experiments – the fire room connected by an open door to a hallway which lead to an open exterior door. The fuel load included an upholstered sofa, a simulated chair side, and carpeting throughout the fire room.

2.1 Experimental Structure

All of the experiments were conducted at full scale in a purpose-built residential structure located on the grounds of the Delaware County Emergency Services Training Center (ESTC) in Sharon Hill, Pennsylvania. The test structure was an approximately 98 m^2 (1,060 ft^2) single story, four bedroom ranch home with 2.4 m (8 ft) ceilings. Figure 2.1 shows photographs of the exterior sides of structure with side A as the front. A floor plan of the test structure with major dimensions is presented in Figure 2.2. The dimensions of the windows and doors are summarized in Table 2.1.

The walls were constructed from nominally 3.81 cm by 8.89 cm (2 in. x 4 in.) wood studs spaced 41 cm (16 in.) on center and filled with R-13 fiberglass insulation. The interior walls were lined with 1.3 cm (1/2 in.) thick gypsum board finished with latex paint. The exterior walls were lined with 0.6 cm (1/4 in.) thick fiber cement board siding, a layer of olefin home wrap, and 1.1 cm (7/16 in.) oriented strand board sheathing.

(a) Side A

(b) Side B

(c) Side C

(d) Side D

Figure 2.1: Exterior photographs of the exterior sides of the experimental structure.

Table 2.1: Window and door schedules for the test structure.

Type	Height [cm (in.)]	Width [cm (in.)]	Sill Height [cm (in.)]
Window	122 (48)	91 (36)	61 (24)
Exterior Door	203 (80)	90 (36)	–
Interior Door	203 (80)	76 (30)	–

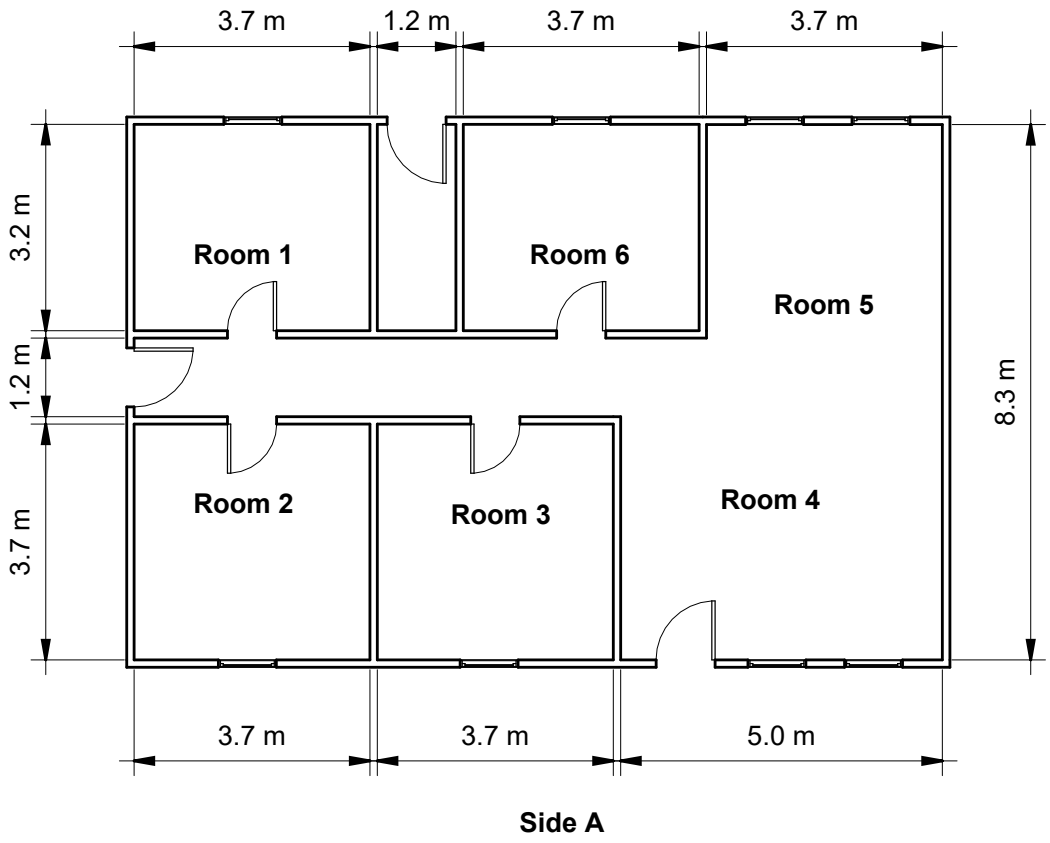

Figure 2.2: Plan view of the test structure including major dimensions.

A pump and tank system, designed to meet NFPA 13D requirements, was used to supply the water spray system in the structure. The system was placed against the Side D exterior wall and routed into the structure via 2.54 cm (1 in.) CVPC piping. Ports for the nozzles/sprinklers were installed in each room (six total). The water spray locations were centered in the 3.7 m x 3.7 m (12 ft x 12 ft) rooms (Rooms 2 and 3). In the other rooms the water sprays were installed off-center to achieve particular distances from the corners of the rooms. In Rooms 1 and 6, the water spray locations were 1.5 m (5 ft) from adjoining walls of one of the corners opposite the door. Likewise, water spray locations were 2.1 m (7 ft) from adjoining walls of corners in Rooms 3 and 4. Figure 2.3 shows the floor plan of the structure with the water spray locations.

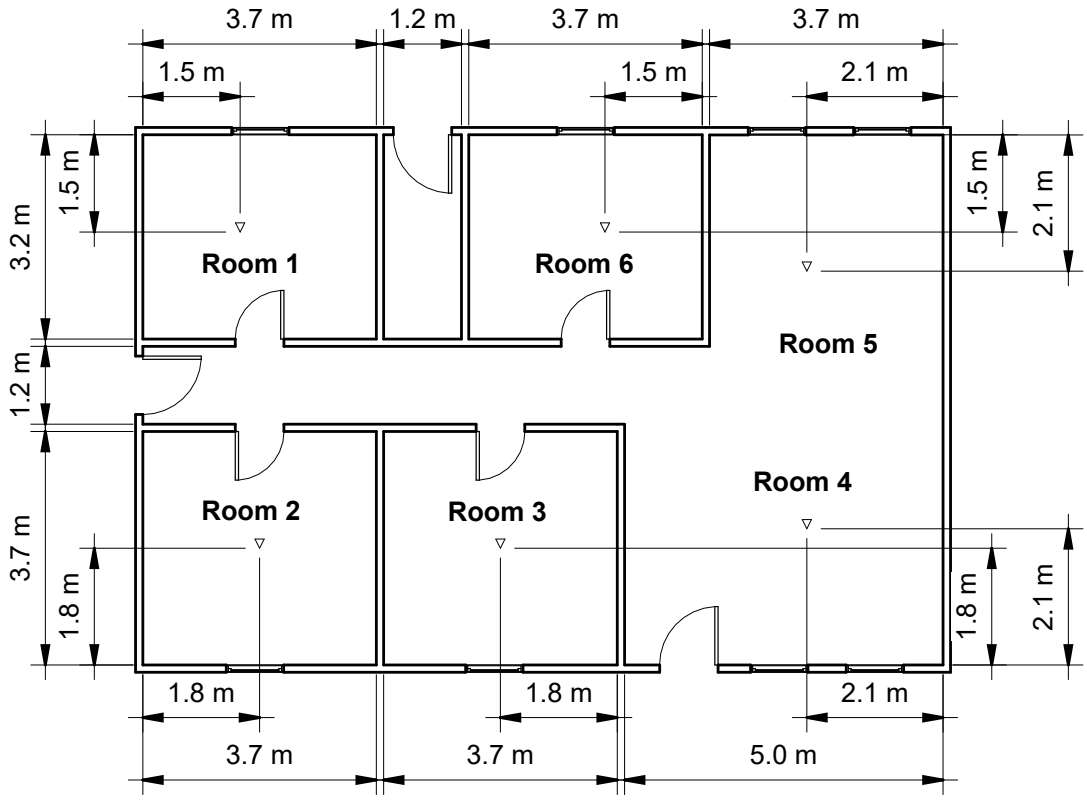

Figure 2.3: Floor plan of the test structure including water spray locations.

Fires were only conducted in Rooms 1, 2, and 3. To ensure consistent flow paths and control volumes between experiments the hallway was modified according to each fire room. The control volumes included the fire room and the length of hallway spanning the width of the fire room. One end of the hallway was closed and the other was open to the exterior. Walls were installed in the hallway to achieve these configurations. Floor plans showing the configurations for each fire room are presented in Figure 2.4.

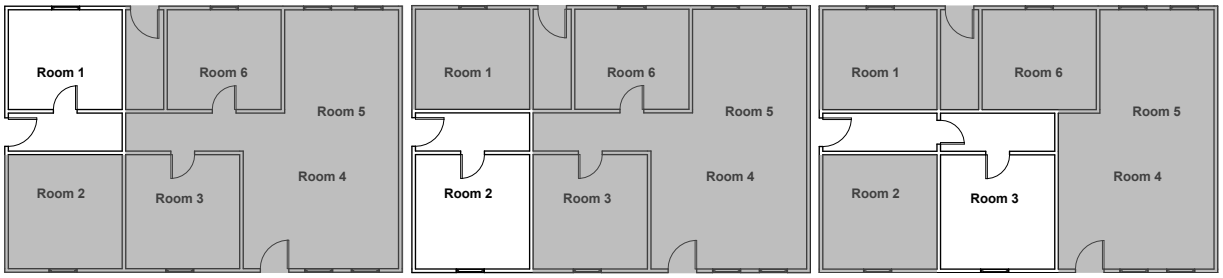

(a) Room 1 (b) Room 2 (c) Room 3

Figure 2.4: Floor plans showing each fire room configuration used in this series. Grey shaded regions indicate areas within the structure that were not considered part of the experimental volume.

2.2 Instrumentation

The structure was instrumented for gas temperature, gas concentration (carbon monoxide, carbon dioxide, and oxygen), heat flux, water flow rate, and sprinkler activation time.

Gas temperatures were measured with 1.27 mm (0.05 in.) bare-bead, chromel-alumel (type K) thermocouples and 1.59 mm (0.0625 in.) inconel-sheathed thermocouples. Sheathed thermocouples allow the instrumentation to be placed in areas where suppression may occur to minimize the affect the water has on the measurement. Small-diameter thermocouples were used during these experiments to limit the impact of radiative heating and cooling. The total expanded uncertainty associated with the temperature measurements from these experiments is estimated to be $\pm$ 15% as reported by researchers at NIST [8, 9].

Total heat flux measurements were made with water-cooled Schmidt-Boelter gauges. The heat flux gauges were oriented vertically and horizontally in the fire room. Results from an international study on total heat flux gauge calibration and response demonstrated that the uncertainty of a Schmidt-Boelter gauge is typically $\pm$ 8% [10].

Gas concentration sampling ports consisted of 9.5 mm (0.375 in.) stainless steel tubing within the structure. Once outside the structure, the sample was drawn through a condensing trap to remove moisture. At the condensate trap exit, the sample was filtered through 5 micron and 2 micron paper filters. Then the sample line transitioned from stainless steel to polyethylene tubing for flexibility. Upstream of the analyzer the sample passed through a fine, 0.01 micron filter. Samples were pulled from the structure through the use of vacuum/pressure diaphragm pump rated at 0.75 CFM.

Gas samples were analyzed through the use of oxygen (paramagnetic alternating pressure) and combination carbon monoxide/carbon dioxide (non-dispersive infrared) analyzers. The gas sampling instruments used throughout the series of tests discussed in this report have demonstrated a relative expanded uncertainty of $\pm$ 1% when compared to span gas volume fractions [11]. Given the non-uniformities and movement of the fire gas environment and the limited set of sampling points in these experiments, an estimated uncertainty of $\pm$ 12% is applied to the results [12].

Water flow rate was measured with a 1.9 cm (0.75 in.) diameter turbine flow meter. The wetted components of the meter are composed of PVC. Flow rate is measured indirectly via the rotational speed of a paddle-wheel that is induced by fluid flow. A built-in display provides the flow rate proportional to the rotational speed of the paddle-wheel. The manufacturer reports a $\pm$ 3.0% calibration uncertainty for the accuracy of the measurement [13]. The flow rate was set manually using a needle valve upstream of the flow meter. An operator observed the flow rate throughout the experiments and maintained it within $\pm$ 1.5 lpm (0.4 gpm).

The spray nozzles did not include a thermally activated bulb or link, therefore a "tell-tale sprinkler" was installed to indicate the activation time. A tell-tale sprinkler was also installed remote from the fire to determine whether a second nozzle would have activated. The bulbs had an activation temperature of 68.3 °C (155 °F). They were connected to pressurized air lines with a pressure switches to detect when the bulb of the tell-tale sprinkler broke.

A load cell was used to weigh the fuels prior to the fire experiments and weigh the water collected in the water distribution tests. The load cell had a range of 0 kg (0 lb) to 200 kg (441 lb) with a resolution of 0.1 kg (0.2 lb) and a calibration uncertainty within 1% [14]. The total expanded uncertainty for the weights measured by the load cell that are presented in this report is estimated to be less than $\pm$ 3%.

All numerical data was recorded with a purpose-built data acquisition systems with specifically programmed software. Temperatures were recorded using specific hardware with built-in cold-junction compensation and raw voltage values were translated to quantities of interest through post-processing software specifically programmed for use with the systems. Data was sampled at 1 Hz.

2.2.1 Measurement Locations

The structure was instrumented with three primary measurement locations per experiment. Position 1 was in the fire room, near the entrance to the room. Position 2 was in the hallway between the fire room door and a doorway leading to the exterior. Position 3 was in the hallway between the fire room door and the closed end of the hallway. Figure 2.5 shows the locations of the measurement locations for an exemplar fire room.

Table 2.2 summarizes the instrumentation at each location. Each measurement location included a thermocouple array consisting of eight thermocouples. The top thermocouple was 2.5 cm (1 in.) below the ceiling and the remaining seven thermocouples were spaced in 30.5 cm (1 ft) intervals below the ceiling such that the bottom thermocouple was 2.1 m (7 ft) below the ceiling. Inconel sheathed thermocouples were used in the thermocouple array at Position 1 to minimize the affect of water on the measurement. Positions 2 and 3 were out of range of the water spray, and therefore consisted of bare-bead thermocouples.

Gas sampling ports were installed 0.9 m (3 ft) and 1.5 m (5 ft) above the floor at Positions 1 and 3. Heat flux was measured at Position 1, 0.9 m (3 ft) above the floor. Two heat flux gauges were

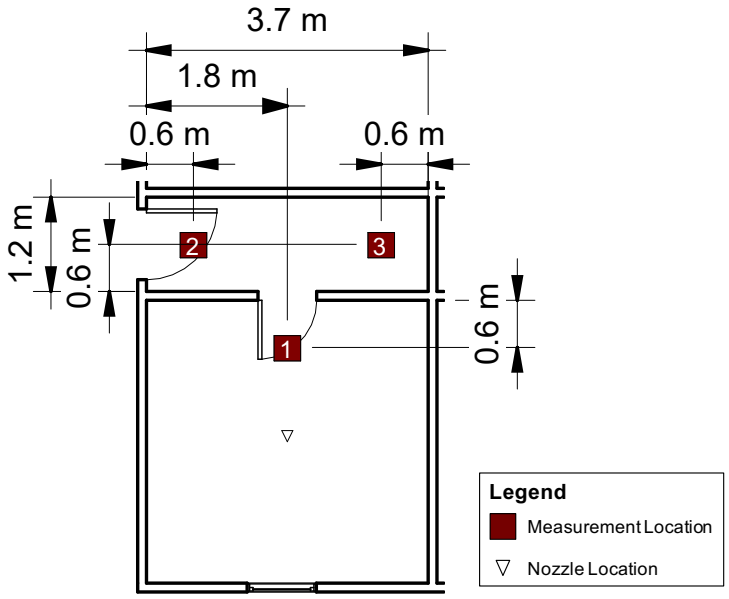

Figure 2.5: Instrumentation locations in an exemplar fire room.

included, one aimed at the ignition location and the other at the ceiling.

A tell-tale sprinkler was installed 10 cm (4 in.) away from the nozzle, and opposite from the ignition corner so that it would not interfere with the water spray pattern from the nozzle. The purpose of the tell-tale sprinkler was to indicate activation time, which prompted manual activation of water flow to the nozzle. A bare-bead thermocouple was installed in the same location to measure gas temperature. A second tell-tale sprinkler was installed at Position 2 (hallway sprinkler) to determine whether a second nozzle would have activated.

Standard video and thermal imaging cameras were installed inside and around the structure to record the experiments. Views from the fire room, hallway, exterior door, and fire room window were included.

Table 2.2: Summary of the instrumentation and their locations used every experiment.

Position	Instrumentation	Elevations
Nozzle	Tell-tale sprinkler	ceiling mounted
	Bare-bead thermocouple	2.5 cm (1 in.) below ceiling
1	Inconel sheathed thermocouple array	0.3 m (1 ft) – 2.4 m (7.9 ft), 0.3 m (1 ft) intervals
	Gas sampling ports	0.9 m (3 ft) and 1.5 m (5 ft)
	Heat flux aimed at ign. location	0.9 m (3 ft)
	Heat flux aimed at the ceiling	0.9 m (3 ft)
2	Bare-bead thermocouple array	0.3 m (1 ft) – 2.4 m (7.9 ft), 0.3 m (1 ft) intervals
	Tell-tale sprinkler	ceiling mounted
3	Bare-bead thermocouple array	0.3 m (1 ft) – 2.4 m (7.9 ft), 0.3 m (1 ft) intervals
	Gas sampling ports	0.9 m (3 ft) and 1.5 m (5 ft)

2.3 Fuel Load

A consistent fuel package was used for this series of experiments. The primary fuel source and ignition location was an upholstered sofa. The room also included an simulated chair side similar in design to the simulated furniture fuel package used in UL 199 [6]. The floor of the fire room was covered by carpeting to allow for the fire to spread beneath the sofa where it would be shielded from the water spray, thereby providing a more realistic challenge to the water spray. The flooring was comprised of a bottom layer of 1.3 cm (0.5 in.) thick plywood sheets, followed by a 1.0 cm (0.4 in.) layer of polyurethane foam padding, and topped by a layer of carpet. The fuels were weighed and measured, and the base materials used in their construction were determined. These details are summarized in Tables 2.3 and 2.4.

Table 2.3: Description of Materials in Fuel Load

Item	Materials
Sofa	PE Fabric, PU Foam & PE Fill, Engineered Wood Frame
Simulated Chair Side	100% PU Foam, 3/4 in. Plywood, 2 x 4 in. Dimensional Lumber
Carpet	100% Olefin Fiber, PP Backing
Padding	PU Rebond Foam

The sofa was placed in one of the corners of the fire room opposite the door. The simulated chair side faced the sofa from 1 m (3.3 ft) away and 10 cm (4 in.) from the back wall. Photographs

Table 2.4: Dimensions and Weights for Each Fuel

Item	Length [cm (in.)]	Width [cm (in.)]	Height [cm (in.)]	Mass
Sofa	218 (87)	91 (36)	86 (34)	53.5 ± 0.7 kg
Sim. Chair Side PU Foam	81 (32)	76 (30)	8 (3)	1.0 ± 0.1 kg
Carpet	-	-	0.5 (0.2)	1.3 ± 0.1 kg/m^2
Padding	-	-	1.0 (0.4)	0.8 ± 0.1 kg/m^2

and a floor plan showing the arrangement of a representative furnished fire room are presented in Figure 2.6.

Figure 2.6: Arrangement of furniture in an exemplar fire room.

2.3.1 Heat Release Rates of the Fuel

The fuels have been characterized in terms of heat release rate (HRR). Upholstered sofas, similar to those used in the furnished room experiments, have been characterized in compartment fires [15]. They were burned under the UL oxygen consumption calorimeter in Northbrook, IL to determine the HRR and the total heat released. The sofa was burned in a 3.7 m x 3.7 m (12 ft x 12 ft) compartment with an open door. Three ignition locations were included: 1) in the corner opposite the door, 2) centered on the wall opposite the door, and 3) centered in the room. Up to three replicates of each location were included. The HRRs from each experiment are presented in Figure 2.7. Including every replicate and ignition location, the average HRR and total energy released were 2729 $\pm$ 335 kW and 839 $\pm$ 67 MJ, respectively. Temperature measurements throughout the compartment indicate flashover conditions were present in every experiment (temperatures exceeded 600 °C (1112 °F)). The sofa alone can create enough energy to flashover the test compartment.

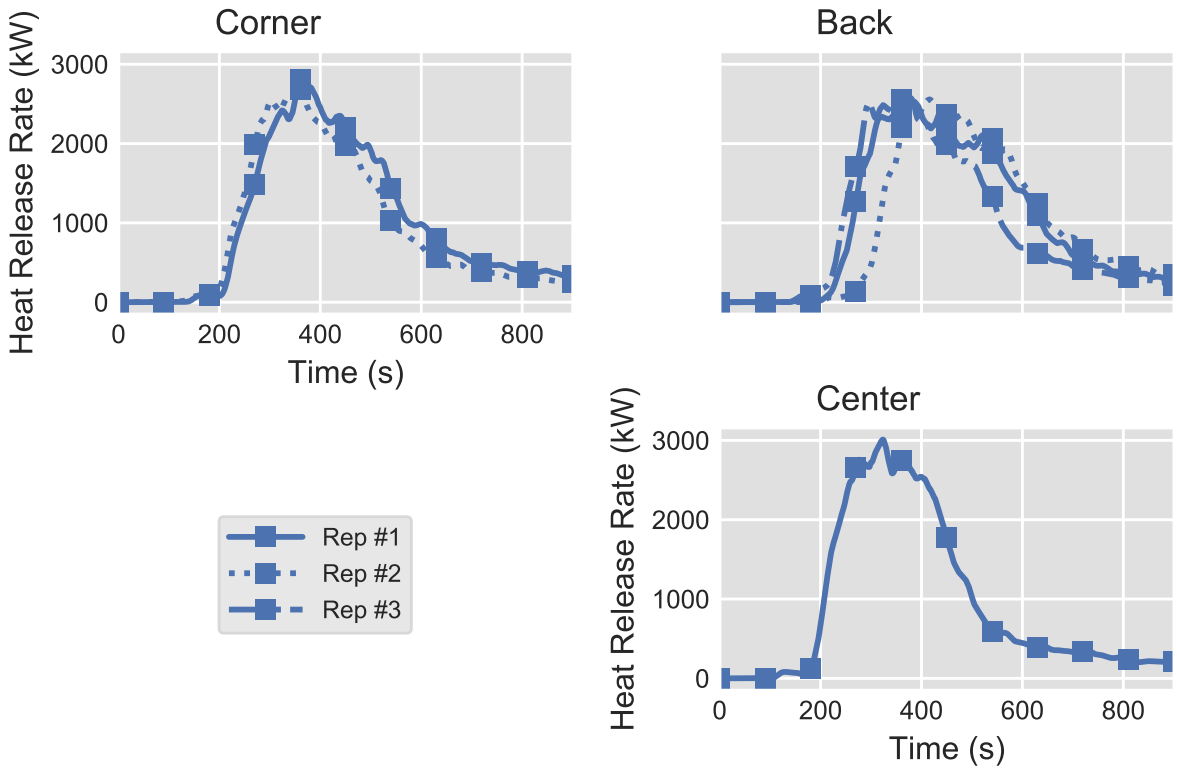

Figure 2.7: Heat release rate time histories of the upholstered sofa burned in different locations within a compartment [15].

The components of the flooring were burned under a lab scale cone calorimeter. Table 2.5 summarizes the data collected with the cone calorimeter for the flooring components. The cone calorimeter data demonstrates that if the flooring, padding, or carpeting under the sofa burned due to being shielded from the water, a significant HRR could be produced.

Table 2.5: Cone calorimeter data for flooring materials. Each material was tested for three replicates under a heat flux exposure of 35 kW/m^2. Reported values are the averages and expanded uncertainties between replicates.

Item	Peak HRR [kW/m^2]	Total Energy Released [MJ/m^2]	Effective Heat of Combustion [MJ/kg]
Carpet	383 ± 22	28 ± 4	42 ± 13
Carpet padding	436 ± 16	23 ± 2	29 ± 4
Plywood	163 ± 18	72 ± 5	13 ± 0.2

2.4 Water Sprays

The primary spray nozzle used in this project was the same spray nozzle used in the furnished room experiments of Phase 1, identified in this report as Nozzle 40W. The nozzle has been characterized and tested in Phase 1, providing a benchmark to compare with the results of Phase 2. Four additional nozzles were evaluated for this study. Water distribution tests were conducted with each nozzle to characterize their spray patterns. The results of the water distribution tests were used to determine the best candidates to be used in the fire tests. Table 2.6 summarizes all of the nozzles used in the water distribution tests. Figure 2.8 shows images of each nozzle while flowing water.

The nozzles varied in three main characteristics: flow capacity, spray angle, and vane design. The flow capacity of a nozzle determines its flow rate for a given pressure and depends on factors such as the orifice size of the nozzle. Findings from Phase 1 demonstrated that a flow rate of 23 lpm (6 gpm) at 1.7 bar (25 psi) was successful, therefore, nozzles with similar flow capacities were chosen. Nozzle spray angles are commonly available at 90° and 120°. Spray angles of 90° or less were not considered as they would likely not provide a large enough coverage area. One nozzle with a 150° spray angle was included, the rest had 120° spray angles.

The vane design of nozzles can generally be categorized as enclosed or open. An enclosed nozzle uses vanes to produce rotational flow inside of a chamber. The liquid atomizes as it exits the nozzle orifice to form a full cone spray pattern. An open nozzle has a continuous spiral vane that is angled to redirect the water flow in a cone pattern. The liquid shears along the spiral profile to achieve atomization. Generally, open nozzles have smaller droplet sizes but less uniform spray patterns when compared to enclosed nozzles. These differences can be visually apparent, as shown between the enclosed nozzles in Figures 2.8a–2.8c and the open nozzles in Figures 2.8d–2.8e.

Table 2.6: Summary of the nozzle characteristics. The flow rates and spray angles are provided by the manufacturers for an operating pressure of 1.4 bar (20 psi).

Nozzle Identifier	Flow Rate [lpm (gpm)]	Spray Angle (degrees)	Design
40W	20.8 (5.5)	120	Enclosed
50W	26.1 (6.9)	120	Enclosed
WL7	19.3 (5.1)	120	Enclosed
N2	28.4 (7.5)	120	Open
TF14-150	21.6 (5.7)	150	Open

(a) 40W

(b) 50W

(c) WL7

(d) N2

(e) TF14-150

Figure 2.8: Photographs of each nozzle during operation.

2.4.1 Water Distribution Tests

The purpose of the water distribution tests was to characterize the spray patterns of the nozzles. The tests were conducted with the nozzles installed in Room 4 to provide the largest possible distribution map.

The water flow patterns were determined by collecting the water in discrete bins. Each bin was square, with side lengths of 50.8 cm (20 in.), covering an area of 0.3 m^2 (2.8 ft^2). The height of the bins was 0.3 m (1 ft). The edge of each bin had a lip to cover the gap between the adjacent bins, ensuring that all of the water was collected. Bins were only placed in one quadrant of the room due to the axial symmetry of the spray pattern. The first bin was placed such that its corner was directly below the water spray. The remaining bins were arranged in adjacent fashion from the first, leaving a 10 cm (4 in.) gap between the bins and the walls. This arrangement fit four rows of four bins each, totaling 16 bins. The arrangement of the bins is pictured in Figure 2.9. To evaluate the assumption of axial symmetry additional tests were conducted with bins in all four quadrants of the room, as shown in Figure 2.10.

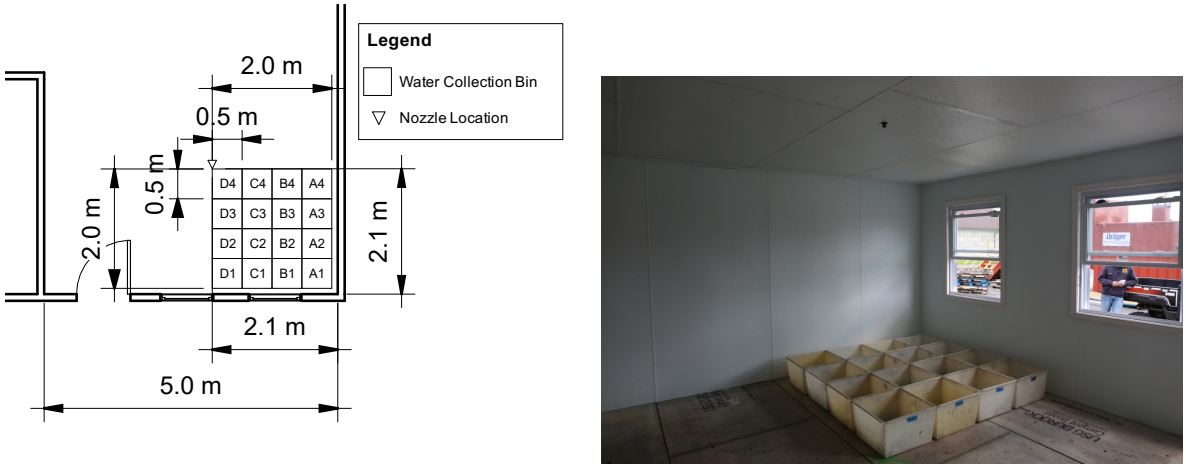

Figure 2.9: Floor plan and picture showing the locations of the collection bins for the water distribution tests measuring one quadrant of the room.

The water distribution was determined by measuring the mass of the water collected in each bin and the duration of the water flow. The duration of each test was 10 minutes. From these values the water flow rate per unit area, *water flux*, was calculated. The water flux was calculated for each bin, and averaged over each replicate. The water flow rate for every test was 23 lpm (6 gpm). Table 2.7 summarizes the results in terms of the average water flux and variance between replicates.

To evaluate the assumption that the nozzles' spray distributions are axial symmetric, one test per nozzle was conducted with bins in all four quadrants of the room, as shown in Figure 2.10. These tests are summarized in Table 2.8. The variance between corresponding bins of each quadrant was

Figure 2.10: Floor plan and picture showing the locations of the collection bins for the water distribution tests measuring all four quadrants of the room.

Table 2.7: Summary of the water distribution tests. The average water flux is an average of both the set of bins in one quadrant of the room (as pictured in Figure 2.9) and of the replicates. The variance is calculated between replicates for each bin, then averaged over every bin.

Nozzle	N	Avg. Water Flux [mm/min (gpm/ft^2)]	Avg. Variance of Replicates [mm/min (gpm/ft^2)]
40W	3	1.3 (0.031)	0.03 (0.0008)
50W	3	1.3 (0.032)	0.00 (0.0001)
WL7	3	1.3 (0.031)	0.22 (0.0054)
N2	1	1.2 (0.030)	-
TF14-150	1	1.0 (0.024)	-

calculated (for example: bins A1, A8, H1, and H8), and the average of those variances is reported in the table. The 40W, 50W, and WL7 nozzles had average variances of less than 0.1 mm/min (0.002 gpm/ft^2), indicating strong axial symmetry. The N2 nozzle, in contrast, had an average variance of 0.7 mm/min (0.0180 gpm/ft^2). This difference in axial symmetry is consistent with the vane design of the nozzles – the N2 nozzle is open and the other nozzles are enclosed. These findings show that using collection bins in only one quadrant of the room is sufficient for understanding the distribution maps of the enclosed nozzles (40W, 50W, and WL7). For the open nozzles (N2, TF14-150), however, there is less certainty that water flux data from one quadrant of the room reflects the distribution map of the entire room.

The total volume of water collected was compared to the expected volume based on the flow rate and duration of flow. With 23 lpm (6 gpm) and a ten minute duration, the expected volume was

Table 2.8: Summary of the water distribution tests that included bins in all four quadrants of the room, as pictured in Figure 2.10. The flow rate was 23 lpm (6 gpm) for each nozzle, and one replicate of each test was conducted. The variance between corresponding bins of each quadrant was calculated (for example: bins A1, A8, H1, and H8), and the average of those variances is reported.

Nozzle	Avg. Variance of Quadrants [mm/min (gpm/ft^2)]
40W	0.08 (0.0020)
50W	0.04 (0.0009)
WL7	0.05 (0.0013)
N2	0.73 (0.0180)

227 L (60 gal). Based on the tests with 64 bins and the 40W and 50W nozzles, the average total volume of water collected was 203 L (54 gal), corresponding to a percent error of 10%. This error resulted from water distributed beyond the area of the bins and on the walls.

The water distribution map for the 40W nozzle flowing at 23 lpm (6 gpm) is visualized by a bar graph in Figure 2.11. The average water flux of the bins was 1.3 mm/min (0.031 gpm/ft^2). The general pattern shows the water flux is highest directly below the nozzle, and decreases with greater radial distance from the nozzle. Although the design of the nozzle is to provide a uniform cone pattern, the droplets do not have enough momentum to maintain straight trajectories. Instead, droplets distributed near the edge of the cone pattern fall short of their initial trajectories, resulting in greater water flux near the center of the cone pattern. The highest water flux was collected by bin C4 with 2.7 mm/min (0.066 gpm/ft^2), and the lowest in bin A1 with 0.1 mm/min (0.002 gpm/ft^2).

Figure 2.12 provides a comparison of the water distribution maps for each nozzle when flowing at 23 lpm (6 gpm). The 40W nozzle was shown to be effective in the fire experiments of Phase 1. It is therefore the benchmark by which to compare the other nozzles.

The 50W nozzle provided a more uniform spray distribution compared to the 40W nozzle, as shown in Figure 2.12b. The water flux ranged between 1.0 mm/min (0.024 gpm/ft^2) and 1.8 mm/min (0.044 gpm/ft^2), with exception of bins B1, A1, and A2. Those bins had lower water flux (less than 0.7 mm/min (0.016 gpm/ft^2)) indicating a sharp limit to the spray radius at about 2.3 m (7.5 ft). In comparison to nozzle 40W, the range of water flux for the same bins (excluding B1, A1, and A2) was between 0.5 mm/min (0.013 gpm/ft^2) and 2.7 mm/min (0.066 gpm/ft^2). A potential explanation for the difference in distribution patterns is that the 50W nozzle is a higher capacity nozzle (lower operating pressure for same flow rate) which creates larger droplet sizes. Larger droplets have greater momentum, allowing them to maintain the trajectories of a uniform cone distribution over greater distances.

The WL7 nozzle provided a similar spray distribution to the 40W nozzle, as shown in Figure 2.12c. This result is unsurprising due to the similar design and flow capacities for these nozzles (see Table 2.6). The greatest difference between nozzles was in the bin closest to the center (bin

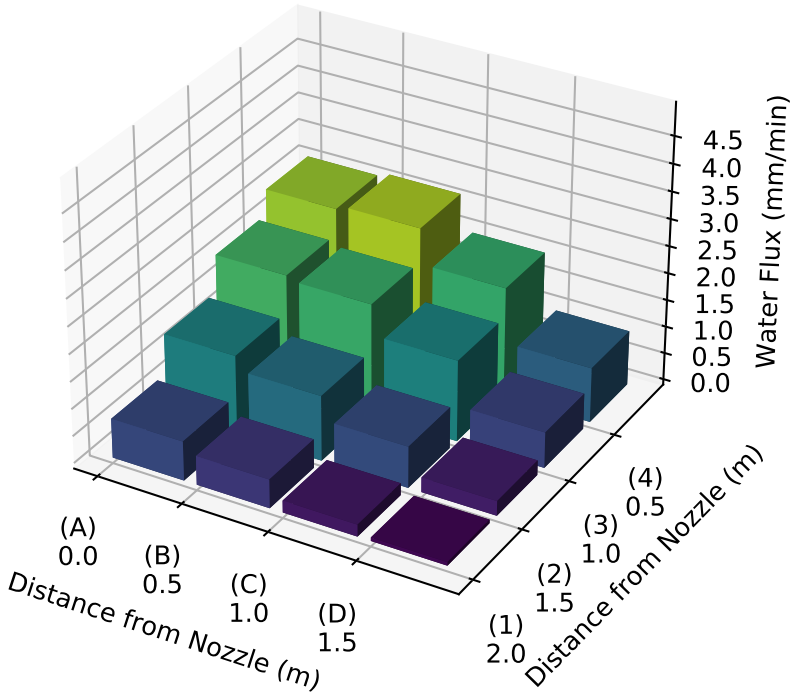

Figure 2.11: Water distribution map for the 40W nozzle flowing at 23 lpm (6 gpm). The bars represent the water flux collected in each bin, averaged over three replicates. The bins were placed in one quadrant of the room (as shown in Figure 2.9), with the outside corner of bin 4D directly below the nozzle.

D4), where the WL7 water flux was 3.8 mm/min (0.093 gpm/ft^2) as compared to 2.6 mm/min (0.064 gpm/ft^2) from the 40W nozzle – a difference of 1.2 mm/min (0.029 gpm/ft^2). In every other bin, the difference in water flux between nozzles was less than 0.7 mm/min (0.016 gpm/ft^2).

The N2 nozzle provided a spray distribution that was concentrated near the center and was less uniform compared to the 40W nozzle (see Figure 2.12d). The bin nearest the nozzle, D4, had a water flux of 4.8 mm/min (0.118 gpm/ft^2), while the bins more than one row away from the nozzle all had less than 2 mm/min (0.05 gpm/ft^2). The lack of uniformity in the distribution pattern is evident by comparing bins that are equidistant from the nozzle. For example, bins D3 and C4 are both one row away from the nozzle, but have water flux of 3.7 mm/min (0.091 gpm/ft^2) and 2.5 mm/min (0.062 gpm/ft^2), respectively. The lack of uniformity is also consistent with the results of the four quadrant distribution test, where the variance between quadrants was significantly higher for the N2 nozzle than the other (enclosed) nozzles (see Table 2.8).

The TF14-150 nozzle provided a similar spray distribution pattern to the 40W nozzle, but with consistently lower water flux in each bin (see Figure 2.12e). The 150° spray angle distributed a

greater portion of water beyond the coverage area of the bins. Therefore the average water flux in the bins was lower for the TF14-150 nozzle (1.0 mm/min (0.024 gpm/ft^2)) than for the 40W nozzle (1.2 mm/min (0.031 gpm/ft^2)) despite equivalent flow rates.

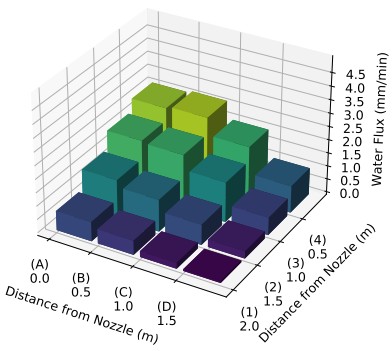

(a) 40W

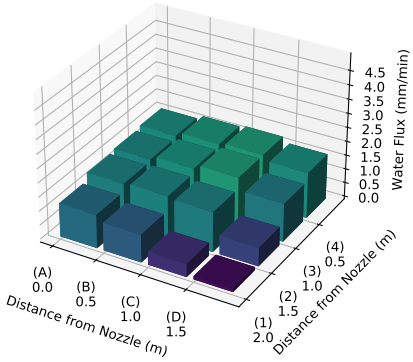

(b) 50W

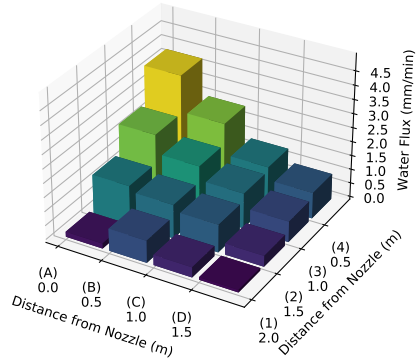

(c) WL7

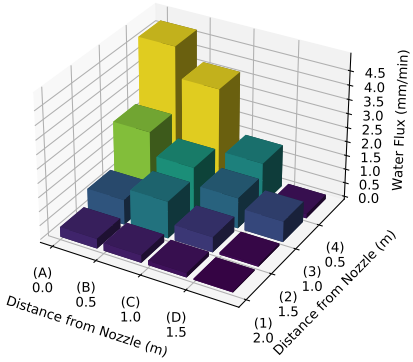

(d) N2

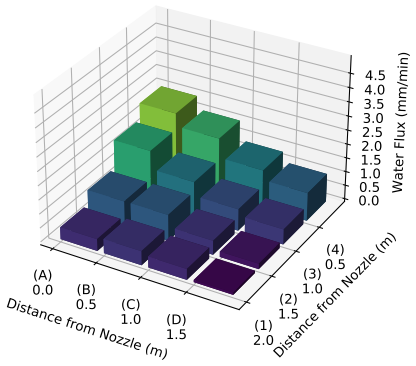

(e) TF14-150

Figure 2.12: Comparison of the water distribution maps for each nozzle when flowing at 23 lpm (6 gpm). The bars represent the water flux collected in each bin. The bins were placed in one quadrant of the room (as shown in Figure 2.9), with the outside corner of bin 4D directly below the nozzle.

2.5 Summary of Experimental Configurations

The purpose of these experiments was to examine the ability of a low flow nozzle to cool and suppress the thermal hazard from a fire generated by interior finishes and fuels that would be found in a residence. The variable adjusted between experiments was the water flux at the ignition location. Results from Phase 1 of this project showed that 1.6 mm/min (0.040 gpm/ft^2) at the ignition location was sufficient to suppress the fire in that scenario, but 1.1 mm/min (0.027 gpm/ft^2) was not. Therefore, the experimental configurations were designed to provide a range of water flux values around 1.1 mm/min (0.027 gpm/ft^2) at the ignition location. One way this variable was adjusted was by changing the nozzle-to-ignition distance via changes in room size and ignition location. The other way was by using different nozzles.

Based on the results from the water distribution tests, only the 40W and 50W nozzles were selected for use in the fire experiments. The WL7 nozzle performed similarly to the 40W nozzle, and thus would not provide additional insight on low flow nozzle performance. The N2 nozzle had the least uniform distribution pattern, likely increasing the dependence of its suppression performance on ignition location. Lastly, the TF14-150 nozzle had a lower average water flux than was expected to be sufficient for fire protection.

Overall, the range of water flux values at the ignition location varied between 0.3 mm/min (0.008 gpm/ft^2) and 1.8 mm/min (0.044 gpm/ft^2). The flow rate was consistent between experiments at 23 lpm (6 gpm). In addition, one experiment was conducted with a residential sprinkler flowing water at 30 lpm (8 gpm) to provide a baseline for comparison. Nine experiments were conducted in total, and are summarized in Table 2.9. The following sections provide details on the configuration for each experiment.

Table 2.9: Summary of Fire Experiments.

Exp #	Water Spray	Ign. Corner-Nozzle Distance [m (ft)]	Water Flux at Ign. [mm/min (gpm/ft^2)]
1A	40W	2.6 m (8.5 ft)	0.3 (0.008)
1B	40W	2.6 m (8.5 ft)	0.3 (0.008)
2	50W	2.6 m (8.6 ft)	0.4 (0.010)
3	50W	2.6 m (8.5 ft)	0.5 (0.012)
4	40W	2.2 m (7.1 ft)	0.8 (0.019)
5	50W	2.4 m (7.8 ft)	0.9 (0.022)
6	50W	2.2 m (7.1 ft)	1.4 (0.035)
7	50W	1.8 m (6.0 ft)	1.8 (0.044)
8	Sprinkler	2.6 m (8.5 ft)	1.8 (0.043)

Additional water distribution tests were conducted in the fire rooms to provide more accurate measurements of the water flux at the ignition locations. A grid of at least 3 x 3 bins was placed against the walls of the ignition corners. Three replicates were collected for each configuration of water spray, room size, and ignition location used in the fire experiments. The results of these tests

are provided for each experiment.

2.5.1 Experiment 1A and 1B

Two replicate experiments with the following configuration were conducted, and are referred to as Experiments 1A and 1B. The fire room was 3.7 m x 3.7 m (12 x 12 ft) with a nozzle centered in the room. The distance between the ignition corner and the nozzle was 2.6 m (8.5 ft). Figure 2.13 shows the dimensioned floor plan for Experiment 1A including the locations of the instrumentation, fuel, and ignition. The setup was identical for Experiment 1B, but located in Room 3 instead of Room 2.

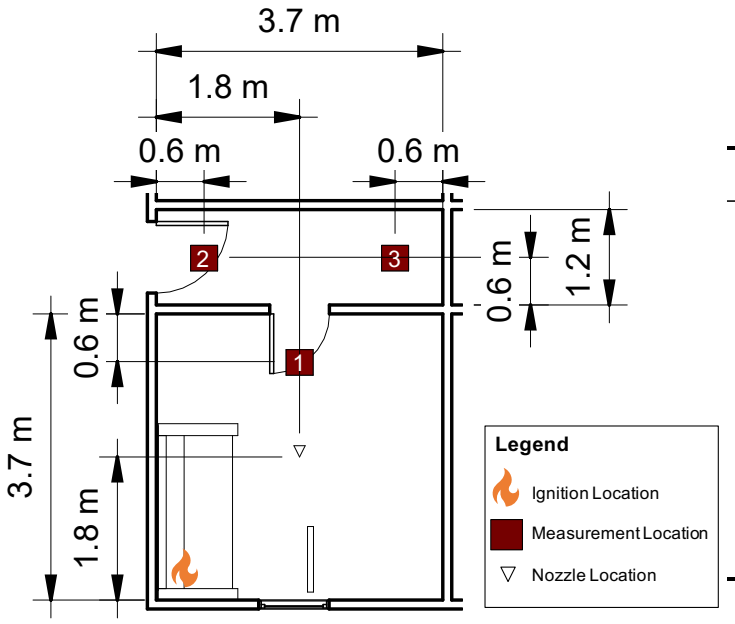

Position	Instrumentation
1	Thermocouple Array, Gas Concentrations, Heat Flux
2	Thermocouple Array, Tell-Tale Sprinkler, Smoke Alarm
3	Thermocouple Array, Gas Concentrations

Figure 2.13: Dimensioned floor plan with the locations of the instrumentation, fuel, and ignition for Experiments 1A and 1B.

The 40W nozzle flowing water at 23 lpm (6 gpm) was used in these experiments. Figure 2.14 shows the water distribution map overlaid on the fire room floor plan. The water flux in the ignition corner (Bin A1) is 0.3 mm/min (0.008 gpm/ft^2). The water flux increases to greater than 0.7 mm/min (0.018 gpm/ft^2) in the bins adjacent to the ignition corner (Bins A2, B1, and B2).

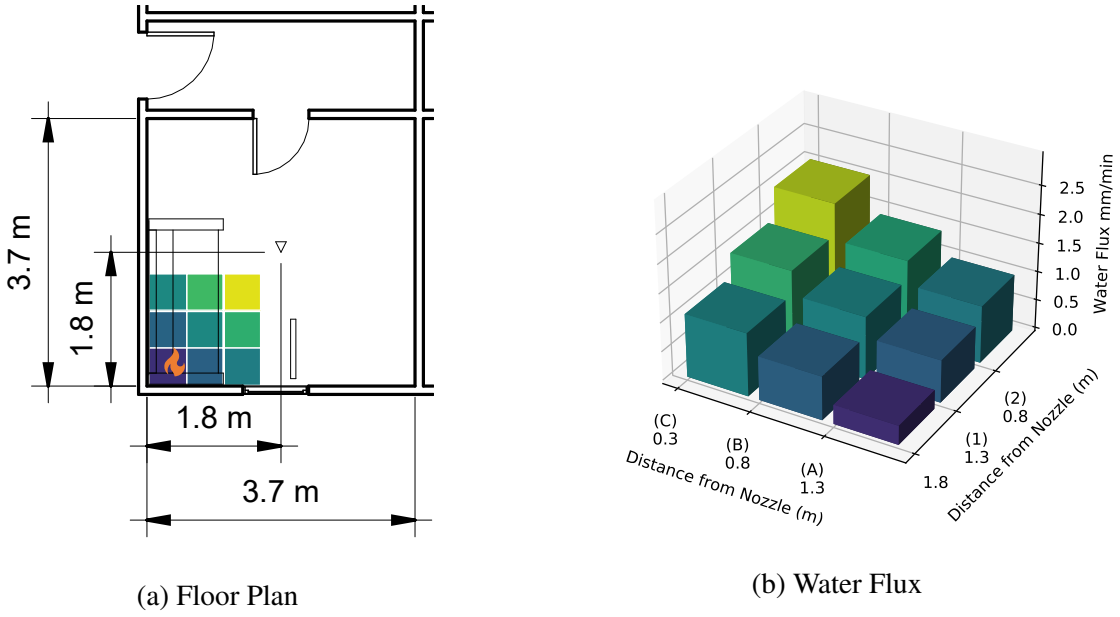

(a) Floor Plan

(b) Water Flux

Figure 2.14: Water distribution map for the nozzle and ignition location in Experiments 1A and 1B. The values in the bar graph represent the water flux collected in each bin, averaged over three replicates. The arrangement of the bins is shown by the floor plan, where Bin A1 corresponds to the ignition location.

2.5.2 Experiment 2

Experiment 2 was conducted in Room 1 which was 3.2 m x 3.7 m (10.5 x 12 ft). The nozzle location was 1.5 m (5 ft) and 2.1 m (7 ft) from the adjoining walls of the ignition corner. Measured directly, the distance between the ignition corner and the nozzle was 2.6 m (8.5 ft). Figure 2.15 shows the dimensioned floor plan including the locations of the instrumentation, fuel, and ignition.

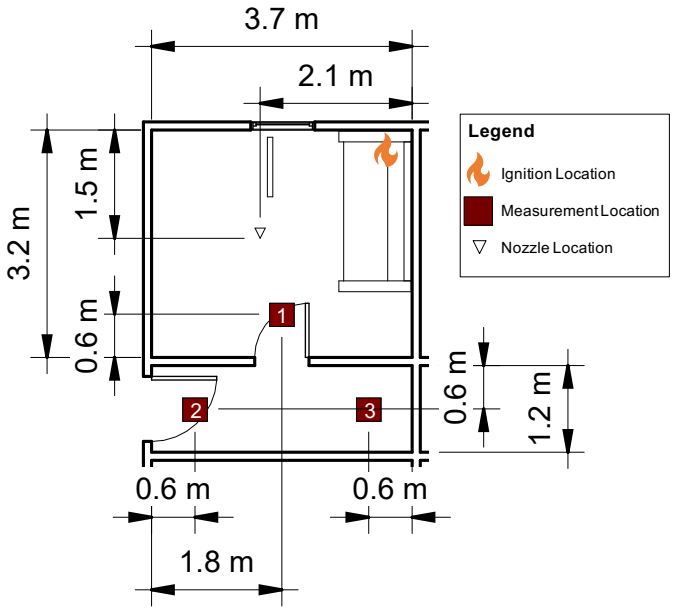

Position	Instrumentation
1	Thermocouple Array, Gas Concentrations, Heat Flux
2	Thermocouple Array, Tell-Tale Sprinkler, Smoke Alarm
3	Thermocouple Array, Gas Concentrations

Figure 2.15: Dimensioned floor plan with the locations of the instrumentation, fuel, and ignition for Experiment 2.

The 50W nozzle flowing water at 23 lpm (6 gpm) was used in this experiment. Figure 2.16 shows the water distribution map overlaid on the fire room floor plan. The water flux in the ignition corner (Bin A1) is 0.4 mm/min (0.010 gpm/ft^2). The water flux increases to greater than 0.9 mm/min (0.023 gpm/ft^2) in the bins adjacent to the ignition corner (Bins A2, B1, and B2).

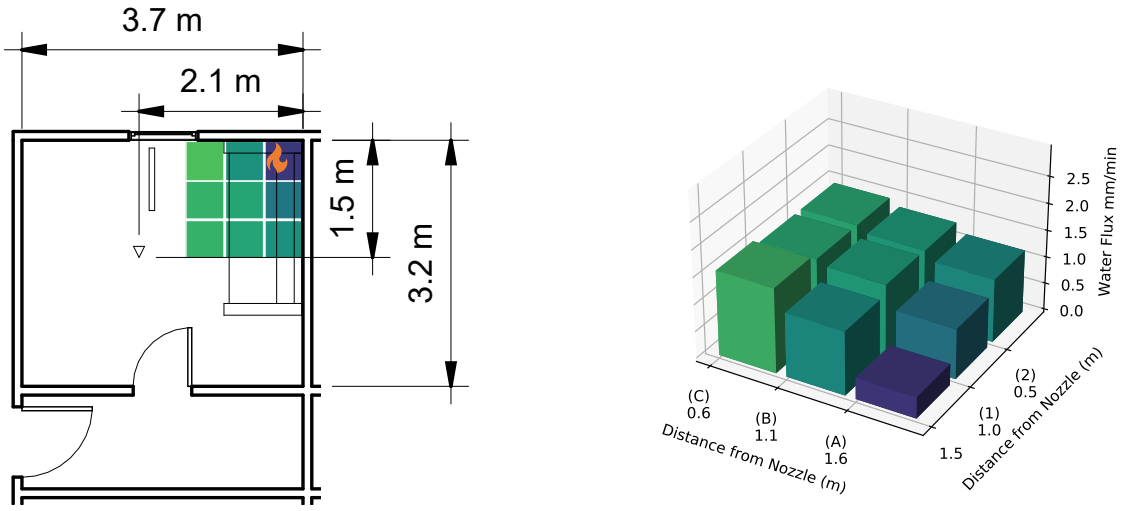

(a) Floor Plan

(b) Water Flux

Figure 2.16: Water distribution map for the nozzle and ignition location in Experiment 2. The values in the bar graph represent the water flux collected in each bin, averaged over three replicates. The arrangement of the bins is shown by the floor plan, where Bin A1 corresponds to the ignition location.

2.5.3 Experiment 3

Experiment 3 was conducted in Room 2, a 3.7 m x 3.7 m (12 x 12 ft) room with a nozzle in the center. The distance between the ignition corner and the nozzle was 2.6 m (8.5 ft). Figure 2.17 shows the dimensioned floor plan for Experiment 3 including the locations of the instrumentation, fuel, and ignition.

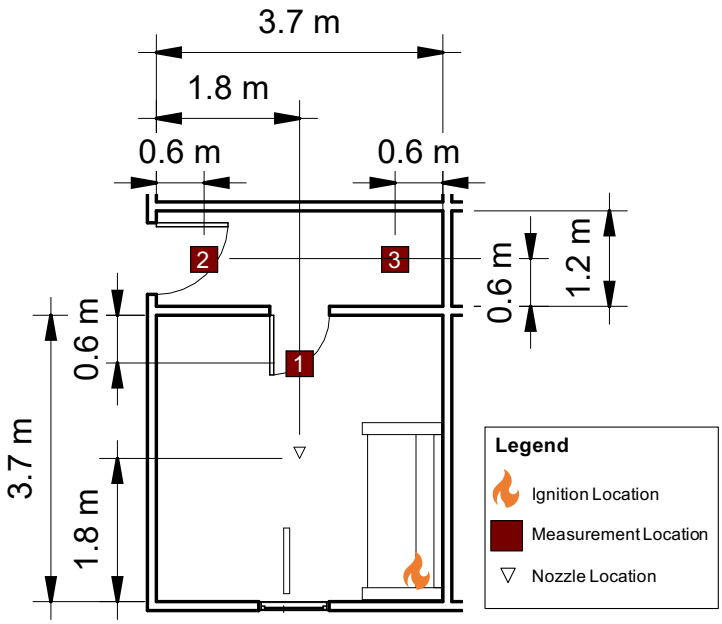

Position	Instrumentation
1	Thermocouple Array, Gas Concentrations, Heat Flux
2	Thermocouple Array, Tell-Tale Sprinkler, Smoke Alarm
3	Thermocouple Array, Gas Concentrations

Figure 2.17: Dimensioned floor plan with the locations of the instrumentation, fuel, and ignition for Experiment 3.

The 50W nozzle flowing water at 23 lpm (6 gpm) was used in this experiment. Figure 2.18 shows the water distribution map overlaid on the fire room floor plan. The water flux in the ignition corner (Bin A1) is 0.5 mm/min (0.012 gpm/ft^2). The water flux increases to greater than 1.2 mm/min (0.029 gpm/ft^2) in the bins adjacent to the ignition corner (Bins A2, B1, and B2).

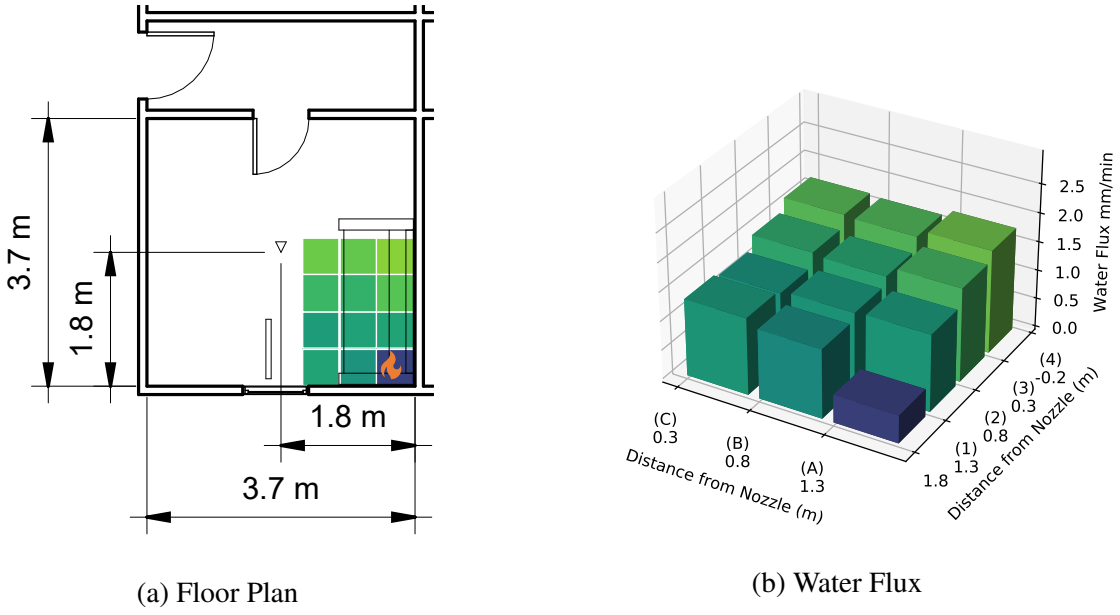

(a) Floor Plan

(b) Water Flux

Figure 2.18: Water distribution map for the nozzle and ignition location in Experiment 3. The values in the bar graph represent the water flux collected in each bin, averaged over three replicates. The arrangement of the bins is shown by the floor plan, where Bin A1 corresponds to the ignition location.

2.5.4 Experiment 4

Experiment 4 was conducted in Room 1, which was 3.2 m x 3.7 m (10.5 x 12 ft). The nozzle location was 1.5 m (5 ft) and 1.5 m (5 ft) from the adjoining walls of the ignition corner. Measured directly, the distance between the ignition corner and the nozzle was 2.2 m (7.1 ft). Figure 2.19 shows the dimensioned floor plan including the locations of the instrumentation, fuel, and ignition.

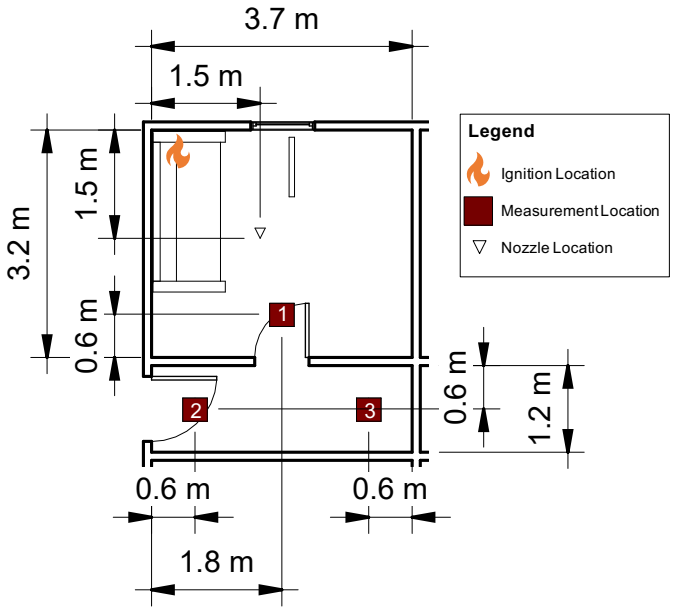

Position	Instrumentation
1	Thermocouple Array, Gas Concentrations, Heat Flux
2	Thermocouple Array, Tell-Tale Sprinkler, Smoke Alarm
3	Thermocouple Array, Gas Concentrations

Figure 2.19: Dimensioned floor plan with the locations of the instrumentation, fuel, and ignition for Experiment 4.

The 40W nozzle flowing water at 23 lpm (6 gpm) was used in this experiment. Figure 2.20 shows the water distribution map overlaid on the fire room floor plan. The water flux in the ignition corner (Bin A1) is 0.8 mm/min (0.019 gpm/ft^2). The water flux increases to greater than 1.3 mm/min (0.031 gpm/ft^2) in the bins adjacent to the ignition corner (Bins A2, B1, and B2).

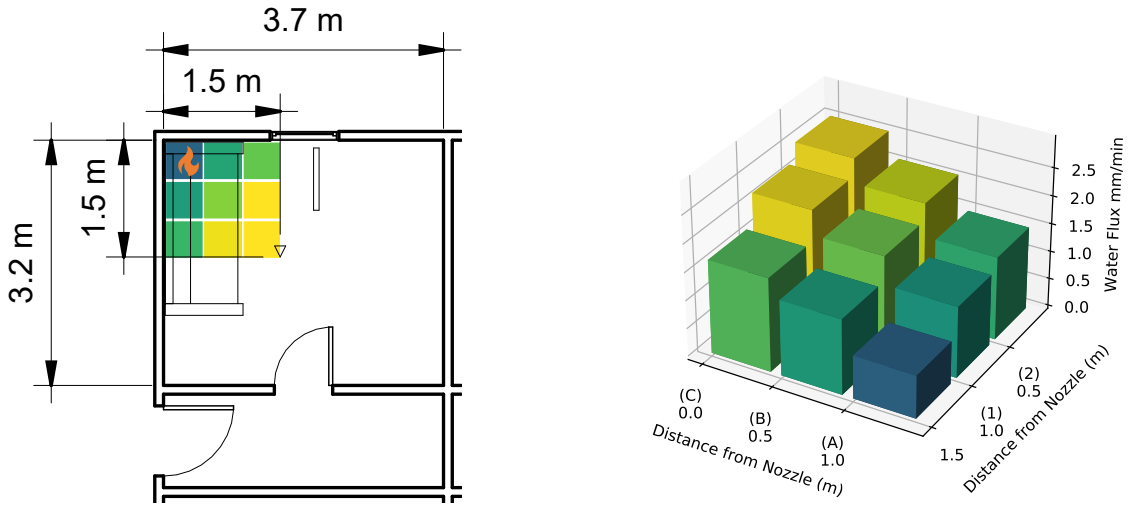

(a) Floor Plan

(b) Water Flux

Figure 2.20: Water distribution map for the nozzle and ignition location in Experiment 4. The values in the bar graph represent the water flux collected in each bin, averaged over three replicates. The arrangement of the bins is shown by the floor plan, where Bin A1 corresponds to the ignition location.

2.5.5 Experiment 5

Experiment 5 was conducted in Room 2, a 3.7 m x 3.7 m (12 x 12 ft) room with a nozzle in the center. Unlike the other experiments, the sofa was shifted 0.3 m (1 ft) away from the back wall of the room. The purpose for this change was to achieve a greater water flux on the ignition location than when the sofa was against the corner. The distance between the ignition location and the nozzle was 2.4 m (7.8 ft). Figure 2.21 shows the dimensioned floor plan including the locations of the instrumentation, fuel, and ignition.

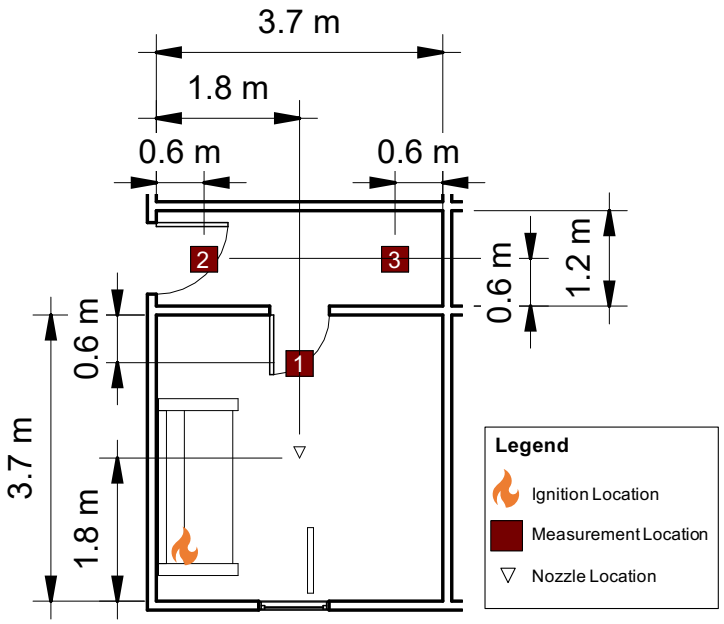

Position	Instrumentation
1	Thermocouple Array, Gas Concentrations, Heat Flux
2	Thermocouple Array, Tell-Tale Sprinkler, Smoke Alarm
3	Thermocouple Array, Gas Concentrations

Figure 2.21: Dimensioned floor plan with the locations of the instrumentation, fuel, and ignition for Experiment 5.

The 50W nozzle flowing water at 23 lpm (6 gpm) was used in this experiment. Figure 2.22 shows the water distribution map overlaid on the fire room floor plan. The water flux in the ignition corner (average of Bins A1 and A2) is 0.9 mm/min (0.022 gpm/ft^2). The water flux increases to greater than 1.2 mm/min (0.029 gpm/ft^2) in the bins adjacent to the ignition corner (Bins A3, B1, and B2).

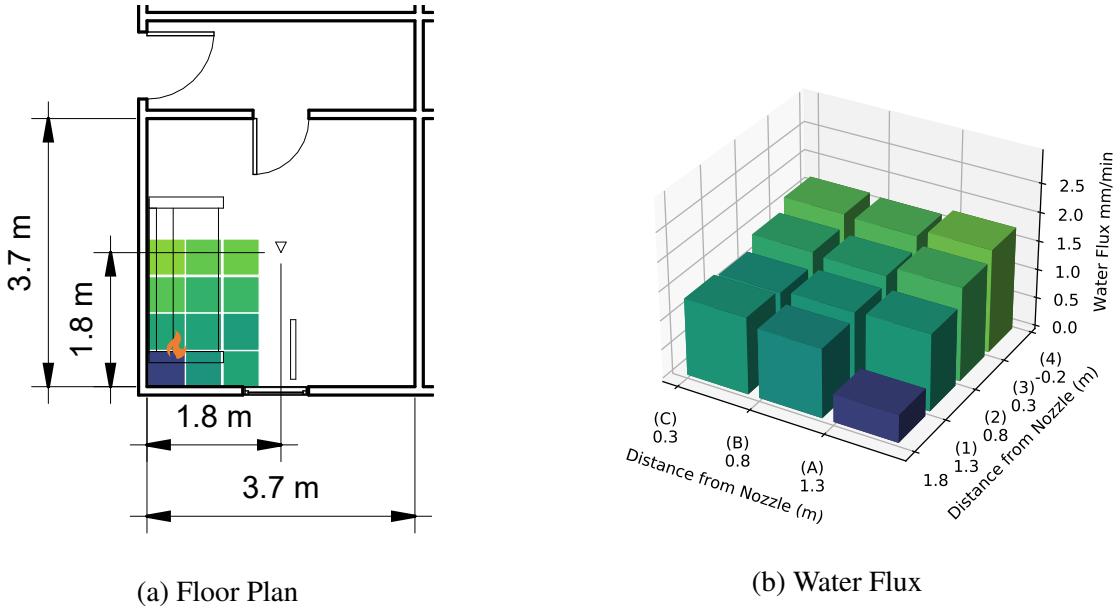

(a) Floor Plan

(b) Water Flux

Figure 2.22: Water distribution map for the nozzle and ignition location in Experiment 5. The values in the bar graph represent the water flux collected in each bin, averaged over three replicates. The arrangement of the bins is shown by the floor plan, where the ignition location is between Bins A1 and A2.

2.5.6 Experiment 6

Experiment 6 was conducted in Room 1, which was 3.2 m x 3.7 m (10.5 x 12 ft). The nozzle location was 1.5 m (5 ft) and 1.5 m (5 ft) from the adjoining walls of the ignition corner. Measured directly, the distance between the ignition corner and the nozzle was 2.2 m (7.1 ft). Figure 2.23 shows the dimensioned floor plan including the locations of the instrumentation, fuel, and ignition.

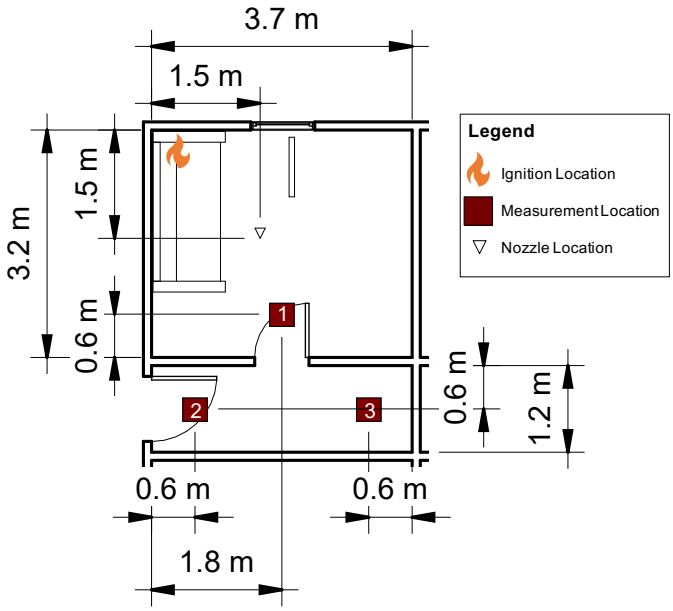

Position	Instrumentation
1	Thermocouple Array, Gas Concentrations, Heat Flux
2	Thermocouple Array, Tell-Tale Sprinkler, Smoke Alarm
3	Thermocouple Array, Gas Concentrations

Figure 2.23: Dimensioned floor plan with the locations of the instrumentation, fuel, and ignition for Experiment 6.

The 50W nozzle flowing water at 23 lpm (6 gpm) was used in this experiment. Figure 2.24 shows the water distribution map overlaid on the fire room floor plan. The water flux in the ignition corner (Bin A1) is 1.4 mm/min (0.035 gpm/ft^2). The water flux is relatively uniform across the measured area, ranging between 1.4 mm/min (0.035 gpm/ft^2) and 1.8 mm/min (0.045 gpm/ft^2).

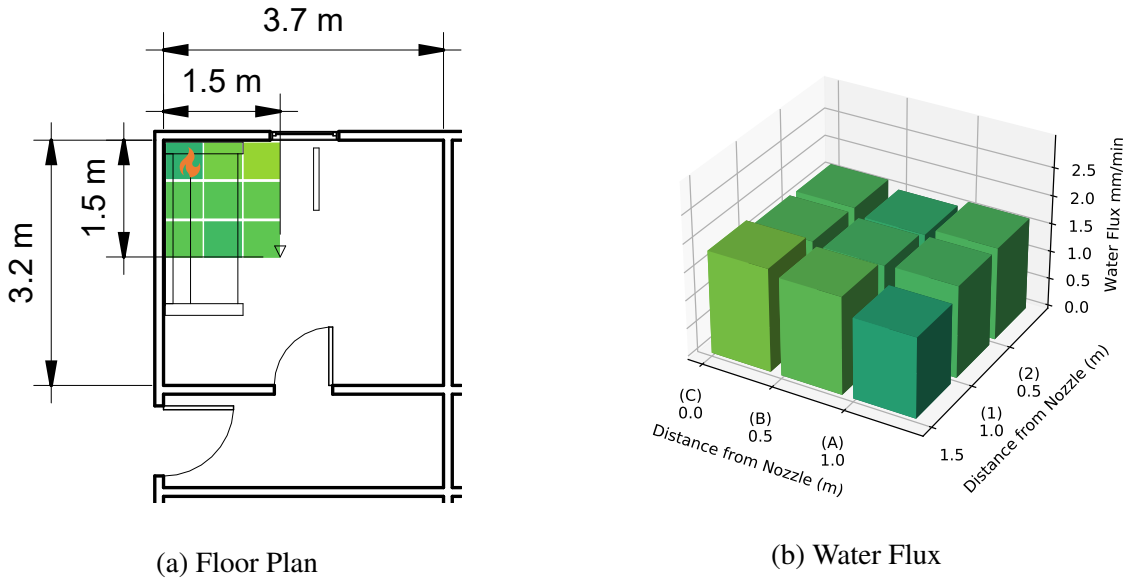

(a) Floor Plan

(b) Water Flux

Figure 2.24: Water distribution map for the nozzle and ignition location in Experiment 6. The values in the bar graph represent the water flux collected in each bin, averaged over three replicates. The arrangement of the bins is shown by the floor plan, where Bin A1 corresponds to the ignition location.

2.5.7 Experiment 7

Experiment 7 was conducted in Room 3, a 3.7 m x 3.7 m (12 x 12 ft) room with a nozzle in the center. Unlike the other experiments, the ignition location was on the opposite end of the sofa which was approximately centered on the wall. The purpose for this change was to achieve a greater water flux at the ignition location. The distance between the ignition location and the nozzle was 1.8 m (6 ft). Figure 2.25 shows the dimensioned floor plan including the locations of the instrumentation, fuel, and ignition.

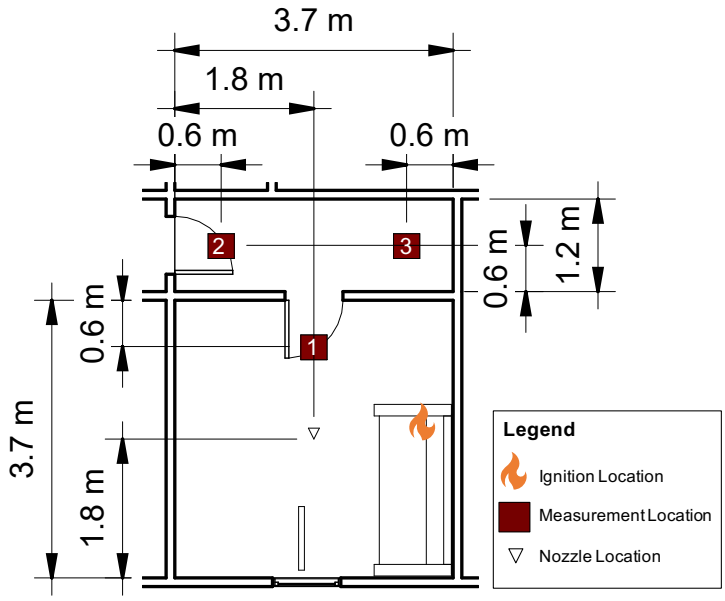

Position	Instrumentation
1	Thermocouple Array, Gas Concentrations, Heat Flux
2	Thermocouple Array, Tell-Tale Sprinkler, Smoke Alarm
3	Thermocouple Array, Gas Concentrations

Figure 2.25: Dimensioned floor plan with the locations of the instrumentation, fuel, and ignition for Experiment 7.

The 50W nozzle flowing water at 23 lpm (6 gpm) was used in this experiment. Figure 2.26 shows the water distribution map overlaid on the fire room floor plan. The water flux at the ignition location (Bin A4) is 1.8 mm/min (0.044 gpm/ft^2). This is the maximum water flux within the measured area. The water flux decreases to less than 1.7 mm/min (0.041 gpm/ft^2) in the adjacent bins (Bins A3, B3, and B4).

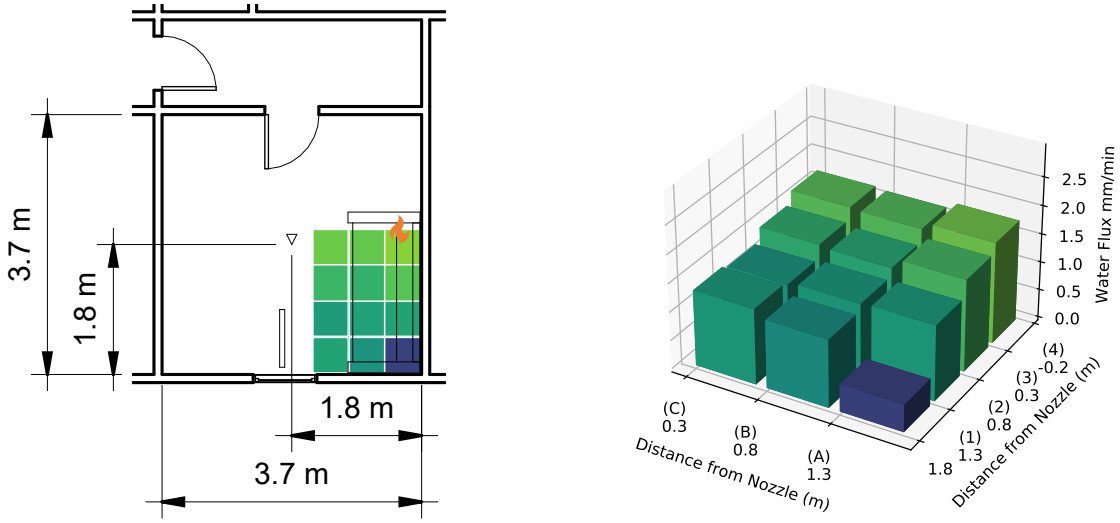

(a) Floor Plan

(b) Water Flux

Figure 2.26: Water distribution map for the nozzle and ignition location in Experiment 7. The values in the bar graph represent the water flux collected in each bin, averaged over three replicates. The arrangement of the bins is shown by the floor plan, where Bin A4 corresponds to the ignition location.

2.5.8 Experiment 8

Experiment 8 tested a standard residential sprinkler to provide a comparison for the performance of the low flow nozzles. The experiment was conducted in Room 2, a 3.7 m x 3.7 m (12 x 12 ft) room with the sprinkler in the center. The distance between the ignition location and the sprinkler was 1.8 m (6 ft). Figure 2.27 shows the dimensioned floor plan including the locations of the instrumentation, fuel, and ignition.

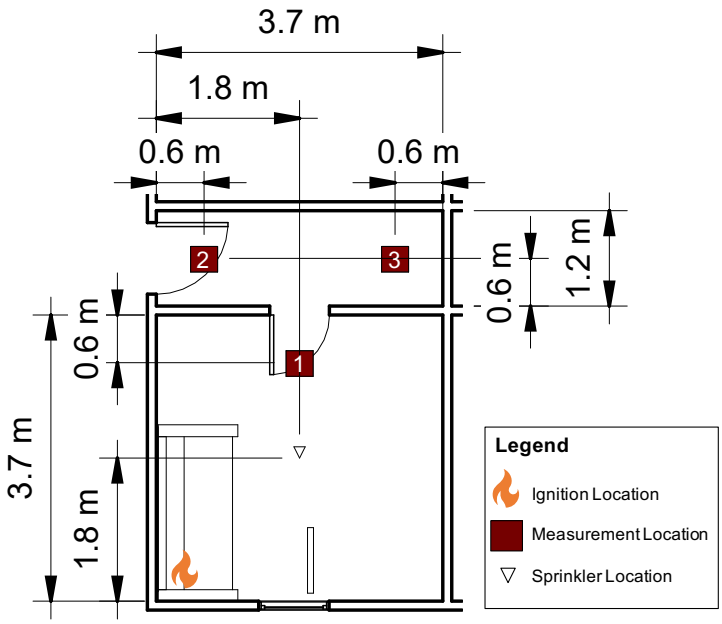

Position	Instrumentation
1	Thermocouple Array, Gas Concentrations, Heat Flux
2	Thermocouple Array, Tell-Tale Sprinkler, Smoke Alarm
3	Thermocouple Array, Gas Concentrations

Figure 2.27: Dimensioned floor plan with the locations of the instrumentation, fuel, and ignition for Experiment 8.

The sprinkler was operated at 30 lpm (8 gpm) which is the minimum flow rate listed by the manufacturer. For the 3.7 m x 3.7 m (12 x 12 ft) room, this equates to an average discharge density of 2.3 mm/min (0.056 gpm/ft^2). This value is slightly greater than the 2.0 mm/min (0.05 gpm/ft^2) minimum discharge density required by NFPA 13D [16]. Figure 2.28 shows the water distribution map overlaid on the fire room floor plan. The water flux in the bins against the walls is greater than 1.4 mm/min (0.033 gpm/ft^2), whereas the other bins are less than 1.2 mm/min (0.029 gpm/ft^2). This reflects the strategy of sprinklers to distribute water high on the walls at the edges of the room, thereby pre-wetting all of the fuels. The water flux at the ignition location (Bin A1) is 1.8 mm/min (0.043 gpm/ft^2).

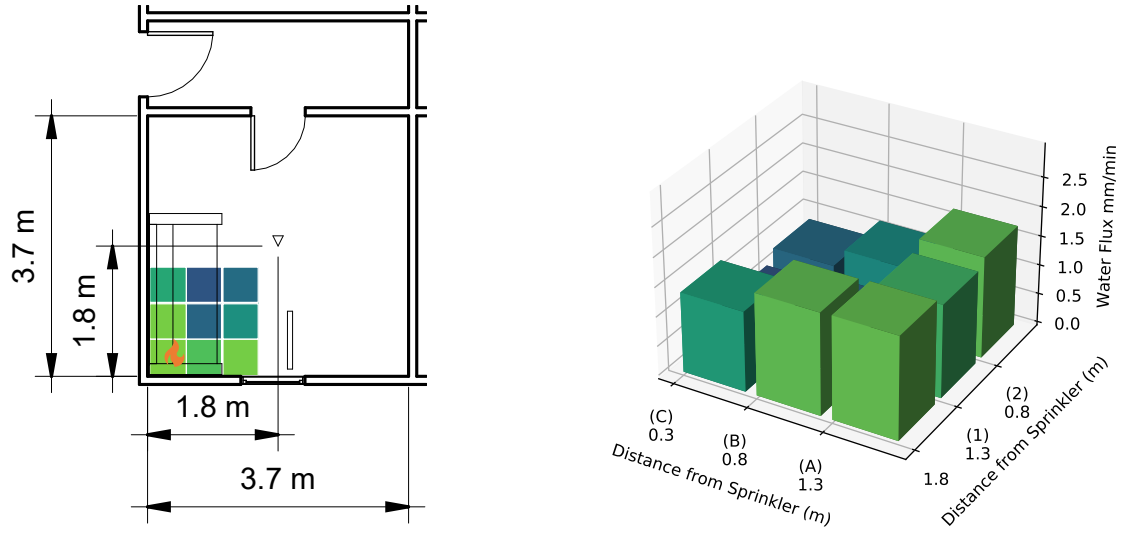

(a) Floor Plan

(b) Water Flux

Figure 2.28: Water distribution map for the nozzle and ignition location in Experiment 8. The values in the bar graph represent the water flux collected in each bin, averaged over three replicates. The arrangement of the bins is shown by the floor plan, where Bin A1 corresponds to the ignition location.

2.6 Experimental Procedure

The test structure was first prepared with the instrumentation and fuel load described in Sections 2.2 and 2.3. The fire room door and front door were left open, and the fire room window was closed. At least 60 seconds of background data was collected to prior to ignition. The fires were started using an electric match placed on the seat cushion of the sofa, in the corner of the arm and back cushion (see Figure 2.29). The electric match consisted of 0.32 mm (28 gauge) nichrome wire coiled through the match heads of a standard matchbook. The matches were ignited remotely by activating a 24 volt power supply connected by extension cord to the nichrome wire. To increase the reliability of ignition and support the propensity for flame spread, a small cut in the fabric (about 15 cm (6 in.)) was made in the back cushion to expose the polyester batting.

The water spray was activated when the thermal conditions in the room triggered the tell-tale sprinkler equipped with a 68.3 °C (155 °F) rated sprinkler bulb. Water flow was initiated by manually opening a ball valve downstream of the pump. The pipe system between the valve and the nozzle was dry prior to this action, which delayed water reaching the nozzle. Combined with communication delay to manually open the valve, the times between the tell-tale sprinkler breaking and water flowing through the nozzle ranged between 5 s and 26 s, with an average of 11 s.

The flow rate was set to 23 lpm (6 gpm) in each experiment. Table 2.10 lists the pressures measured

Figure 2.29: Image of an example ignition setup.

at the water sprays. Water was discharged for 10 minutes to reflect the minimum sprinkler operation time required by the NFPA 13D standard [16]. After the water flow was turned off, the fire was observed for a brief period to evaluate its recovery. Then firefighters entered with a hoseline for final suppression. Photographs of the fire room were taken after the fire was extinguished.

Table 2.10: Summary of the pressures measured immediately upstream of the nozzles/sprinkler for each flow rate.

Water Spray	Water Flow Rate [lpm (gpm)]	Pressure [bar (psi)]
40W Nozzle	23 (6)	1.7 (24)
50W Nozzle	23 (6)	1.0 (15)
Sprinkler	30 (8)	0.3 (5)

Experiment 8 included a residential sprinkler in place of the low flow nozzle, and therefore followed a slightly adjusted procedure. The sprinkler included its own activation bulb, making the fire room tell-tale sprinkler unnecessary. The water line to the sprinkler was pressurized prior to

ignition and set to flow water at 30 lpm (8 gpm) – the minimum flow rate listed by the sprinkler manufacturer.

3 Results

Nine experiments were conducted in total, including eight experiments with a low flow nozzle and one with a residential sprinkler. Flashover was prevented in four of the experiments, including the experiment with a residential sprinkler. The fire size diminished after water flow activation and conditions remained steady for the remainder of the water flow duration. In the other five experiments the fire size was similarly reduced after water flow activation, but only for a limited duration until the fire recovered. These fires were able to burn from a protected location behind and underneath the sofa which allowed a second fire growth phase. Conditions in the fire room became untenable according to UL 199 criteria in each of these experiments. At approximately the same time as conditions became untenable, the second sprinkler in the hallway activated. Although flashover was prevented in these experiments, the activation of a second sprinkler makes this result inconclusive. In a completed system, the activation of the second sprinkler would reduce the water flow to the fire room, potentially leading to flashover.

Due to the similarities between experiments with each outcome, one experiment with a tenable outcome and one with an untenable outcome are described in the following sections. Data from the remaining experiments is provided in Appendix A.

3.1 Experiment 1A – Example of an Untenable Outcome

Experiment 1A is described here as an example experiment where conditions in the structure became untenable according to UL 199 criteria. Other experiments with the same outcome followed a similar pattern, differing mostly in timing and values for peak measurements. The configuration for this experiment is described in Section 2.5.1.

The fire was ignited in the sofa located in the back corner of the room (t = 0 s). Initial flame spread moved up the back cushion and across the arm of the sofa. The fire room tell-tale sprinkler activated at 140 s (2:20) after ignition, when the gas temperature at the sprinkler was 143 °C (290 °F). This was followed by initiating water flow to the nozzle at 166 s (2:46) (Figure 3.1). The water spray rapidly eliminated the flames that were visible on the sofa (Figure 3.2). It also caused mixing of the smoke layer that reduced visibility at all elevations in the fire room.

The fire was not extinguished, however, and began to regrow behind and beneath the sofa where it was protected from the water spray. From this protected position the fire began a second growth phase that substantially worsened conditions in the structure, and eventually triggered the hallway tell-tale sprinkler at 367 s (6:07) (Figure 3.3). According to UL 199 criteria, conditions in the fire room became untenable two seconds earlier (at 365 s (6:05)) when the gas temperature measured near the nozzle exceeded 316 °C (600 °F). The second growth phase peaked at around 400 s (6:40), then conditions became steady due to the water spray limiting further fire growth.

The total duration for water flow was ten minutes, ending at 772 s (12:52) after ignition. At that time the fire was still limited to the ignition corner, burning underneath the sofa arm and first seat cushion (Figure 3.4). Firefighter intervention began one minute later at 836 s (13:56) to extinguish the fire. The fire size increased during the one minute between deactivating the nozzle and firefighter suppression (Figure 3.5).

Figure 3.1: Standard and thermal imaging views of conditions in the fire room at nozzle activation, 166 s (2:46) after ignition, in Experiment 1A.

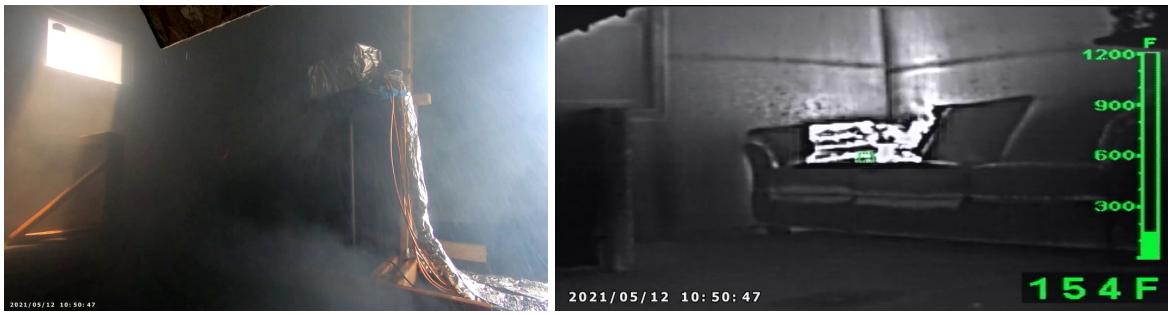

Figure 3.2: Standard and thermal imaging views of conditions in the fire room 30 s after nozzle activation (196 s (3:16) after ignition) in Experiment 1A.

Figure 3.3: Standard and thermal imaging views of conditions in the fire room at time of hallway tell-tale sprinkler activation, 367 s (6:07) after ignition, in Experiment 1A.

Figure 3.4: Standard and thermal imaging views of conditions in the fire room at end of water flow duration, 772 s (12:52) after ignition, in Experiment 1A.

Figure 3.5: Standard and thermal imaging views of conditions in the fire room at start of suppression, 836 s (13:56) after ignition, in Experiment 1A.

Figure 3.6 shows post-test photos of the fire room and sofa. Burn patterns on the walls show damage in the ignition corner that reflect the fire plume. Soot deposition on the upper half of the walls indicates the boundary between the smoke layer and spray pattern of the nozzle. The fire consumed the fabric and foam in the left arm, left seat cushion, and left two back cushions of the sofa. The wood structure underlying those parts of the sofa remained, but was partially burned through and heavily charred. There was no visible fire damage to the right half of the sofa due to the surfaces of the fuel being pre-wet by the water spray. Damage to the carpet shows where burning occurred beneath the left seat cushion of the sofa. Some of the unburned carpet beneath the sofa appears dry, demonstrating the ability of the sofa to protect fuels from the water spray. The simulated chair side was undamaged.

Figure 3.6: Post-test pictures of the fire room in Experiment 1A.

The time histories of the fire room temperatures are presented in Figure 3.7. Temperatures near the ceiling began increasing by 1 minute after ignition. A smoke layer formed in the fire room and began descending, elevating temperatures within 0.9 m (3 ft) of the ceiling. When the nozzle was activated at 166 s (2:46), temperatures within 0.9 m (3 ft) of the ceiling ranged between 65 °C (150 °F) and 110 °C (225 °F). Fire room temperatures initially decreased in response to the water spray, and reached below 40 °C (100 °F) at all elevations by 250 s (4:10). The temperatures were increasing again by 300 s (5:00) in response to the second growth phase of the fire. At about 390 s (6:30) the fire room temperatures reached a peak that ranged between 285 °C (546 °F) and 315 °C (600 °F) at elevations within 0.6 m (2 ft) of the ceiling. The temperature 0.9 m (3 ft) below the ceiling increased to 143 °C (290 °F), and temperatures at lower elevations remained below 93 °C (200 °F). After this peak the fire room temperatures became steady: temperatures

within 0.6 m (2 ft) of the ceiling ranged between 115 °C (240 °F) and 235 °C (455 °F) while temperatures at lower elevations remained below 65 °C (150 °F). These conditions continued for the remaining duration of water flow, which ended at 772 s (12:52). Immediately following water off, temperatures within 1.2 m (4 ft) of the ceiling increased. Manual suppression began one minute later at 836 s (13:56), at which time those temperatures ranged between 105 °C (225 °F) and 300 °C (570 °F).

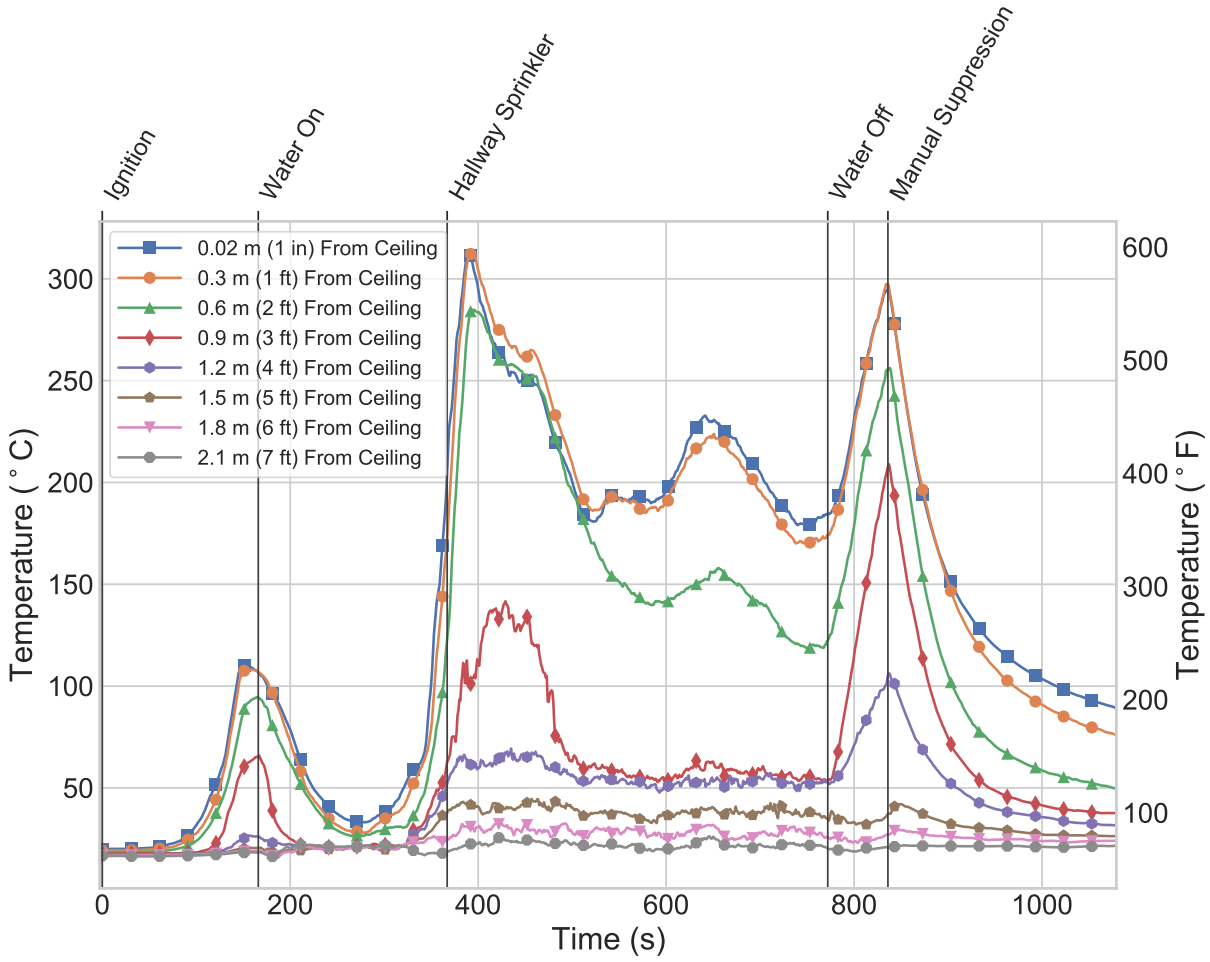

Figure 3.7: Fire room (Position 1) temperatures for Experiment 1A.

The temperatures measured in the hallway showed a similar response to those measured in the fire room, but with lower peaks (see Figure 3.8). Both locations had three temperatures peaks which correspond to the fire growth prior to nozzle activation, the second fire growth phase during water flow, and the fire recovery after water flow ended. At the time of nozzle activation, 166 s (2:46) after ignition, the peak hallway temperature was 75 °C (170 °C), measured 2.5 cm (1 in.) below the ceiling at Position 3. During the second fire growth phase the hallway temperature peaked at 370 °C (700 °F), measured 2.5 cm (1 in.) below the ceiling at Position 2. The temperatures within 0.9 m (3 ft) of the ceiling then remained elevated and steady, ranging between 30 °C (85 °F)

and 130 °C (270 °F). Temperatures at the 1.6 m (4 ft) elevation and below remained below 65 °C (150 °F) for the entire experiment.

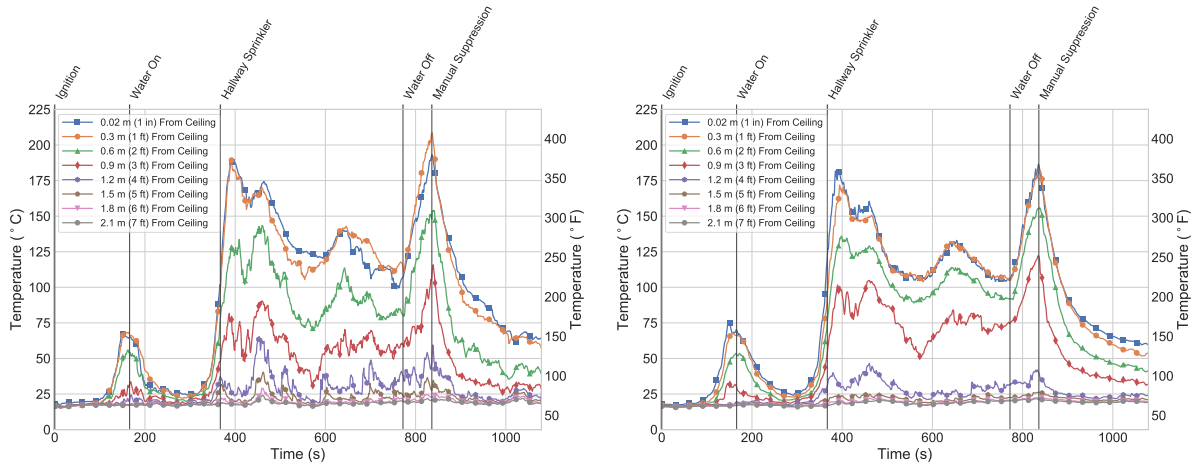

(a) Front Door End of the Hallway (Position 2)

(b) Closed End of the Hallway (Position 3)

Figure 3.8: Hallway temperatures for Experiment 1A.

Gas concentrations were measured at 0.9 m (3 ft) and 1.5 m (5 ft) above the floor at Positions 1 (fire room) and 3 (hallway) (see Figure 3.9). The gas concentrations 1.5 m (5 ft) above the floor responded similarly to the temperature measurements with peak values occurring near the same times. At nozzle activation, the 1.5 m (5 ft) gas concentrations reached peaks of 19.7% O_2 and 1.3% CO_2 in the fire room and 20.3% O_2 and 0.6% CO_2 in the hallway (CO concentration was negligible at both locations). A second peak occurred at about 420 s (7:00) in response to the second growth phase of the fire. Peak gas concentrations of 12.1% O_2, 8.2% CO_2, and 0.32% CO were measured in the fire room and 14.9% O_2, 5.7% CO_2, and 0.22% CO in the hallway. Gas concentrations at the 0.9 m (3 ft) elevation showed a smaller response. For the entire experiment, peak values at the 0.9 m (3 ft) level in the fire room were 19.7% O_2, 1.1% CO_2, and 0.05% CO. In the hallway, the peak 0.9 m (3 ft) gas concentrations were 20.6% O_2, 0.4% CO_2, and 0.014% CO in the hallway.

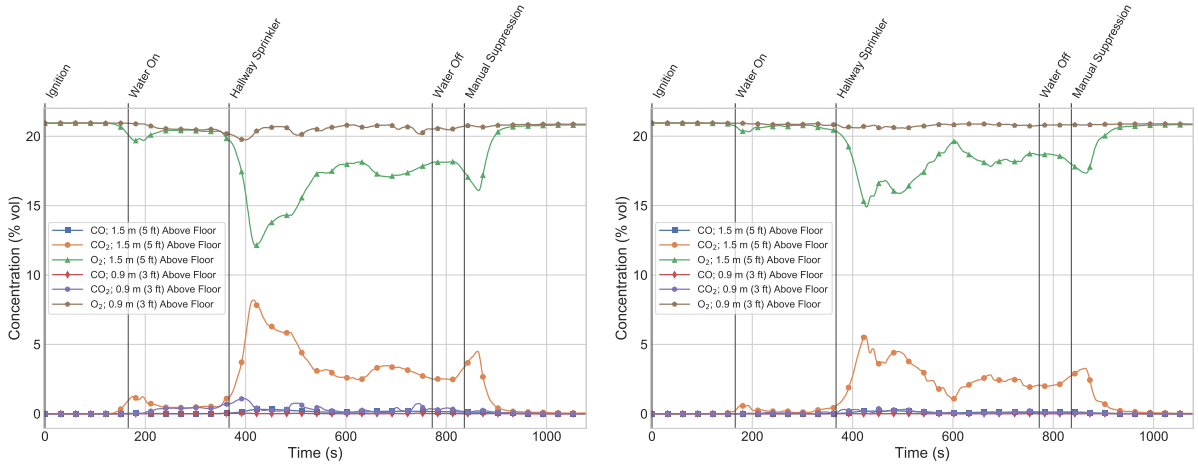

(a) Fire Room (Position 1)

(b) Hallway (Position 3)

Figure 3.9: Gas concentration measurements for Experiment 1A.

Heat flux was measured at 0.9 m (3 ft) above the floor in the fire room (Position 1) (Figure 3.10). One heat flux gauge was oriented vertically to look at the ceiling, and the other was oriented horizontally to look at the ignition corner. Both heat flux measurements increased prior to water activation and reach peaks of 1.4 kW/m^2 measured horizontally and 0.4 kW/m^2 measured vertically. The heat flux measurements decreased prior to water on, starting at 142 s (2:22). This resulted from the polyester batting in the back cushion breaking through the burning fabric and spilling forward onto the fire, which briefly smothered the flames.

Water droplets from the nozzle directly impacted the heat flux gauges which is apparent in the data as increased signal noise. It is also likely that the presence of water on the surface of the gauges biased the measurements towards lower values. Regardless, the heat flux measurements increased during the second fire growth phase and reached peaks of about 6 kW/m^2 measured horizontally and 3 kW/m^2 measured vertically. The signal noise and heat flux magnitudes decreased immediately after water flow ended. Note that there was likely water remaining on the surface of the gauges that impacted the measurements. After water flow ended, the heat flux measured by both gauges was between 1.0 kW/m^2 and 1.5 kW/m^2. These values increased in to response to the fire recovery and reached peaks of 4 kW/m^2 measured horizontally and 2 kW/m^2 measured vertically.

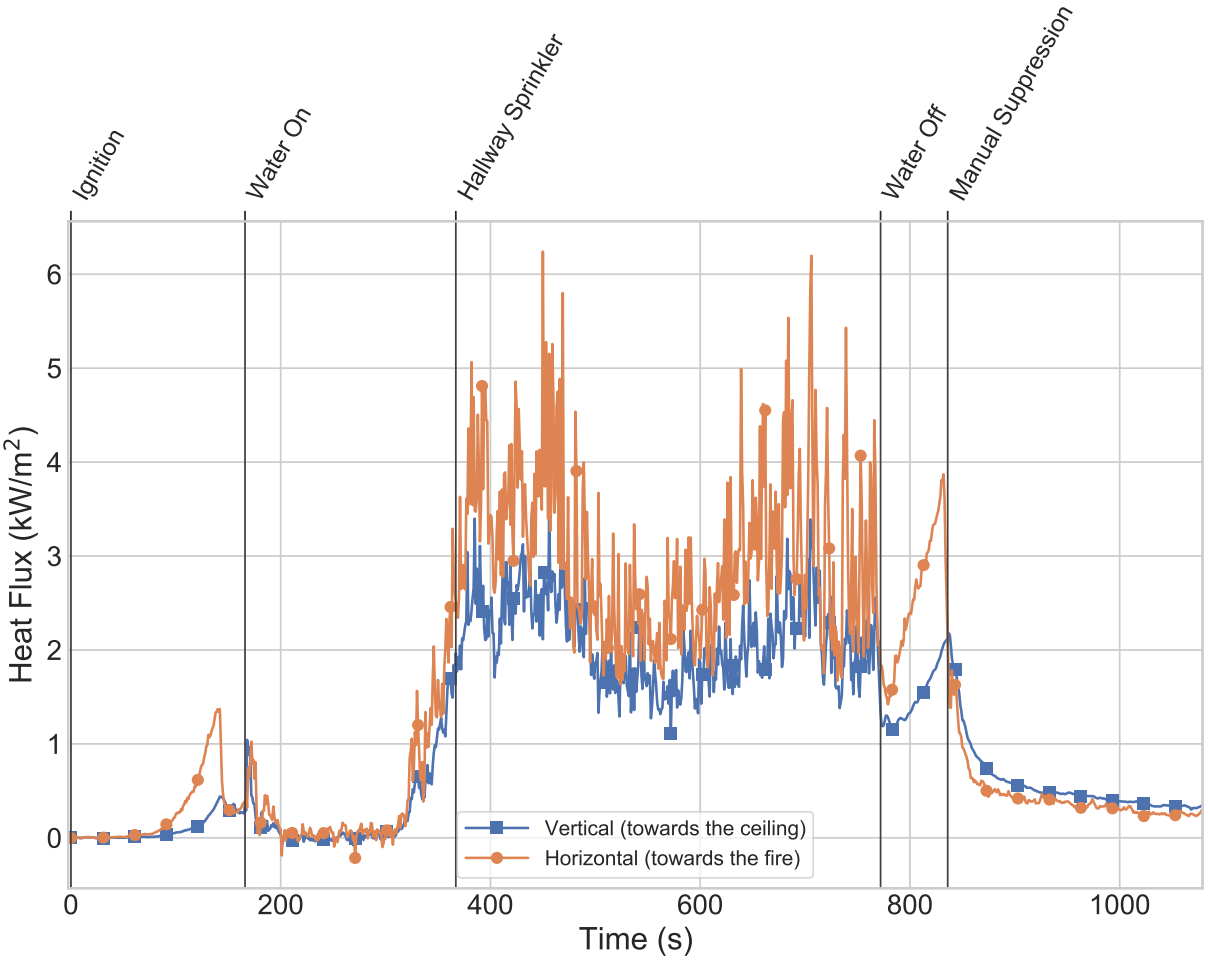

Figure 3.10: Heat flux measurements 0.9 m (3 ft) above the floor in the fire room (Position 1) for Experiment 1A.

3.2 Experiment 5 – Example of a Tenable Outcome

Experiment 5 is described here as an example experiment where conditions in the structure remained tenable according to UL 199 criteria. Other experiments with the same outcome followed a similar pattern. The configuration for this experiment is described in Section 2.5.5.

The fire was ignited in the sofa located in the back corner of the room, shifted 0.3 m (1 ft) away from the back wall (t = 0 s). Initial flame spread moved up and across the back cushion. The fire room tell-tale sprinkler activated at 117 s (1:57) after ignition, when the gas temperature at the sprinkler was 138 °C (280 °F). This was followed by initiating water flow to the nozzle at 126 s (2:46) (Figure 3.11). The water spray rapidly eliminated the flames that were visible on the sofa (Figure 3.12). The fire was not extinguished, but there was not any visible or measured growth for the duration of the water flow. The tell-tale sprinkler located in the hallway did not trigger during

the experiment.

The total duration for water flow was ten minutes, ending at 734 s (12:14) after ignition. The water spray had caused mixing of the smoke layer that reduced visibility at all elevations in the fire room. However, the thermal imaging view did not show any active flames (Figure 3.13). Over two minutes were observed to assess potential fire regrowth, resulting in flames reestablishing in the ignition corner (Figure 3.14). Firefighters entered and extinguished the fire with a hoseline at 874 s (14:34).

Figure 3.11: Standard and thermal imaging views of conditions in the fire room at nozzle activation, 126 s (2:06) after ignition, in Experiment 5.

Figure 3.12: Standard and thermal imaging views of conditions in the fire room 30 s after nozzle activation (156 s (2:36) after ignition) in Experiment 5.

Figure 3.13: Standard and thermal imaging views of conditions in the fire room at end of water flow duration, 734 s (12:14) after ignition, in Experiment 5.

Figure 3.14: Standard and thermal imaging views of conditions in the fire room at start of suppression, 874 s (14:34) after ignition, in Experiment 5.

Figure 3.15 shows post-test photos of the fire room and sofa. There was soot deposition on the wall behind the sofa resulting from the fire plume. Similarly, the tops of the walls and the ceiling had soot deposition resulting from the smoke layer. Neither the walls nor ceiling, however, had any thermal damage from the fire. Fire damage to the sofa included burning of the synthetic materials near the ignition location. There was almost no charring in any of the wood frame of the sofa. Horizontal flame spread was limited to less than half of both the seat cushion and the arm cushion. Instead, the fire had burned below the sofa and reached the carpet. In addition, most of the first back cushion and part of the second were consumed. The simulated chair side was undamaged.

Figure 3.15: Post-test pictures of the fire room in Experiment 5.

The time histories of the fire room temperatures are presented in Figure 3.7. A smoke layer formed in the fire room and began descending, elevating temperatures within 0.9 m (3 ft) of the ceiling. When the nozzle was activated at 126 s (2:04), temperatures within 0.9 m (3 ft) of the ceiling ranged between 65 °C (150 °F) and 90 °C (195 °F). Temperatures above 1.5 m (5 ft) from the ceiling continued increasing for about 20 s, then decreased. At one minute after water activation (186 s (3:06) after ignition), temperatures at all elevations were below 65 °C (150 °F). The temperatures continued decreasing during the ten minutes of water flow, reaching below 32 °C (90 °F) at all elevations. After water flow ended at 734 s (12:14), temperatures within 0.6 m (2 ft) of the ceiling increased until manual suppression extinguished the fire 140 s (2:20) later. Those temperatures reached peaks between 40 °C (105 °F) and 43 °C (110 °F).

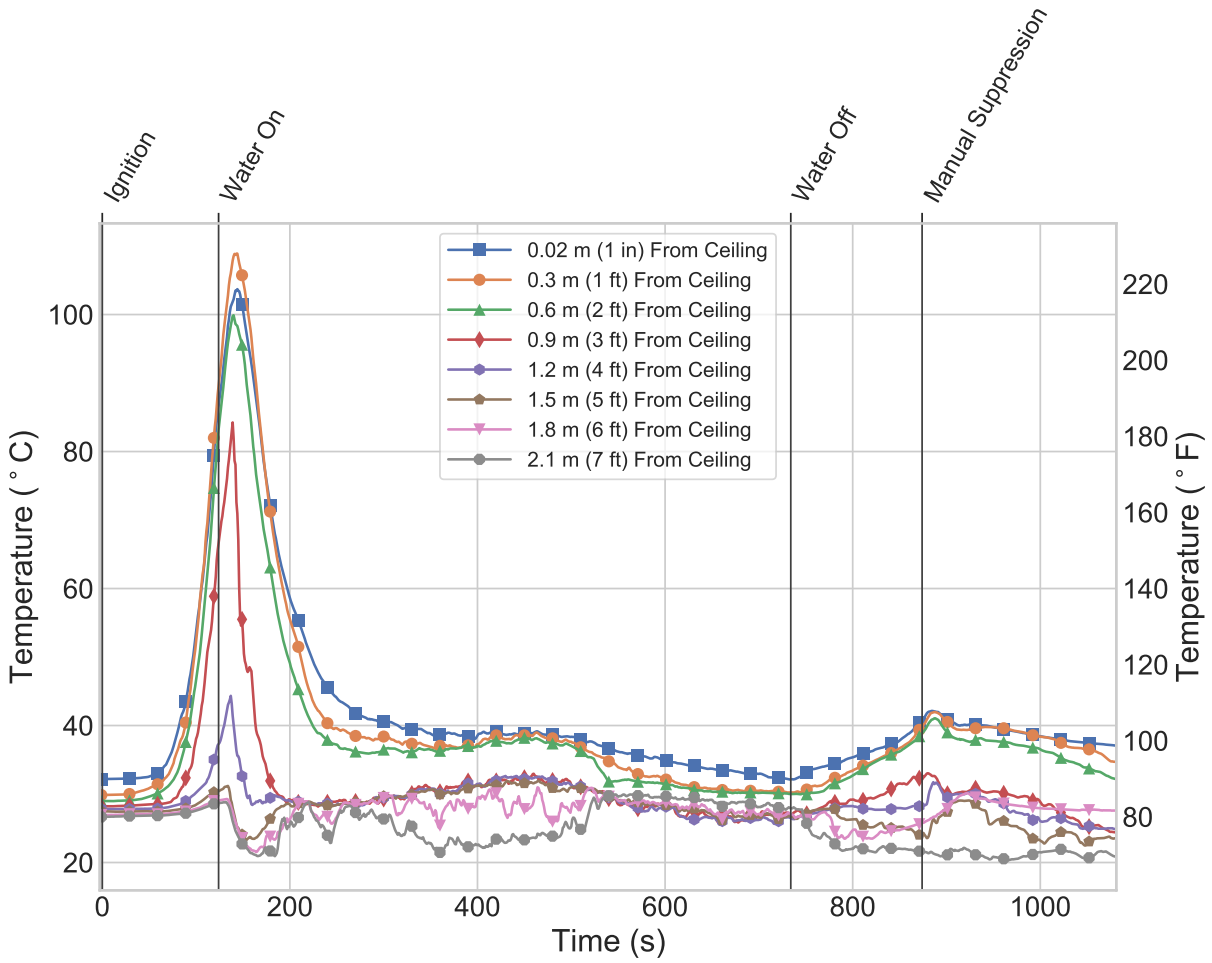

Figure 3.16: Fire room (Position 1) temperatures for Experiment 5.

The temperatures measured in the hallway showed a similar response to those measured in the fire room, but with lower peaks (see Figure 3.8). Temperatures within 0.9 m (3 ft) of the ceiling became elevated due to the descending smoke layer. These temperatures reached peaks within 20 s after nozzle activation, which ranged between 46 °C (115 °F) and 91 °C (196 °F). The temperatures then descended, reaching below 38 °C (100 °F) at all elevations by 255 s (4:15). The temperatures continued returning towards ambient conditions until water off at 734 s (12:14). The fire regrowth after water flow ended caused hallway temperatures to increase again, but they remained below 40 °C (104 °F). Temperatures at elevations below 0.9 m (3 ft) from the ceiling did not exceed 35 °C (95 °F) throughout the experiment.

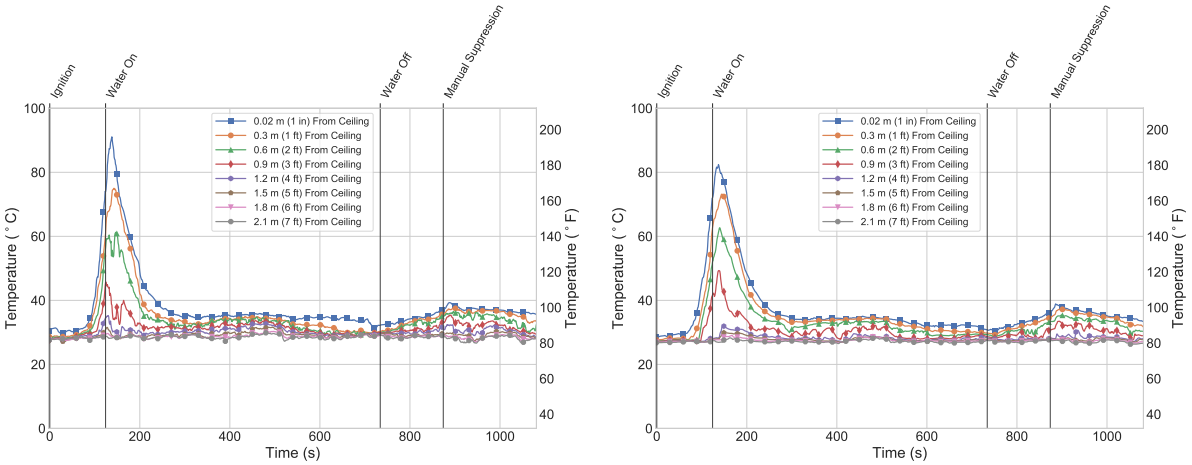

(a) Front Door End of the Hallway (Position 2)

(b) Closed End of the Hallway (Position 3)

Figure 3.17: Hallway temperatures for Experiment 1A.

Gas concentrations were measured at 0.9 m (3 ft) and 1.5 m (5 ft) above the floor at Positions 1 (fire room) and 3 (hallway) (see Figure 3.18). The gas concentrations at 1.5 m (5 ft) above the floor were the first to respond, and reached a peaks at 170 s (2:50), 44 s after nozzle activation. The peak values were 19.4% O_2, 1.4% CO_2, and 0.06% CO in the fire room and 20.2% O_2, 0.8% CO_2, and 0.05% CO in the hallway. The gas concentrations then improved in response to the reduced fire size, but did not return to ambient levels. The water spray caused mixing of the smoke layer that impacted gas concentrations at both the 1.5 m (5 ft) and 0.9 m (3 ft) elevations in the fire room. The fire room gas concentrations at both elevations remained in the following ranges until after the fire was extinguished: 20.1%–20.5% O_2, 0.4%–0.7% CO_2, 0.0%–0.1% CO. Similarly, gas concentrations at 1.5 m (5 ft) above the floor in the hallway fluctuated in the following ranges: 20.4%–20.9% O_2, 0.0%–0.5% CO_2, 0.0%–0.1% CO. Gas concentrations at 0.9 m (3 ft) above the floor in the hallway were the least affected, reaching peak values of 20.7% O_2, 0.1% CO_2, and 0.01% CO.

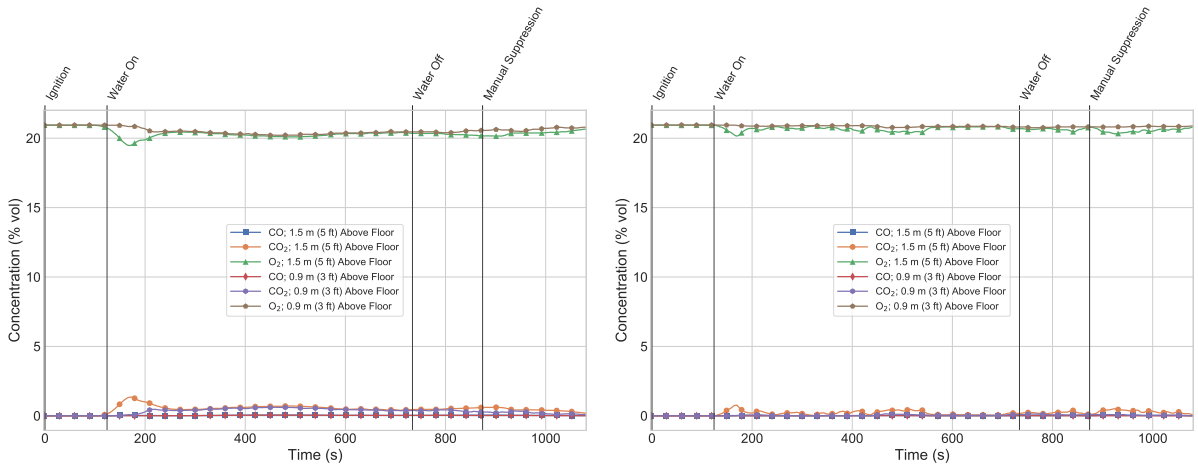

(a) Fire Room (Position 1)

(b) Hallway (Position 3)

Figure 3.18: Gas concentration measurements for Experiment 5.

Heat flux was measured at 0.9 m (3 ft) above the floor in the fire room (Position 1) (Figure 3.19). One heat flux gauge was oriented vertically to look at the ceiling, and the other was oriented horizontally to look at the ignition corner. Both heat flux measurements increased prior to water activation and reach peaks of 1.8 kW/m^2 measured horizontally and 0.5 kW/m^2 measured vertically. Water droplets from the nozzle directly impacted the heat flux gauges which is apparent in the data as increased signal noise. It is also likely that the presence of water on the surface of the gauges biased the measurements towards lower values. Both heat flux measurements decreased after nozzle activation and remained below 1 kW/m^2 for the rest of the experiment.

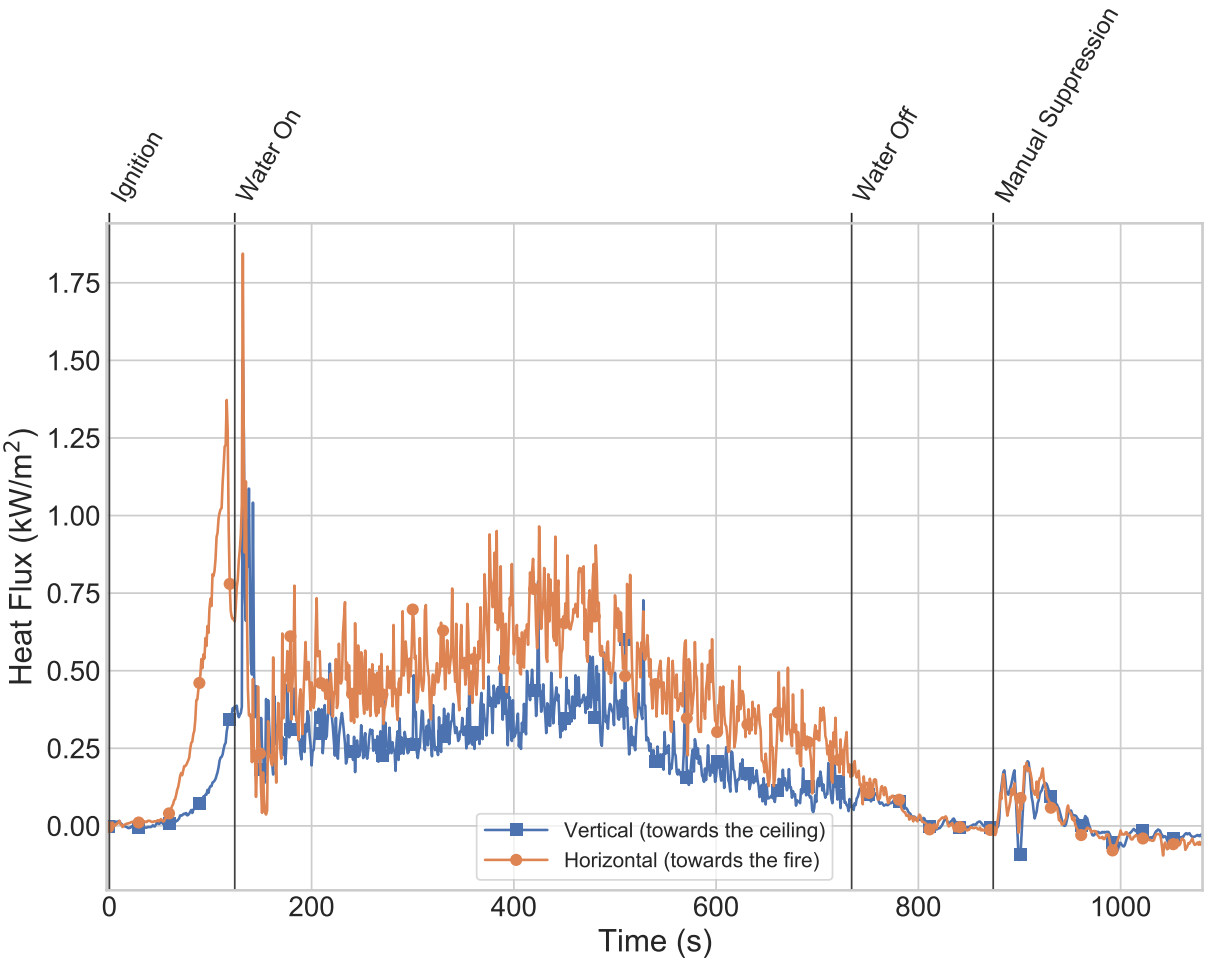

Figure 3.19: Heat flux measurements 0.9 m (3 ft) above the floor in the fire room (Position 1) for Experiment 5.

3.3 Summary

Of the 9 experiments conducted, 5 experiments resulted in untenable conditions according to UL 199 criteria. The criteria that provided the earliest and most consistent indication for untenability was when the temperature measured at the water spray exceeded 316 °C (600 °F). The temperature at the water spray from each experiment is presented in Figure 3.20. Due to variability in the initial fire growth, the time histories are shifted to begin at water spray activation. For the experiments that remained tenable, the temperatures at the water spray were closely aligned. The temperatures increased to between 100 °C (212 °F) and 200 °C (392 °F) prior to water spray activation, then decreased to below 100 °C (212 °F) for the remainder of the experiments. The experiments where conditions became untenable were more varied in terms of the times until untenable and the peak temperatures.

The patterns shown by the temperatures at the water spray are consistent with the other measurements in the structure. When conditions in the fire room exceeded UL 199 tenability criteria, conditions in the hallway also became untenable. However, the times until untenable were longer and the peak temperatures were lower than in the fire room.

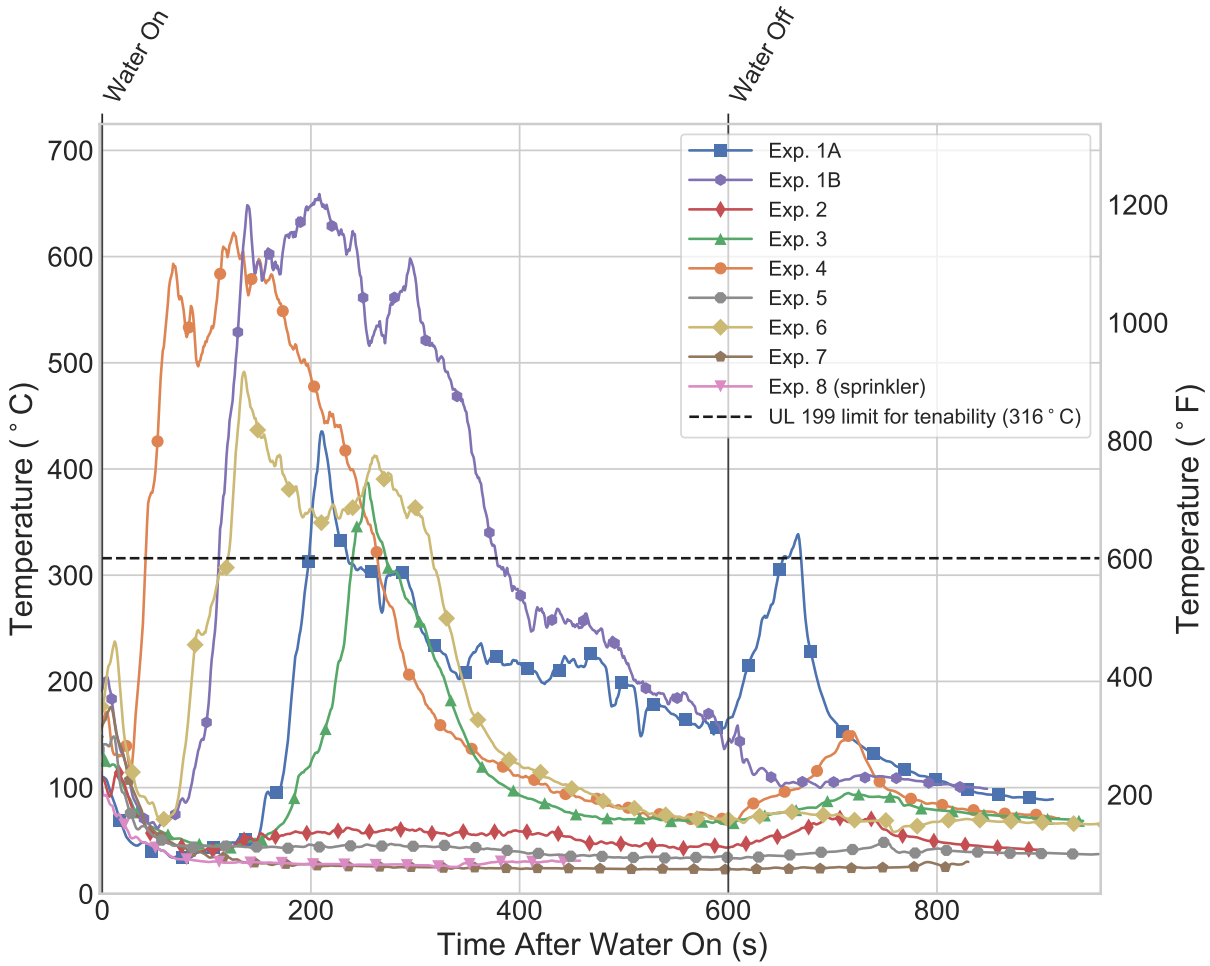

Figure 3.20: Comparison of the temperature time histories measured at the water spray for each experiment. The experiment times are shifted so that t = 0 s corresponds to the water spray activation. The UL 199 limit for tenability, 316 °C (600 °F), is included for reference.

The peak values measured in the fire room (Position 1) during water spray operation in each experiment are summarized in Table 3.1. For experiments where conditions remained tenable, all of the measurements are similar between experiments. Conditions were least severe in Experiment 8 where the residential sprinkler was used. However, the low flow nozzle experiments reached similar values and were substantially below the temperature limit for tenability. For experiments where conditions became untenable, there was relatively greater disparity between results. In particular, Experiments 1B and 4 reached dramatically worse conditions than the other experiments according to every measurement.

Table 3.1: Summary of peak values measured in the fire room (Position 1). The bounds defining water spray operation are between 30 seconds after activation and when the water spray was deactivated. The peak values for O_2 concentration are minimums and the other values are maximums. Temperature and gas concentrations were measured 1.5 m (5 ft) above the floor and heat flux was measured 0.9 m (3 ft) above the floor, looking at the ignition location.

Exp #	Water Flux at Ign. [mm/min (gpm/ft^2)]	Peak Measurements During Water Spray Operation Temp [°C (°F)]	HF [kW/m^2]	O_2 [%]	CO [%]	CO_2 [%]
Conditions exceeded UL 199 tenability criteria:						
1A	0.3 (0.008)	142 (288)	6.2	12.1	0.32	8.2
1B	0.3 (0.008)	358 (677)	17.2	2.4	2.71	15.6
3	0.5 (0.012)	89 (192)	4.2	12.2	0.24	7.8
4	0.8 (0.019)	347 (657)	13.3	5.2	1.51	13.4
6	1.4 (0.044)	75 (167)	5.3	10.3	0.41	9.6
Conditions remained tenable:						
2	0.4 (0.010)	34 (93)	0.7	19.6	0.03	1.2
5	0.9 (0.022)	49 (120)	1.0	19.5	0.06	1.4
7	1.8 (0.044)	55 (131)	0.8	19.2	0.05	1.6
8 (sprinkler)	1.8 (0.043)	36 (97)	0.3	20.0	0.02	0.8
UL 199 Tenability Criteria (measured 1.6 m (5.25 ft) above the floor)		93 (200)				
IDLH Values for 30 min Exposure					0.012	4.0

The times when conditions became untenable are summarized in Table 3.2. The times relative to water spray activation provide a better comparison between experiments due to the variability in activation times. The times for untenability were similar to the activation times of the hallway tell-tale sprinkler, which occurred within 16 s of the fire room conditions becoming untenable. Conversely, the hallway tell-tale sprinkler was not triggered in any experiment where conditions remained tenable. Had a second water spray been installed in the hallway to flow water, the flow rate through each water spray would have decreased when the second water spray activated. With a water supply limited to a total flow rate of 23 lpm (6 gpm), the flow rate through each water spray would be approximately 11 lpm (3 gpm). If this decrease in flow rate occurred during the fires, it is possible that conditions in the fire room would have become worse.

Table 3.2: Times relative to water spray activation when conditions exceeded UL 199 limits for tenability and when the hallway tell-tale sprinkler activated in each experiment.

Exp #	Water Flux at Ign. [mm/min (gpm/ft^2)]	Time after Water On (s)	
		Untenable	Hallway Sprinkler Activation
1A	0.3 (0.008)	199	201
1B	0.3 (0.008)	111	124
2	0.4 (0.010)	–	–
3	0.5 (0.012)	241	240
4	0.8 (0.019)	42	51
5	0.9 (0.022)	–	–
6	1.4 (0.035)	122	106
7	1.8 (0.044)	–	–
8 (sprinkler)	1.8 (0.043)	–	–

4 Discussion

Each experiment demonstrated one of two distinct patterns: 1) the water flow reduced the fire's size and maintained tenable conditions in the structure, or 2) the fire size was initially reduced by the water spray activation, but eventually began a second growth phase that caused conditions in the structure to become untenable and triggered the second sprinkler in the hallway. The water flux at the ignition location, however, was not a reliable predictor for these outcomes. Instead, the outcomes depended strongly on variability in the initial fire growth.

4.1 Activation Timing

The sprinkler (or tell-tale sprinklers) had activation temperatures of 68.3 °C (155 °F). Therefore, the timing for activating the sprinkler or nozzles depended on the initial growth rate of the fire. Table 4.1 summarizes the times and temperatures at which the sprinkler or tell-tale sprinklers activated. The temperature measurements reflect the gas temperature at the sprinkler, not the temperature of the sprinkler bulb. Due to the time required for heat to transfer to the bulb, the gas temperatures at activation are higher than the activation temperature of the bulb. The activation timing ranged between 113 s and 239 s after ignition. Therefore, comparisons between experiments are focused on timing relative to the activation times.

Table 4.1: Times and the associated gas temperatures when the fire room tell-tale sprinkler (or water pressurized sprinkler in Exp. 8) was triggered in each experiment. The averages and expanded uncertainties are included.

Exp #	Time [s]	Temperature [°C (°F)]
Conditions exceeded UL 199 tenability criteria:		
1A	140	147 (297)
1B	126	175 (347)
3	113	109 (228)
4	114	148 (298)
6	235	152 (306)
Conditions remained tenable:		
2	130	125 (257)
5	118	142 (288)
7	151	143 (289)
8 (sprinkler)	129	131 (268)
$\bar{x} \pm 2\sigma$	140 ± 76	141 ± 37 (286 ± 99)

Paragraph copied from Phase 1: Because the fire started from a small flaming source, such as you might have from ignition sources in a home (e.g. small overheated battery or a candle), the initial growth rate varied. While the sofa and small flaming ignition source provide a realistic scenario that could be found in many homes, it does exhibit variations in burning behavior typically within the first minute or two after ignition. The ignition device is placed on the seat cushion in a crevice formed by the side arm and the back cushion of the sofa. In some cases, the ignition flame may initially burn into the side of the sofa as opposed to the first flames extending up the back cushion of the sofa. The heat to activate the sprinkler must be transferred by the convective thermal plume/ceiling jet that is evolving, early in the fire, from the back cushion of the sofa. When heat is being lost to the arm of the sofa in the early seconds of the fire and delaying the flame spread on the back cushion, this has some impact on the activation time of the sprinkler.

Section 2.3 describes how other research has characterized the sofa in terms of HRR, which was shown to be a consistent fuel source. The results from that research, however, also includes variations in the timing of the initial fire growth. The value, *growth start time*, was defined as the first instance at which a temperature change of more than 5 °C (9 °F) over 10 seconds occurred in the hot gas layer (HGL) temperature or as the time when the HGL temperature exceeded 15 °C (27 °C) above the ambient temperature – whichever occurred first. Of the seven experiments conducted, including three different ignition locations, the growth start time ranged between 107 s and 236 s, with an average and expanded uncertainty of 150 ± 104 s [15]. This variance is similar to the variance in times when the tell-tale sprinkler was triggered.

It is necessary to determine whether the fire size at water spray activation was similar between experiments. Due to its proximity to the fire, the temperature measured at the tell-tale sprinkler is the most sensitive indicator for fire size. There was not a statistically significant difference between the temperatures at water spray activation for the experiments with tenable outcomes versus untenable outcomes (two-sample t-test, p-value = 0.39). The failure to find statistical significance suggests that the fire size at the time of water spray activation was similar between experiments. However, it does not preclude the possibility that differences in fire size at water spray activation affected the outcomes. In particular, the failure to find statistical significance could be a result of insufficient statistical power due to the small sample size.

4.2 Repeatability

The following sections describe one-to-one comparisons between experiments based on camera views of the fires. These comparisons show how differences in the initial fire growth impacted the outcome, independent of the water spray.

Experiments 1A and 1B

Experiments 1A and 1B were replicate configurations, but Experiment 1B resulted in peak temperature and heat flux measurements that were more than double the values in Experiment 1A (Table 3.1). The difference is also apparent visually, as shown by Figure 4.1. The times for the images correspond to when the fires reached peak sizes according to the heat flux measurements.

(a) Experiment 1A, 450 s (7:30) after ignition, 284 s (4:44) after water on

(b) Experiment 1B, 457 s (7:37) after ignition, 314 s (5:14) after water on

Figure 4.1: Standard and thermal imaging views of peak conditions in the fire room in Experiments 1A and 1B. The times of each image correspond to when the heat flux measurements looking at the fires reached maximums.

The difference between the results of Experiments 1A and 1B is primarily a result of differences in the initial fire growth. This is made apparent by Figure 4.2 which shows camera views of both fires immediately prior to nozzle activation. The fire in Experiment 1B is noticeably larger than in Experiment 1A. This difference is substantiated by the nozzle temperature at activation: 147 °C (297 °F) in Experiment 1A and 175 °C (347 °F) in Experiment 1B.

(a) Experiment 1A at nozzle activation, 166 s (2:46) after ignition

(b) Experiment 1B at nozzle activation, 143 s (2:19) after ignition

Figure 4.2: Standard and thermal imaging views of conditions in the fire room immediately prior to nozzle activation in Experiments 1A and 1B.

Experiments 2 and 6

The water flux at the ignition location was more than three times greater in Experiment 6 than in Experiment 2 – 1.4 mm/min (0.035 gpm/ft^2) versus 0.4 mm/min (0.008 gpm/ft^2), respectively. Yet, Experiment 6 resulted in untenable conditions while Experiment 2 resulted in a small, controlled fire. The experiments were conducted in the same room and with the same nozzle. The difference in water flux was only a result of changing the ignition location to achieve different nozzle-to-ignition distances. The factor responsible for the outcomes of these experiments was the direction of the initial fire growth – a result of random variation.

Figure 4.3 shows images of the fires in each experiment one minute prior to nozzle activation. The fire in Experiment 2 spread across a larger surface area relative to the fire in Experiment 6, and over a shorter period of time. The fire in Experiment 6 developed slowly, and remained concentrated in the crevice between the back cushion and the arm of the sofa. It dug deeper in the seat cushion rather than spreading across the surface of the back cushion. This resulted in the conditions shown in Figure 4.4 which presents images of the fire rooms one minute after nozzle activation. In Experiment 6, the fire moved behind and below the sofa to a shielded position, evident in Figure 4.4b as an orange glow below the sofa. From this position, the fire was able to grow uninhibited by the water spray for a period of time. Figure 4.4a shows that the fire in Experiment 2 was only

visible near the top of the back cushion, where the water flux was lowest. Those flames eventually diminish since there is there is no path for growth. This comparison demonstrates how the initial fire growth can have a greater affect on the outcome than the water distribution.

(a) Experiment 2, 76 s (1:16) after ignition (b) Experiment 6, 183 s (3:03) after ignition

Figure 4.3: Camera views of conditions in the fire room 60 s (1:00) prior to nozzle activation in Experiments 2 and 6.

(a) Experiment 2, 196 s (3:16) after ignition (b) Experiment 6, 303 s (5:03) after ignition

Figure 4.4: Camera views of conditions in the fire room 60 s (1:00) after nozzle activation in Experiments 2 and 6.

4.3 Minimum Water Flux for Success

The metric for success used to analyze the results of this study has been the UL 199 criteria for tenability. This method divides the experiments in a way that reflects distinct patterns in the results. A more relevant metric is whether or not the compartment transitioned to flashover. Unfortunately, this metric cannot be applied to these experiments. When conditions in an experiment became untenable, the tell-tale sprinkler located in the hallway triggered at approximately the same time. If the water spray system had been "real", then water would have begun flowing through a second nozzle in the hallway, thereby reducing the flow rate through the fire room nozzle. With a water

supply limited to a total flow rate of 23 lpm (6 gpm), the flow rate through each nozzle would be approximately 11 lpm (3 gpm). It cannot be determined whether the reduced water flow would have prevented flashover. However, the low flow nozzles delayed fire growth in every experiment. Following water spray activation, conditions in both the fire room and the hallway improved according to every measurement.

Using UL 199 tenability criteria as the metric for success, the minimum water flux capable of maintaining tenability was 0.4 mm/min (0.010 gpm/ft^2), as demonstrated by Experiment 2. However, three experiments with greater water flux, as much as 1.4 mm/min (0.0035 gpm/ft^2), resulted in untenable conditions. Therefore, a water flux greater than 1.4 mm/min (0.0035 gpm/ft^2) was necessary to reliably maintain tenability.

The amount of time until conditions became untenable can also be used to evaluate success. The water spray delayed fire growth in every experiment, however there was no clear relationship between time until untenable and water flux. This is most apparent by comparing the experiments with the longest and shortest times until untenable (Table 3.2). The longest time (241 s (4:01) after nozzle activation) occurred in Experiment 3 with a water flux of 0.5 mm/min (0.012 gpm/ft^2), and the shortest time (42 s after nozzle activation) occurred in Experiment 4 which had a slightly greater water flux, 0.8 mm/min (0.019 gpm/ft^2). Since increasing the water flux did not consistently increase the time until untenable, it is unclear how much water is necessary.

Experiment 8 showed that an NFPA 13D sprinkler system was the most successful in terms of peak values during operation and preventing fire regrowth after water flow ended. NFPA 13D lists the minimum average water flux for a sprinkler system as 2.0 mm/min (0.05 gpm/ft^2) or the sprinkler rating, whichever is greater. The average water flux refers to the distribution over the entire compartment, in contrast to the water flux applied to the ignition location which was the focus in this study. The nozzle experiments used a flow rate of 23 lpm (6 gpm) in 11.7 m^2 (126 ft^2) and 13.4 m^2 (144 ft^2) rooms, corresponding to average water flux values of 1.9 mm/min (0.048 gpm/ft^2) and 1.7 mm/min (0.042 gpm/ft^2), respectively. The sprinkler used in Experiment 8 was rated for a minimum flow rate of 30 lpm (8 gpm) which corresponds to an average water flux of 2.3 mm/min (0.056 gpm/ft^2). The success of the sprinkler in Experiment 8 compared with the uneven suppression performance of the nozzles supports the minimum water flux listed in NFPA 13D.

The search for a minimum water flux for suppression has been made by other researchers using different approaches. Tamanini tested the performance of full cone nozzles to suppress wood crib fires [17]. Four nozzles at 90° were oriented horizontally towards a wood crib, and the water application rate was varied. A critical rate of water application was determined, below which there was complete loss of the structure. The critical values are 0.090 mm/min (0.0022 gpm/ft^2) for openly packed cribs and 0.180 mm/min (0.0044 gpm/ft^2) for densely packed cribs. It is unsurprising that Tamanini's values are much lower than found in this study when considering the more efficient water application and the easier challenge of wood crib fires compared to compartment fires with real furnishings. However, the two-fold difference between the critical application rates for openly packed and densely packed cribs demonstrates how sensitive the critical water application rate is to changes in fire challenge.

Tamanini noted a behavior related to large cribs with low burn times prior to water application. For water application rates above the critical value, the flame was extinguished quickly. And for water application rates below the critical value, the water had little effect and the fire grew to almost free-burn levels. This behavior appears similar to the divergent outcomes observed in this study. The fires were either quickly controlled, or developed a second growth phase that grew well above the limits for tenability – there was nothing in between. This behavior supports the existence of a critical water application rate for these fire scenarios. In these experiments, once the burning fuel was shielded from the water spray, the reduced water flow from the nozzles could not stop the regrowth of the fire which led to untenable conditions in the fire room. In an actual multi-nozzle system, the regrowth would have led to additional nozzles activating which would reduce the water flow rate in the fire room and potentially lead to flashover.

5 Research Needs

There are several components of this study that could be improved upon in future research efforts. Smaller water collection pans would improve the resolution of the spray density measurements. A fully functional prototype flashover prevention system would eliminate the need for manual water activations based on a tell-tale sprinkler activation, and would allow for multiple points of automatic activation through out the structure.

If this concept is accepatable in terms of flashover delay versus prevention, then additional challenges related to nozzle design would need to be addressed. Primarily, the nozzle would need to be thermally activated. Additional concerns such as nozzle clogging could be an issue as the nozzle diameters may be smaller than than those found in current residential sprinkler designs.

6 Summary

The purpose of this study was to investigate the feasibility of a residential flashover prevention system with reduced water flow requirements relative to a residential sprinkler system designed to meet NFPA 13D requirements. The flashover prevention system would be designed for retrofit applications where water supplies are limited. In addition to examining the water spray's impact on fire growth, this study utilized thermal tenability criteria as defined in UL 199, Standard for Automatic Sprinklers for Fire-Protection Service. The strategy investigated was to use full cone spray nozzles that would discharge water low in the fire room and directly onto burning surfaces of the contents in the room. Where as current sprinkler design discharges water in a manner that cools the hot gas layer, wets the walls and wets the surface of the contents in the fire room.

A series of fire experiments were conducted in which the water flux at the ignition location was varied, but the flow rate was consistent at 23 lpm (6 gpm). The water flux was adjusted by changes in room size, ignition location, and nozzle type. The water flux at the ignition location varied between 0.3 mm/min (0.008 gpm/ft^2) and 1.8 mm/min (0.044 gpm/ft^2) among eight experiments. In three experiments the water spray from the nozzle quickly reduced the fire's size and maintained tenable conditions in the structure. In the remaining five experiments, the fire size was initially reduced, but eventually began a second growth phase that caused conditions in the fire room to become untenable. The relationship between water flux and tenability was not consistent. Untenable conditions occurred with water flux up to 1.4 mm/min (0.0035 gpm/ft^2) while tenable conditions were maintained with water flux as low as 0.4 mm/min (0.010 gpm/ft^2).

At approximately the same time as the untenability criteria were reached, the second sprinkler in the hallway activated. In a completed system, the activation of the second sprinkler would reduce the water flow to the fire room, which would potentially lead to flashover. Natural variations in the burning behavior of the sofa resulted in shielded fires which led to the loss of effectiveness of the reduced flow solid cone water sprays. As a result of these variations, a correlation between discharge density at the lower water flows could not be determined given the limited number of experiments.

These experiments only concluded that the water spray system reliably delayed fire growth. This delay was quantified as the time until conditions became untenable or when the second sprinkler would have activated, and ranged between 42 s and 241 s among the experiments that became untenable. The tenability criteria surpassed in the cases where fire regrowth occurred was a temperature of 93 ^{o}C (200 ^{o}F) at 1.6 m (5.25 ft) above the floor in the fire room.

An additional experiment was conducted with an NFPA 13D sprinkler system flowing 30 lpm (8 gpm). The sprinkler was more effective than the lower flow nozzles in terms of limiting peak temperatures during operation and preventing fire regrowth after water flow ended. This study supports the minimum minimum discharge water flux listed in NFPA 13D.

An additional experiment using a UL listed residential sprinkler designed for flowing 30 lpm (8

gpm). The sprinkler demonstrated more effective suppression than any of the experiments with a nozzle. The success of the sprinkler compared with the unreliable suppression performance of the lower flow nozzles supports the minimum discharge density requirements of 2 mm/min (0.05 gpm/ft^2) from NFPA 13D. The low flow nozzle system tested in this study reliably delayed fire growth, but would not reliably prevent flashover.

References

[1] National Fire Protection Association, Quincy, Massachusetts. *NFPA 13D, Standard for the Installation of Sprinkler Systems in One- and Two-Family Dwellings and Manufactured Homes*, 2022.

[2] M. Ahrens. U.S. Experience with Sprinklers. Report, National Fire Protection Agency (NFPA), July 2017. https://www.nfpa.org/-/media/Files/News-and-Research/Fire-statistics-and-reports/Suppression/ossprinklers.pdf.

[3] J. Rudden. Number of housing units in the United States from 1975 to 2018. *Statista*, July 2019. https://www.statista.com/statistics/240267/number-of-housing-units-in-the-united-states/.

[4] Home Fire Sprinkler Coalition. Retrofitting a House with Fire Sprinklers. https://homefiresprinkler.org/retrofitting-fire-sprinklers-video/. [Online; accessed 23-April-2020].

[5] R.P. Fleming and D. Madrzykowski. *NFPA Fire Protection Handbook*, chapter Residential Sprinkler Systems. National Fire Protection Association, Quincy, Massachusetts, 20th edition, 2008.

[6] Underwriters Laboratories, Northbrook, Illinois. *UL 199, Standard for Automatic Sprinklers for Fire-Protection Service*, April 2020.

[7] NIOSH. Current Intelligence Bulletin 66: Derivation of Immediately Dangerous to Life or Health (IDLH) Values. US Department of Health and Human Services, Centers for Disease Control and Prevention, National Institute for Occupational Safety and Health, DHHS (NIOSH), Cincinnati, OH, 2013.

[8] L.G. Blevins. Behavior of bare and aspirated thermocouples in compartment fires. In *National Heat Transfer Conference, 33rd Proceedings*, pages 15–17, 1999.

[9] W.M. Pitts, E. Braun, R. Peacock, H. Mitler, E. Johnson, P. Reneke, and L.G. Blevins. Temperature uncertainties for bare-bead and aspirated thermocouple measurements in fire environments. *ASTM Special Technical Publication*, 1427:3–15, 2003.

[10] W.M. Pitts, A.V. Murthy, J.L. de Ris, J. Filtz, K. Nygård, D. Smith, and I. Wetterlund. Round robin study of total heat flux gauge calibration at fire laboratories. *Fire Safety Journal*, 41(6):459–475, 2006.

[11] M. Bundy, A. Hamins, E.L. Johnsson, S.C. Kim, G.H. Ko, and D.B. Lenhart. Measurements of Heat and Combustion Products in Reduced-Scale Ventilated-Limited Compartment Fires. NIST Technical Note 1483, National Institute of Standards and Technology, Gaithersburg, MD, 2007.

[12] A. Lock, M. Bundy, E.L. Johnsson, A. Hamins, G.H. Ko, C. Hwang, P. Fuss, and R. Harris. Experimental study of the effects of fuel type, fuel distribution, and vent size on full-scale underventilated compartment fires in an ISO 9705 room. NIST Technical Note 1603, National Institute of Standards and Technology, Gaithersburg, MD, 2008.

[13] Great Plains Industries, Inc., Wichita, KS. *TM Series Electronic Water Meters Owner's Manual*, 2015.

[14] Ohaus Corporation, Pine Brook, New Jersey. *Manual for ES Series Bench Scale*, 2002.

[15] J. Willi, D. Madrzykowski, and M. McKinnon. Repeatability of Thermal Measurements in Furniture-Fueled Compartment Fires. Technical report, UL Firefighter Safety Research Institute, Columbia, Maryland, July 2021.

[16] National Fire Protection Association, Quincy, Massachusetts. *NFPA 13, Standard for the Installation of Sprinkler Systems*, 2019.

[17] F. Tamanini. The application of water sprays to the extinguishment of crib fires. *Combustion Science and Technology*, 14(1-3):17–23, 1976.

Appendix A Experiment Results

A.1 Experiment 1B

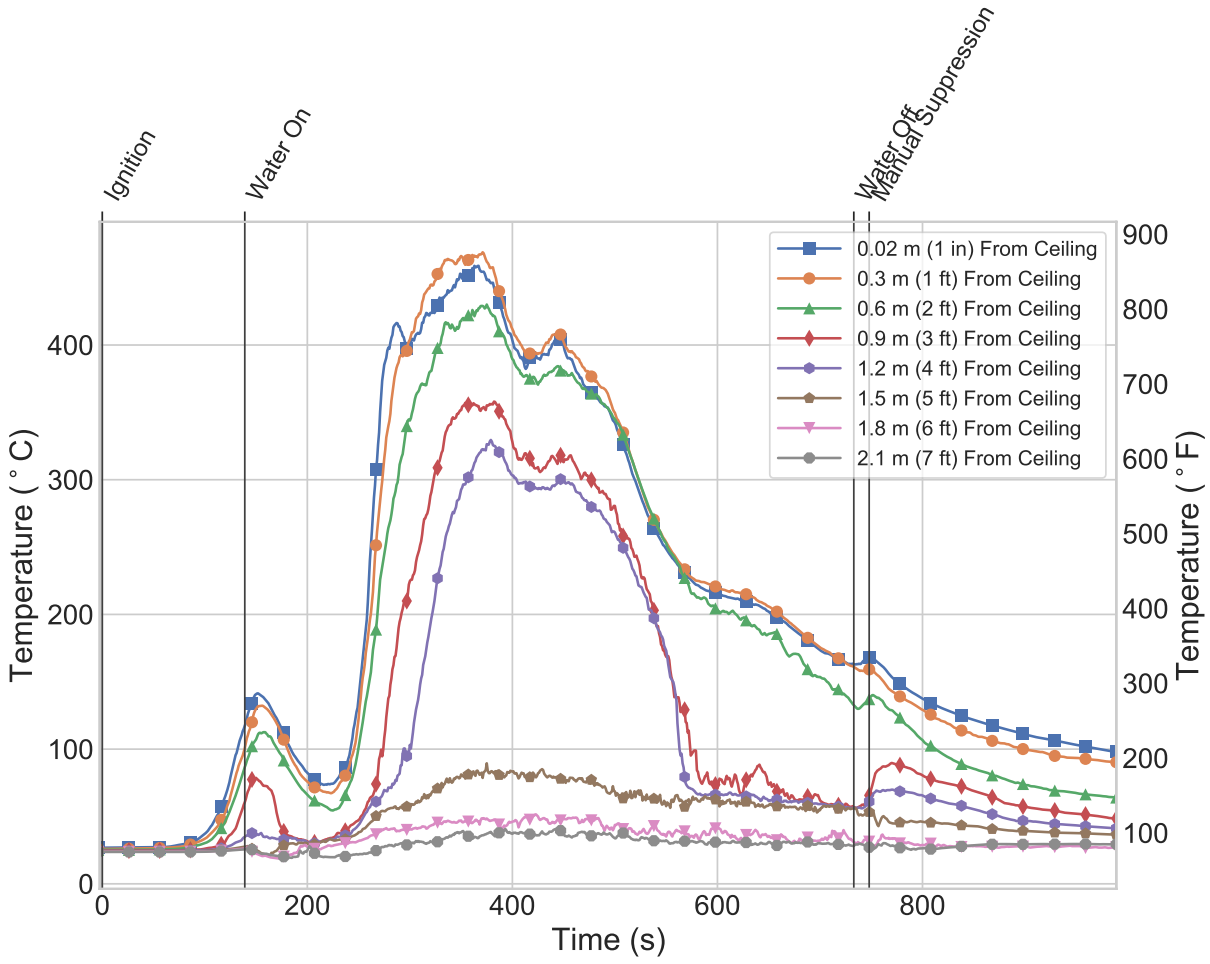

Figure A.1: Fire room (Position 1) temperatures for Experiment 1B.

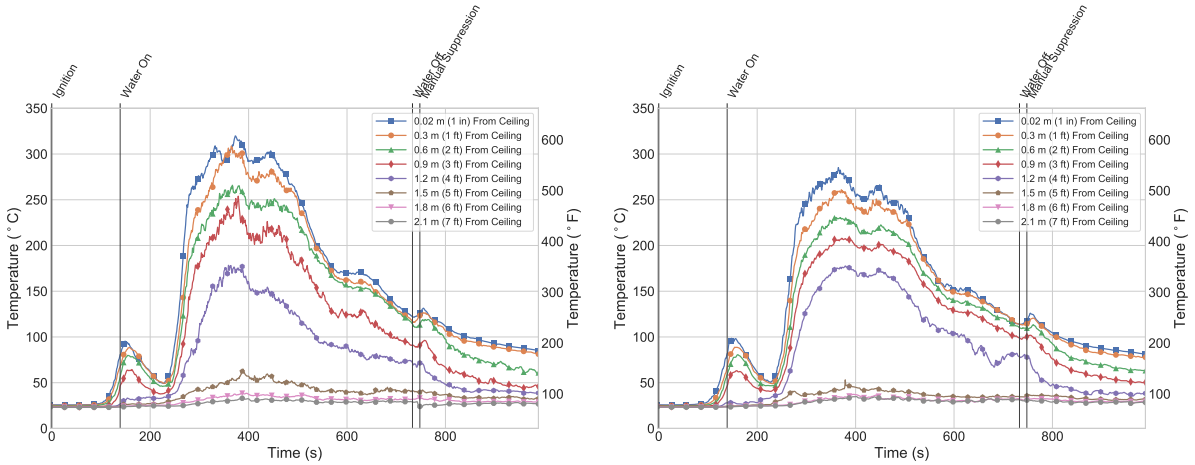

(a) Front Door End of the Hallway (Position 2) (b) Closed End of the Hallway (Position 3)

Figure A.2: Hallway temperatures for Experiment 1B.

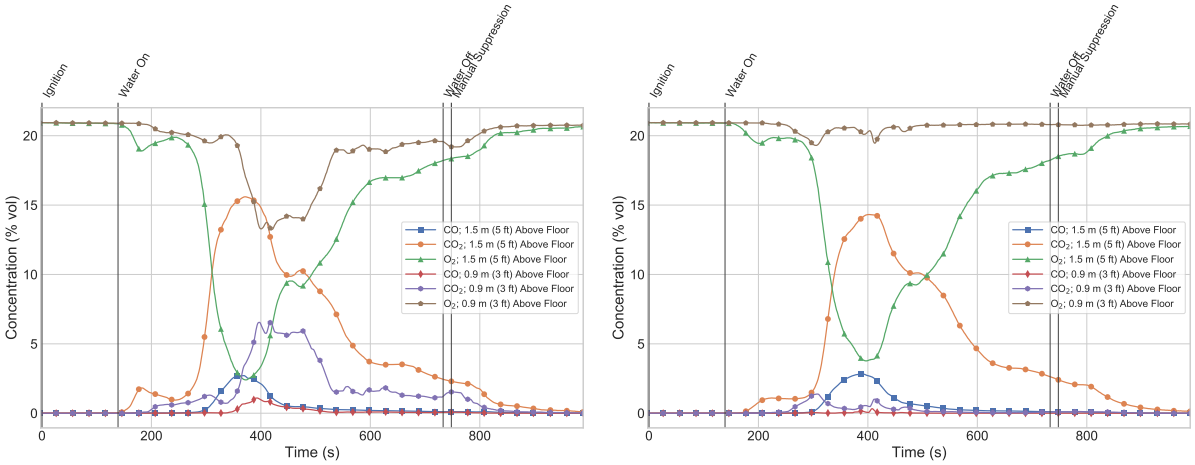

(a) Fire Room (Position 1) (b) Hallway (Position 3)

Figure A.3: Gas concentration measurements for Experiment 1B.

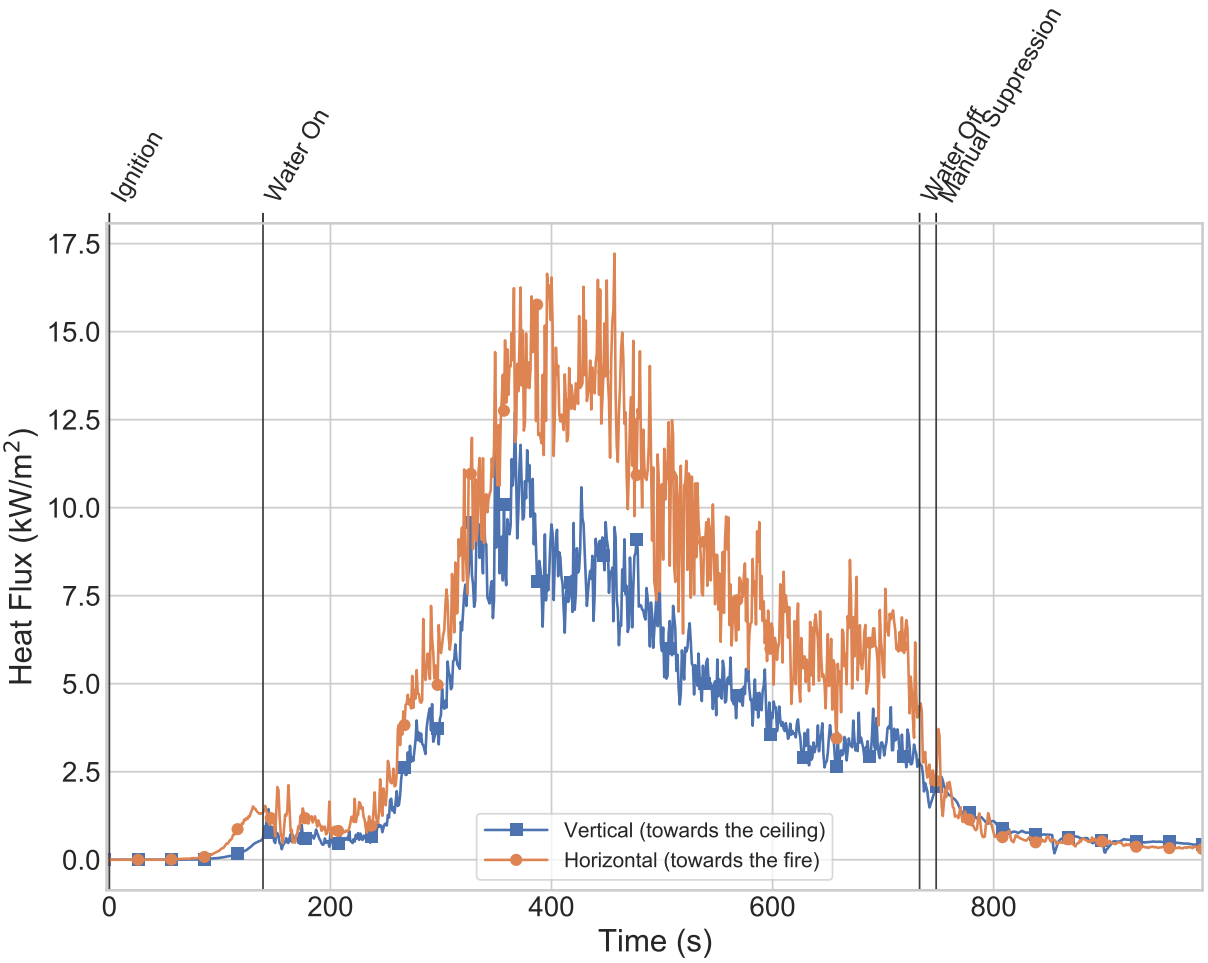

Figure A.4: Heat flux measurements 0.9 m (3 ft) above the floor in the fire room (Position 1) for Experiment 1B.

A.2 Experiment 2

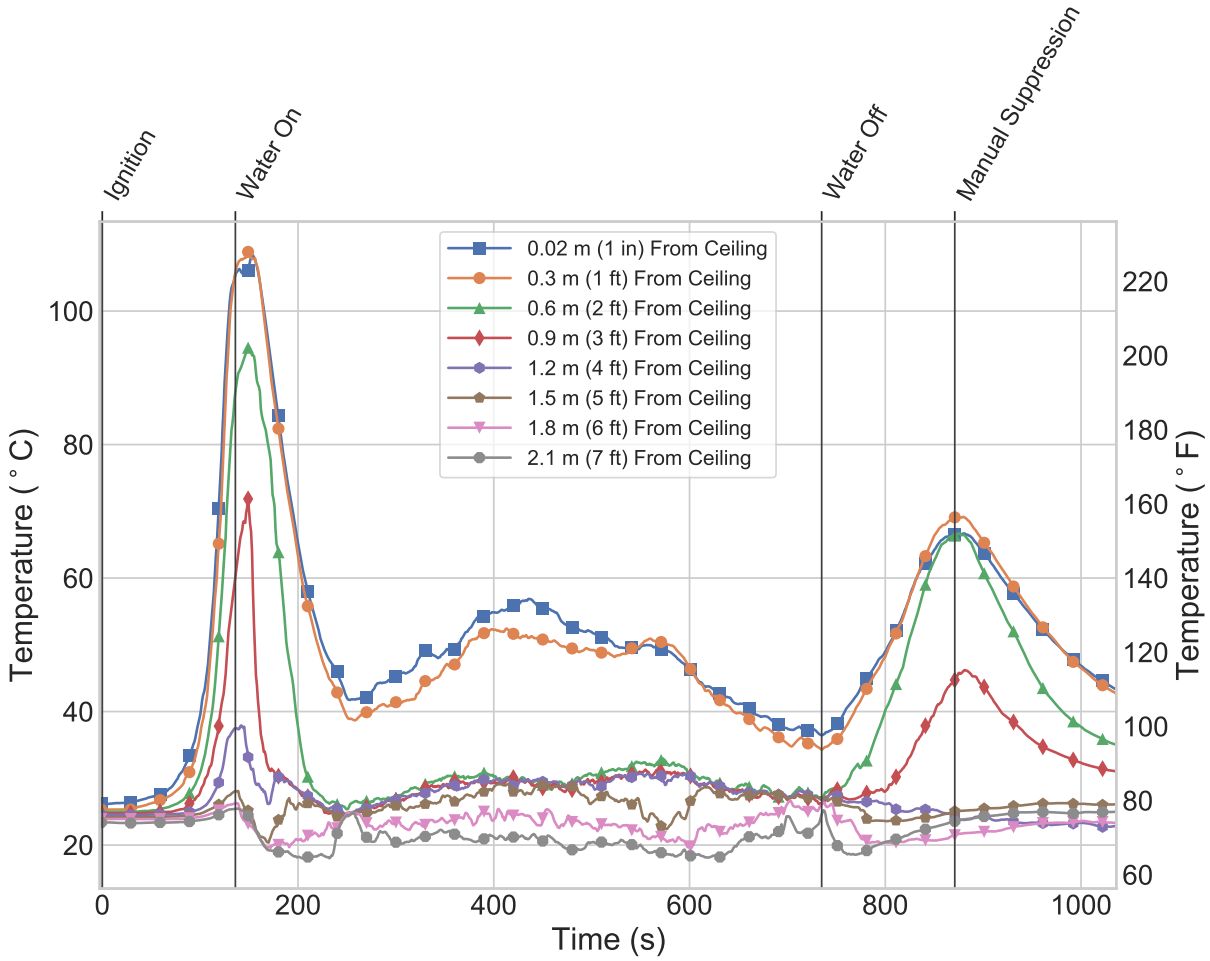

Figure A.5: Fire room (Position 1) temperatures for Experiment 2.

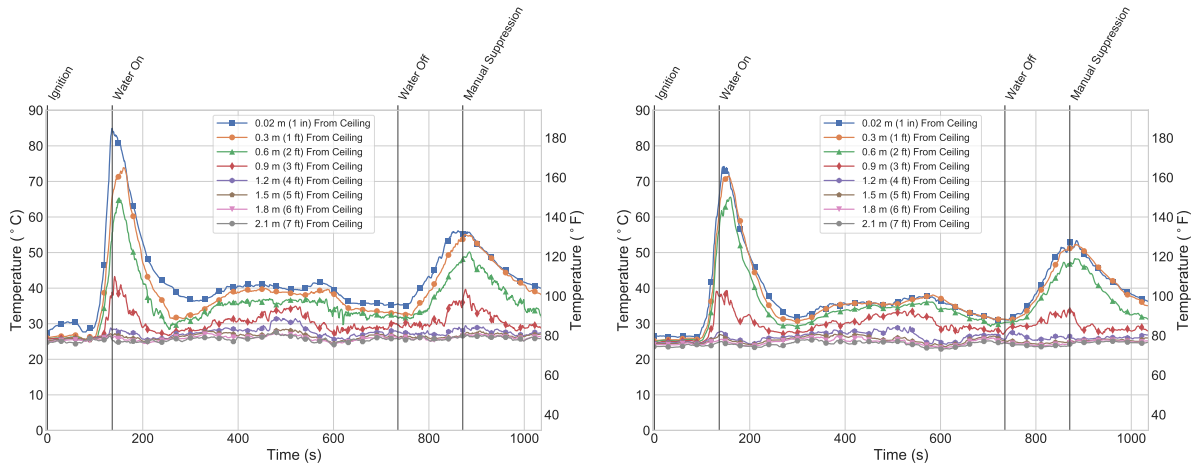

(a) Front Door End of the Hallway (Position 2) (b) Closed End of the Hallway (Position 3)

Figure A.6: Hallway temperatures for Experiment 2.

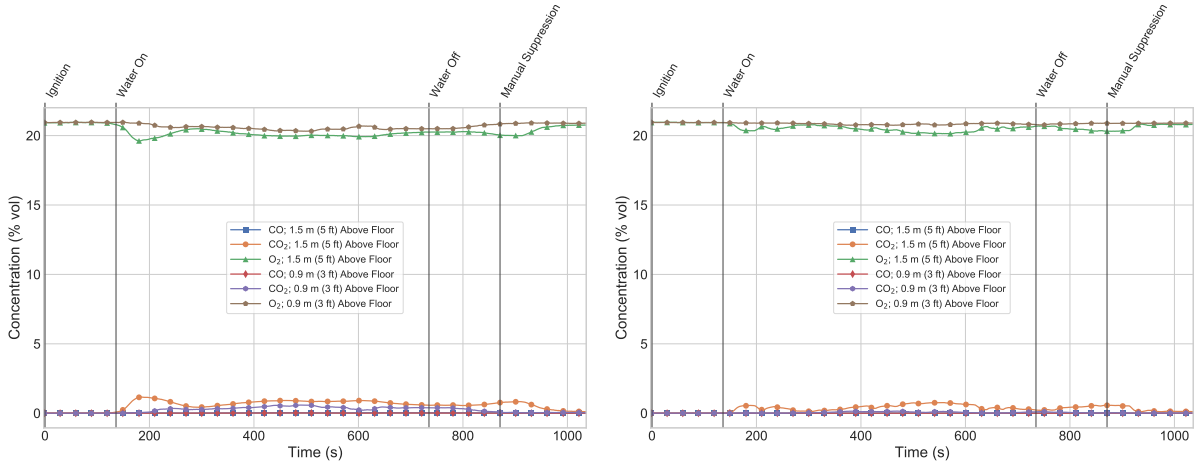

(a) Fire Room (Position 1) (b) Hallway (Position 3)

Figure A.7: Gas concentration measurements for Experiment 2.

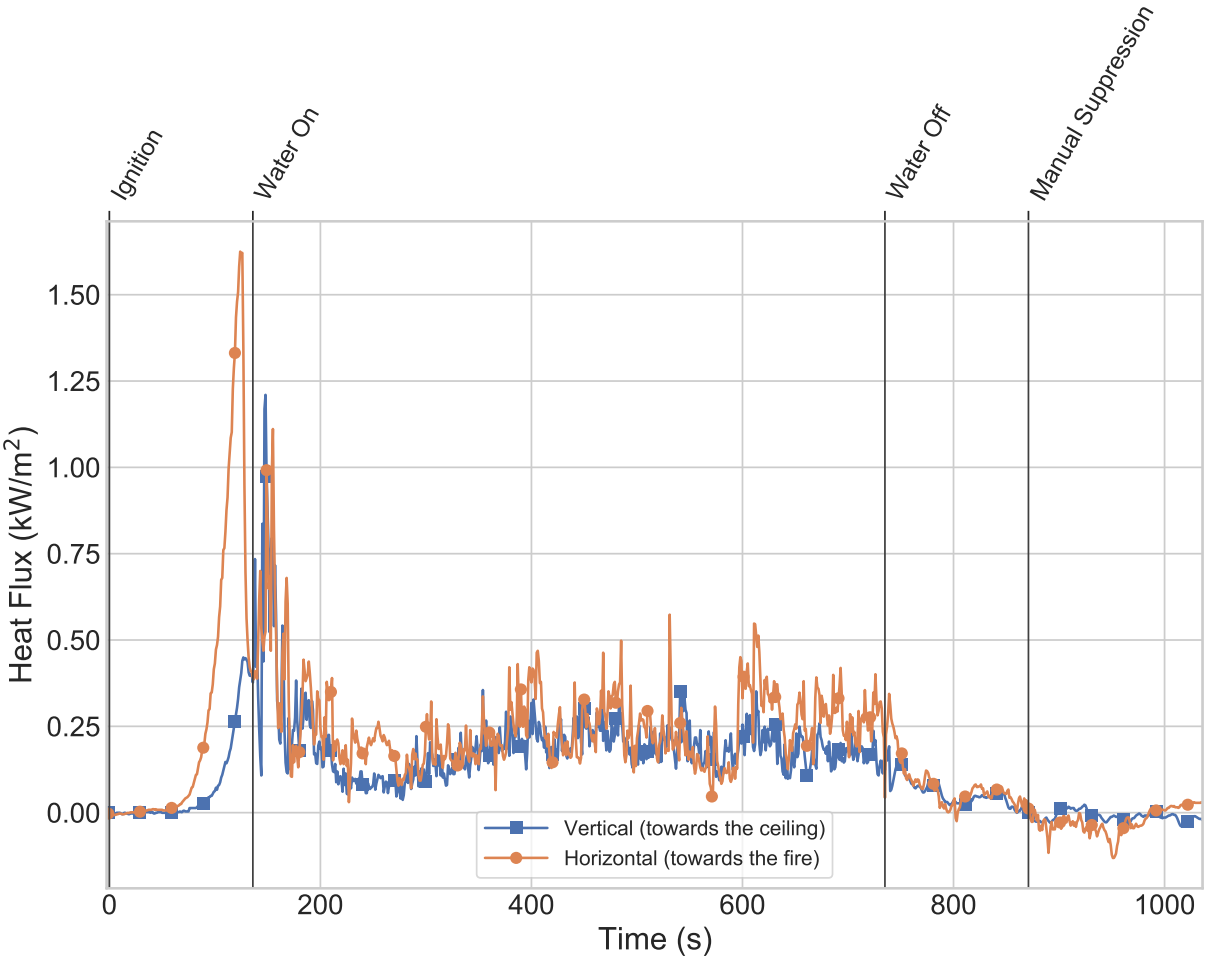

Figure A.8: Heat flux measurements 0.9 m (3 ft) above the floor in the fire room (Position 1) for Experiment 2.

A.3 Experiment 3

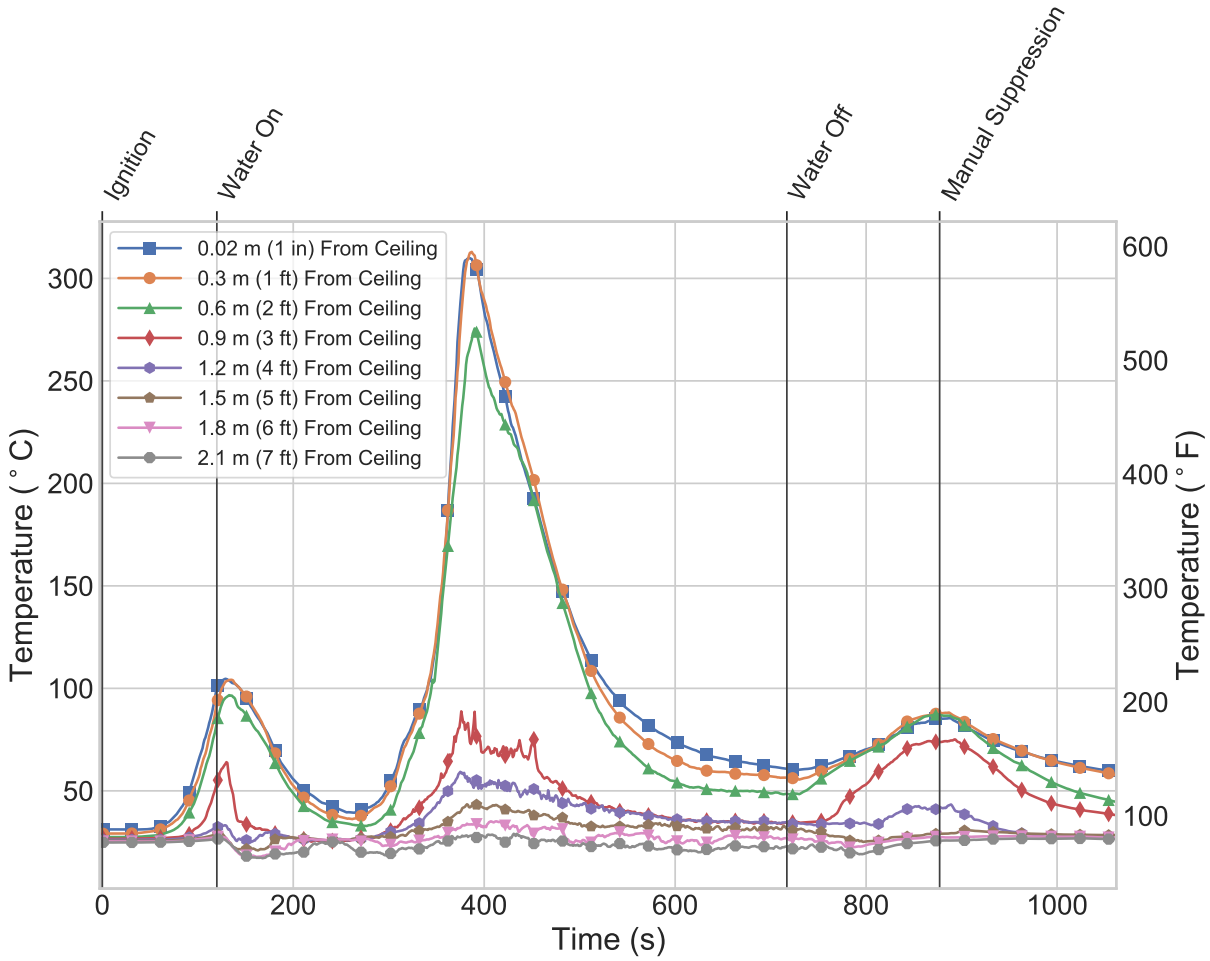

Figure A.9: Fire room (Position 1) temperatures for Experiment 3.

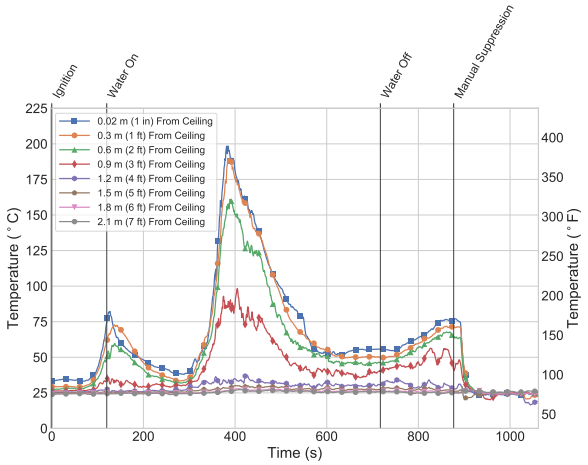

(a) Front Door End of the Hallway (Position 2)

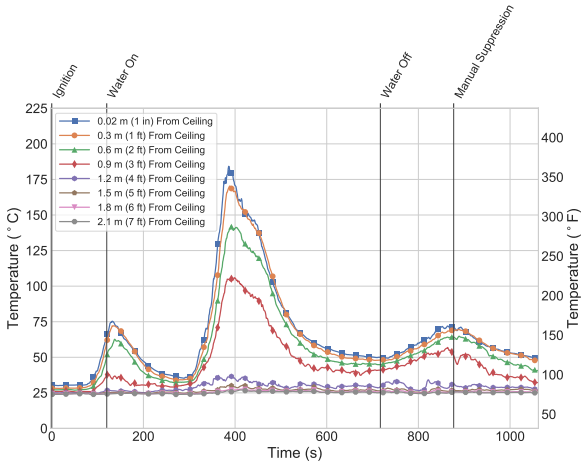

(b) Closed End of the Hallway (Position 3)

Figure A.10: Hallway temperatures for Experiment 3.

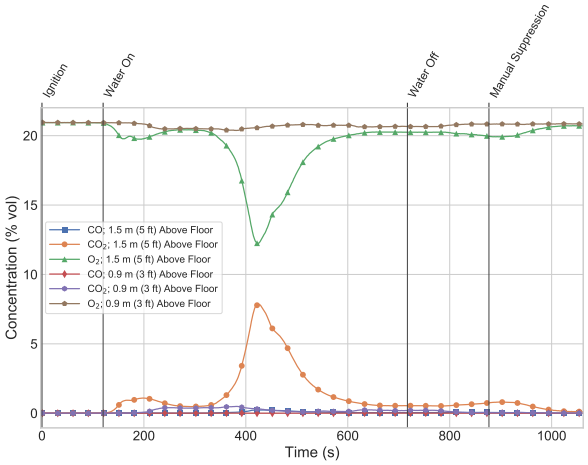

(a) Fire Room (Position 1)

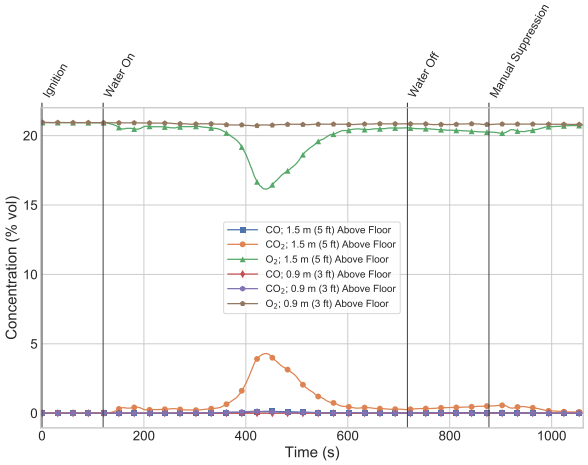

(b) Hallway (Position 3)

Figure A.11: Gas concentration measurements for Experiment 3.

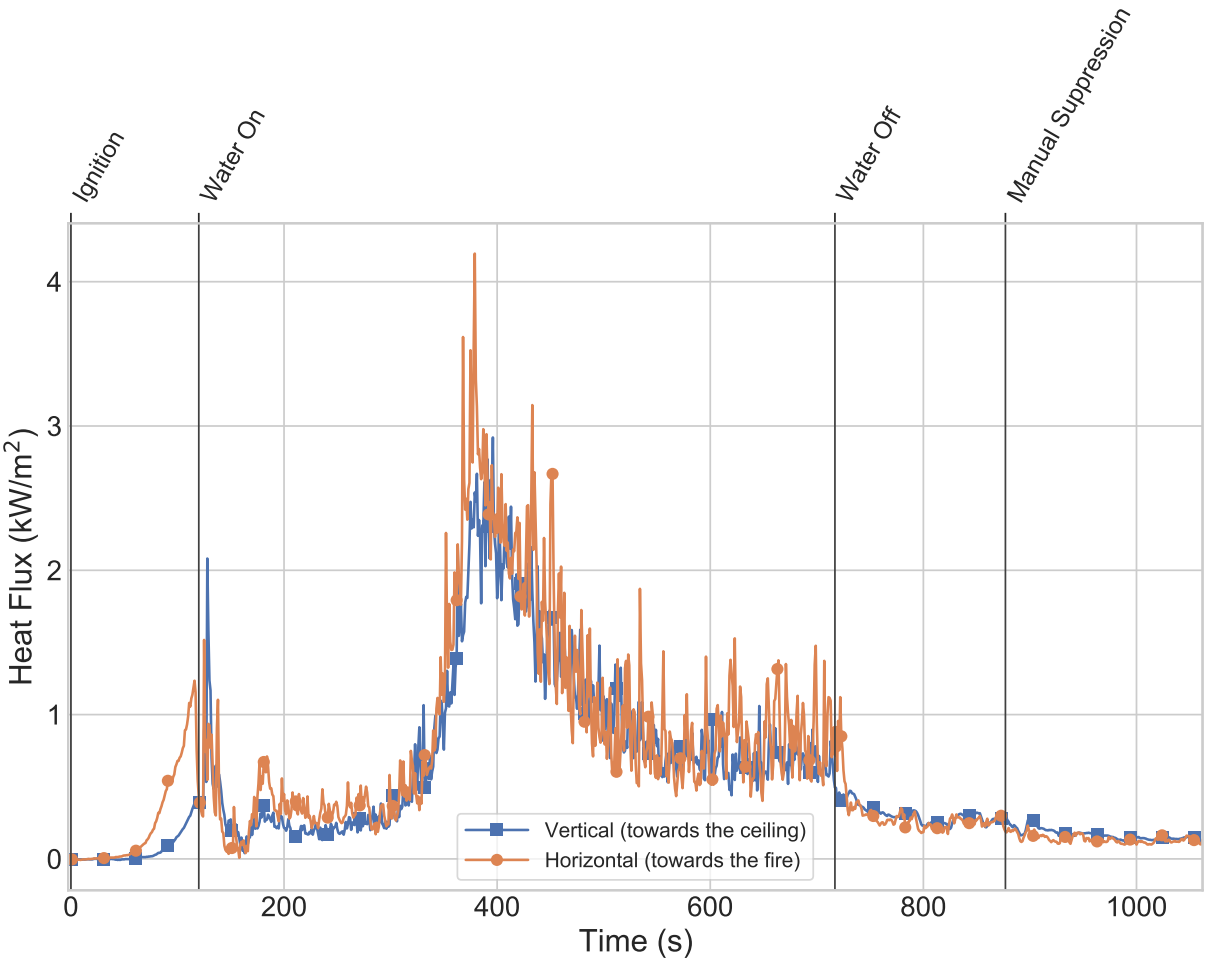

Figure A.12: Heat flux measurements 0.9 m (3 ft) above the floor in the fire room (Position 1) for Experiment 3.

A.4 Experiment 4

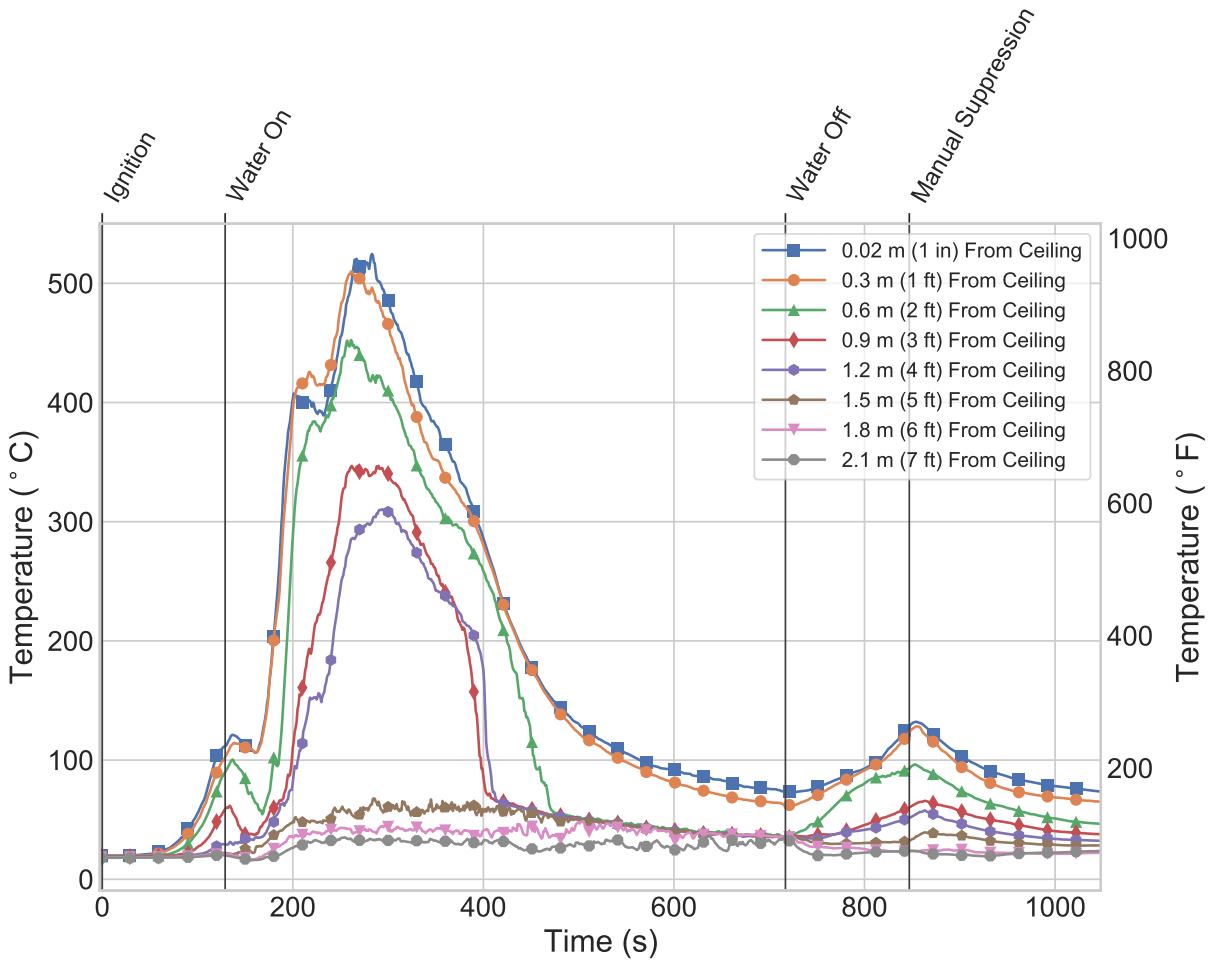

Figure A.13: Fire room (Position 1) temperatures for Experiment 4.

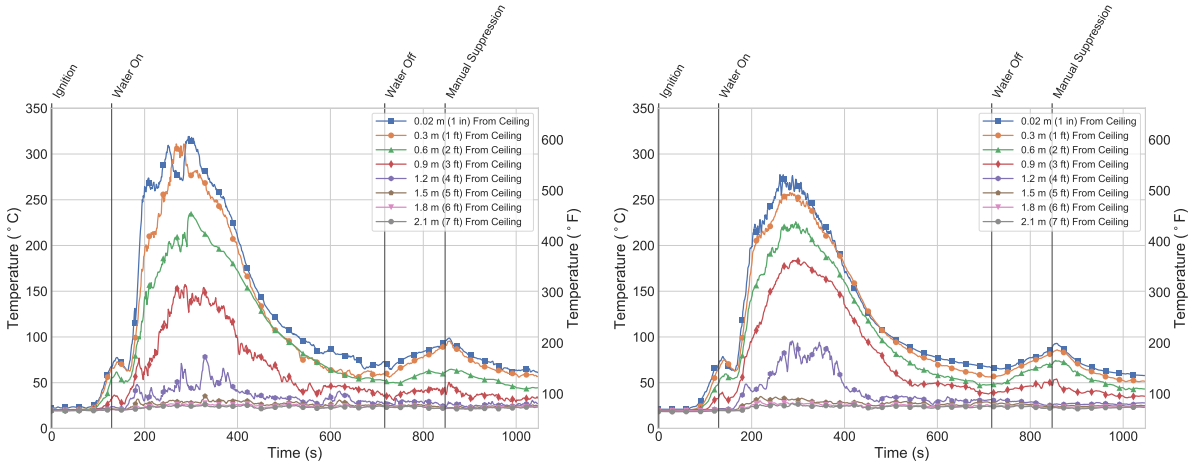

(a) Front Door End of the Hallway (Position 2) (b) Closed End of the Hallway (Position 3)

Figure A.14: Hallway temperatures for Experiment 4.

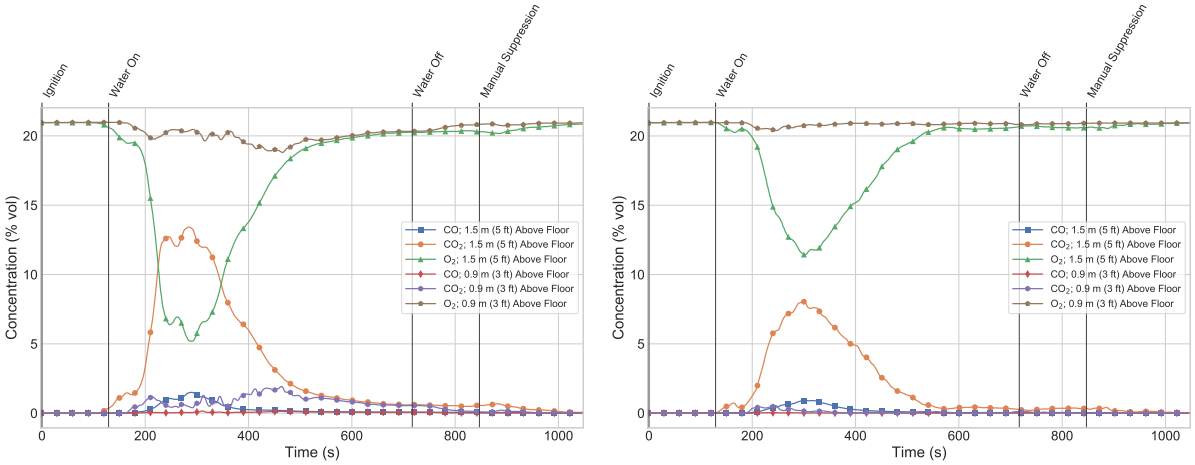

(a) Fire Room (Position 1) (b) Hallway (Position 3)

Figure A.15: Gas concentration measurements for Experiment 4.

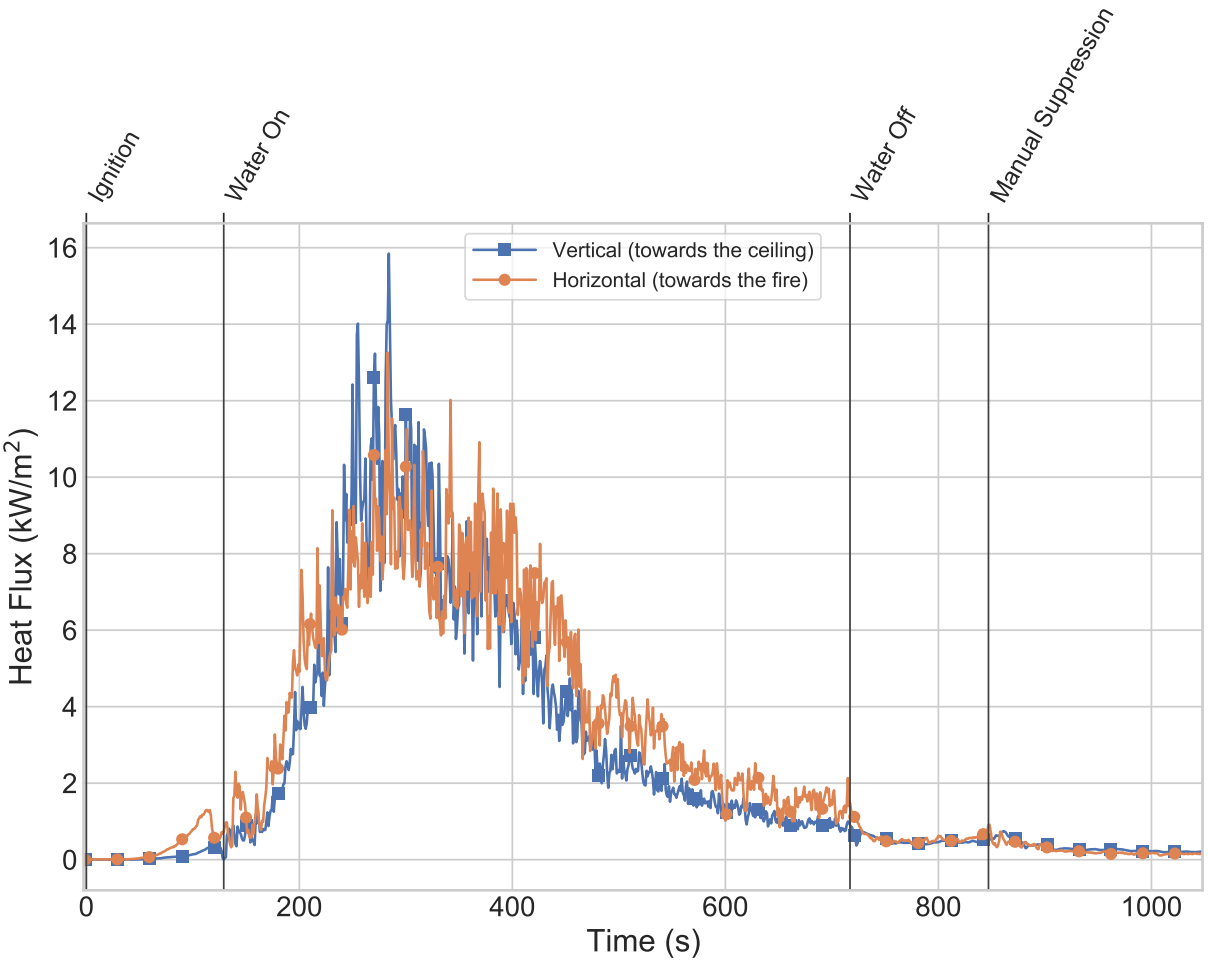

Figure A.16: Heat flux measurements 0.9 m (3 ft) above the floor in the fire room (Position 1) for Experiment 4.

A.5 Experiment 6

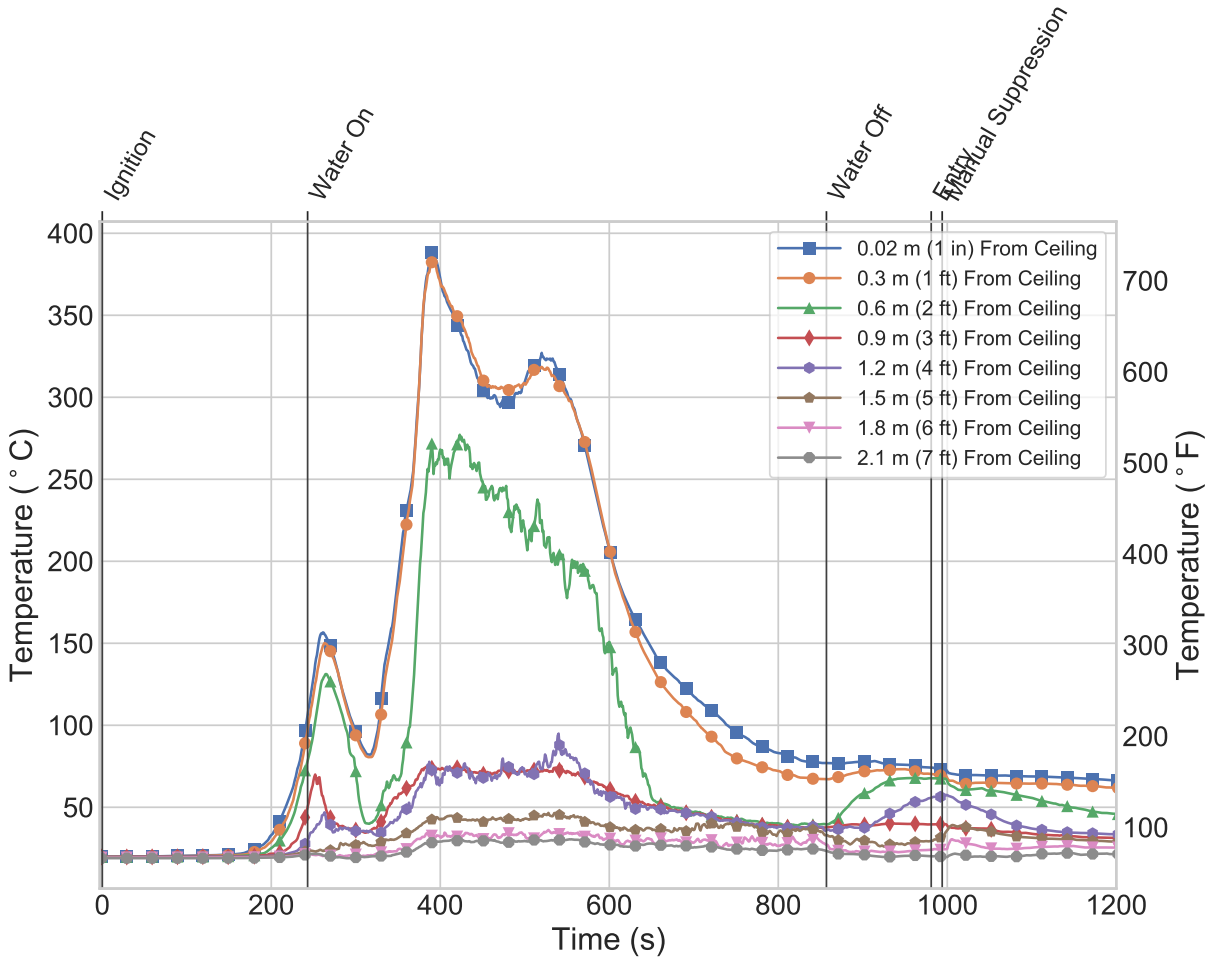

Figure A.17: Fire room (Position 1) temperatures for Experiment 6.

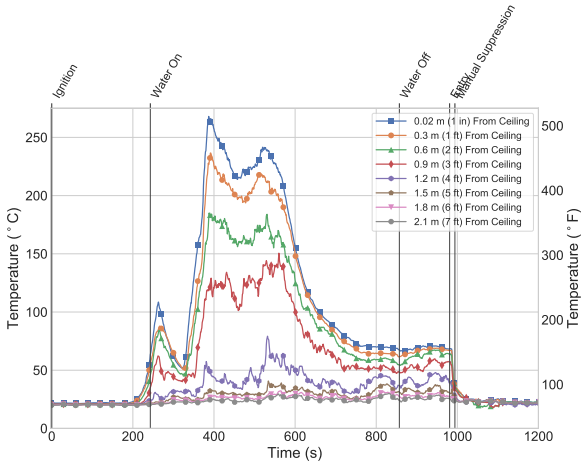

(a) Front Door End of the Hallway (Position 2)

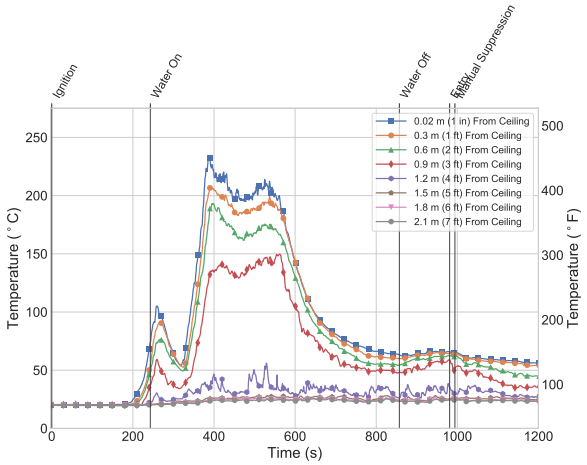

(b) Closed End of the Hallway (Position 3)

Figure A.18: Hallway temperatures for Experiment 6.

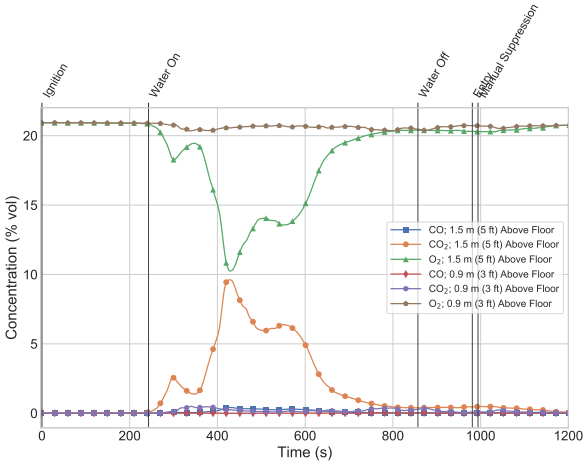

(a) Fire Room (Position 1)

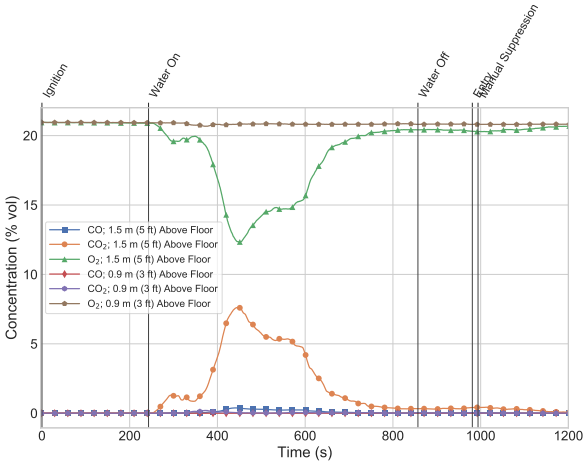

(b) Hallway (Position 3)

Figure A.19: Gas concentration measurements for Experiment 6.

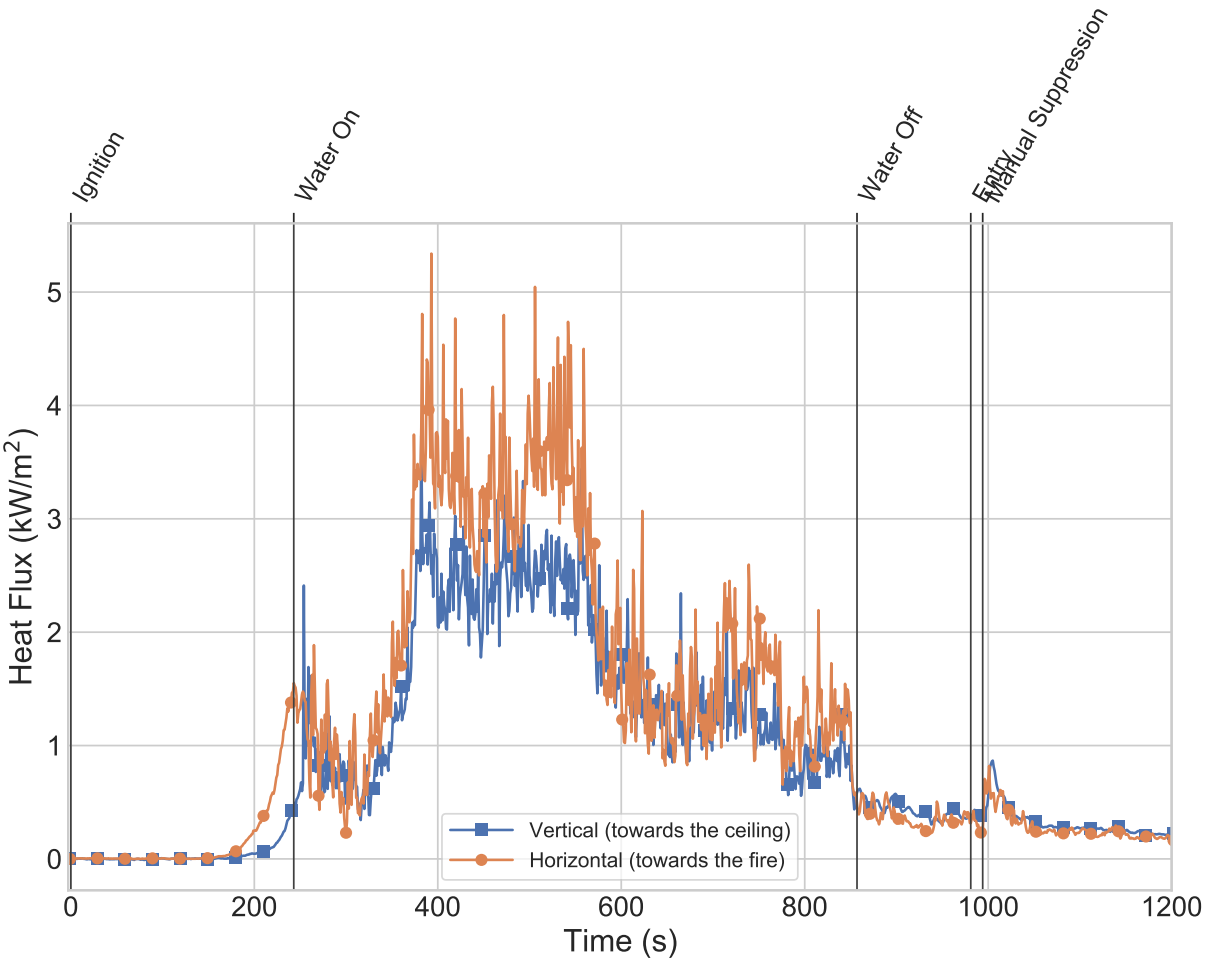

Figure A.20: Heat flux measurements 0.9 m (3 ft) above the floor in the fire room (Position 1) for Experiment 6.

A.6 Experiment 7

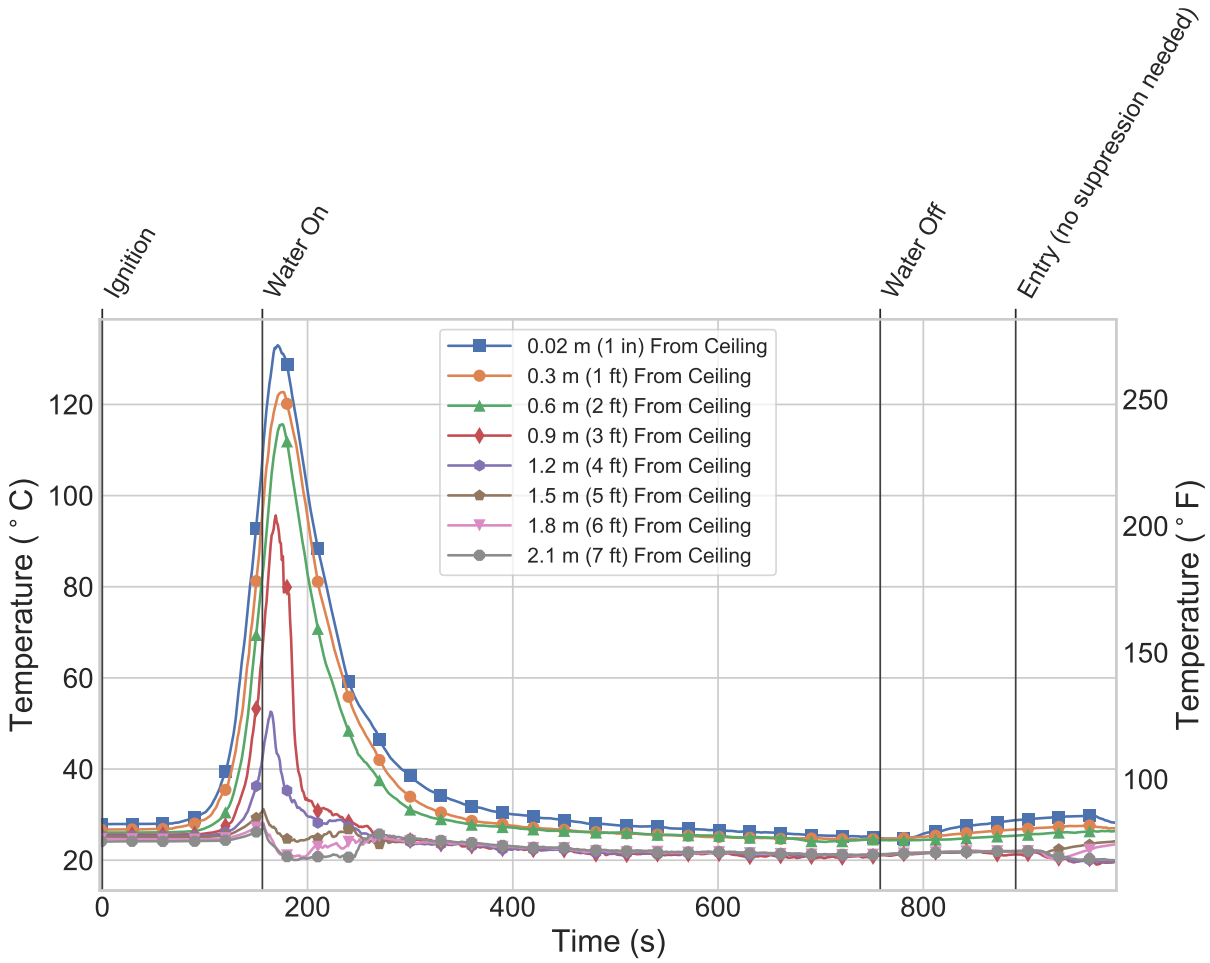

Figure A.21: Fire room (Position 1) temperatures for Experiment 7.

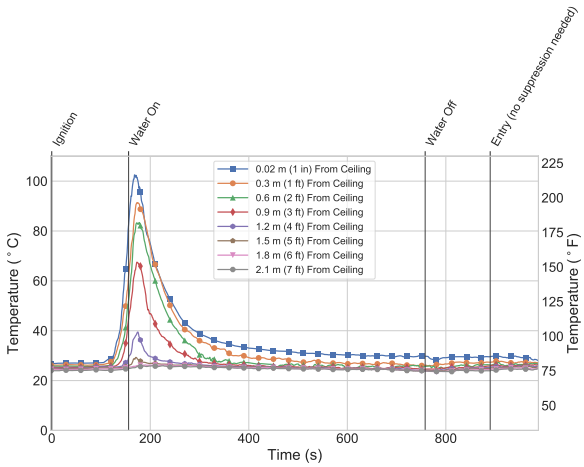

(a) Front Door End of the Hallway (Position 2)

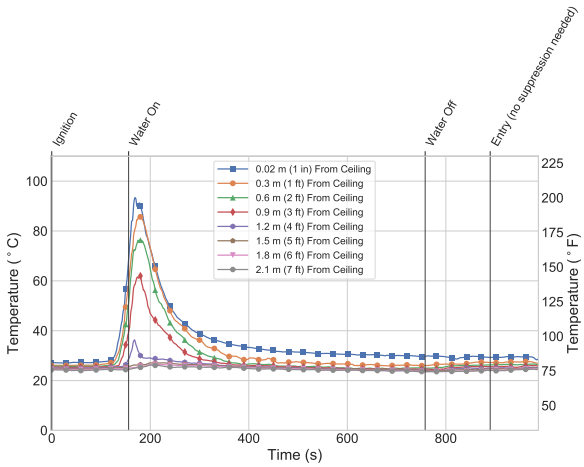

(b) Closed End of the Hallway (Position 3)

Figure A.22: Hallway temperatures for Experiment 7.

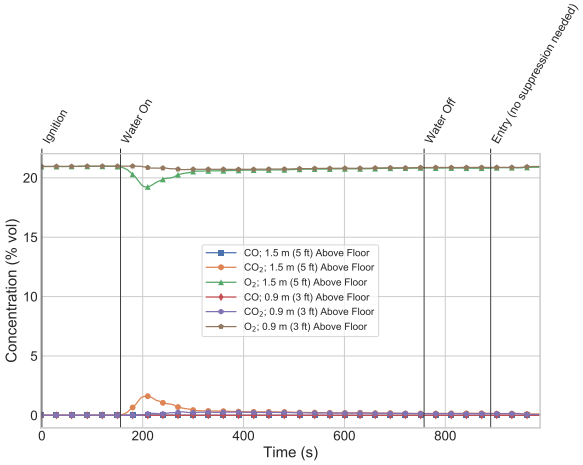

(a) Fire Room (Position 1)

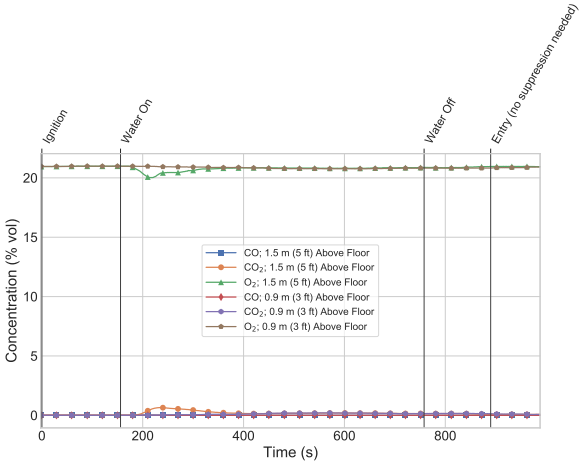

(b) Hallway (Position 3)

Figure A.23: Gas concentration measurements for Experiment 7.

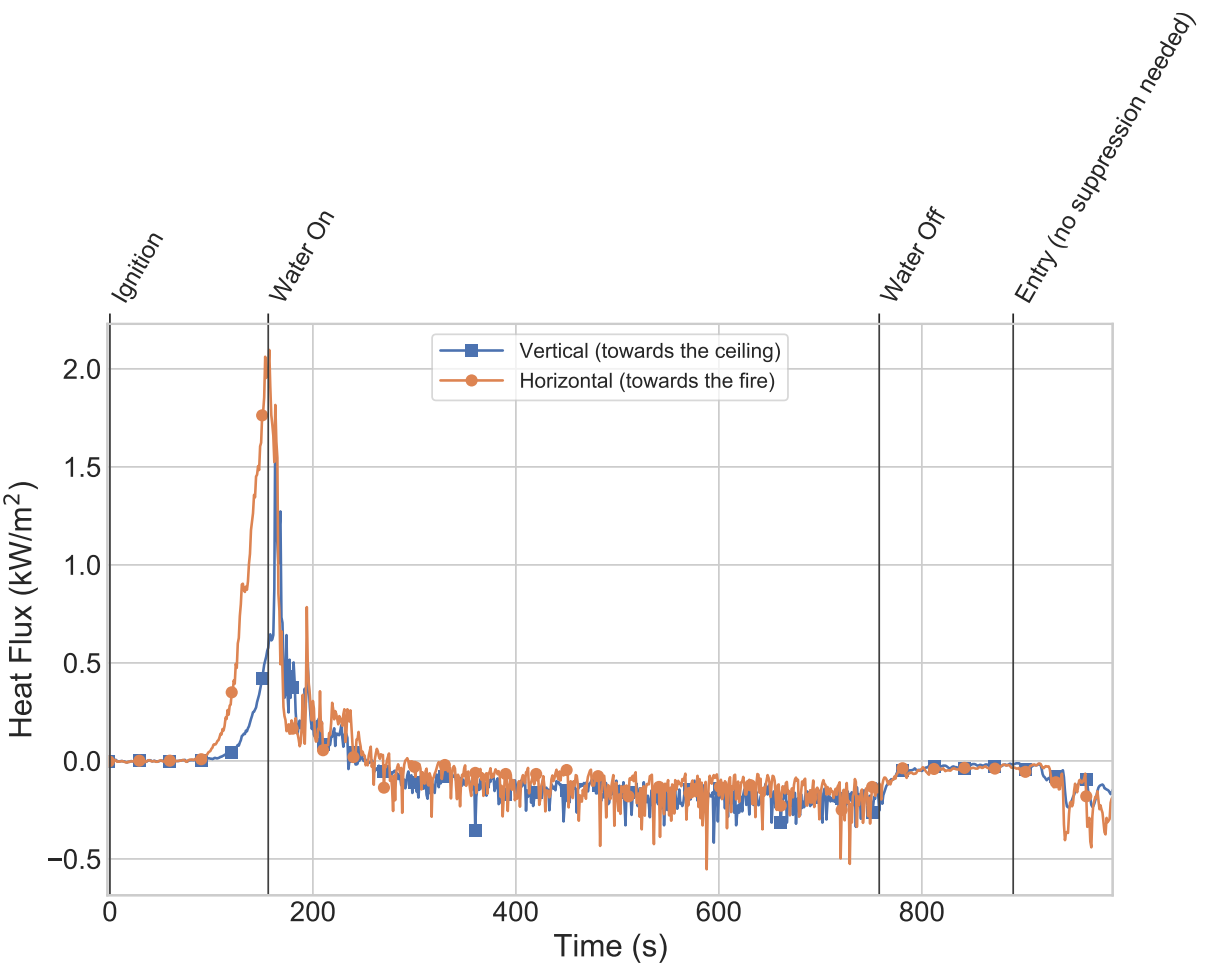

Figure A.24: Heat flux measurements 0.9 m (3 ft) above the floor in the fire room (Position 1) for Experiment 7.

A.7 Experiment 8

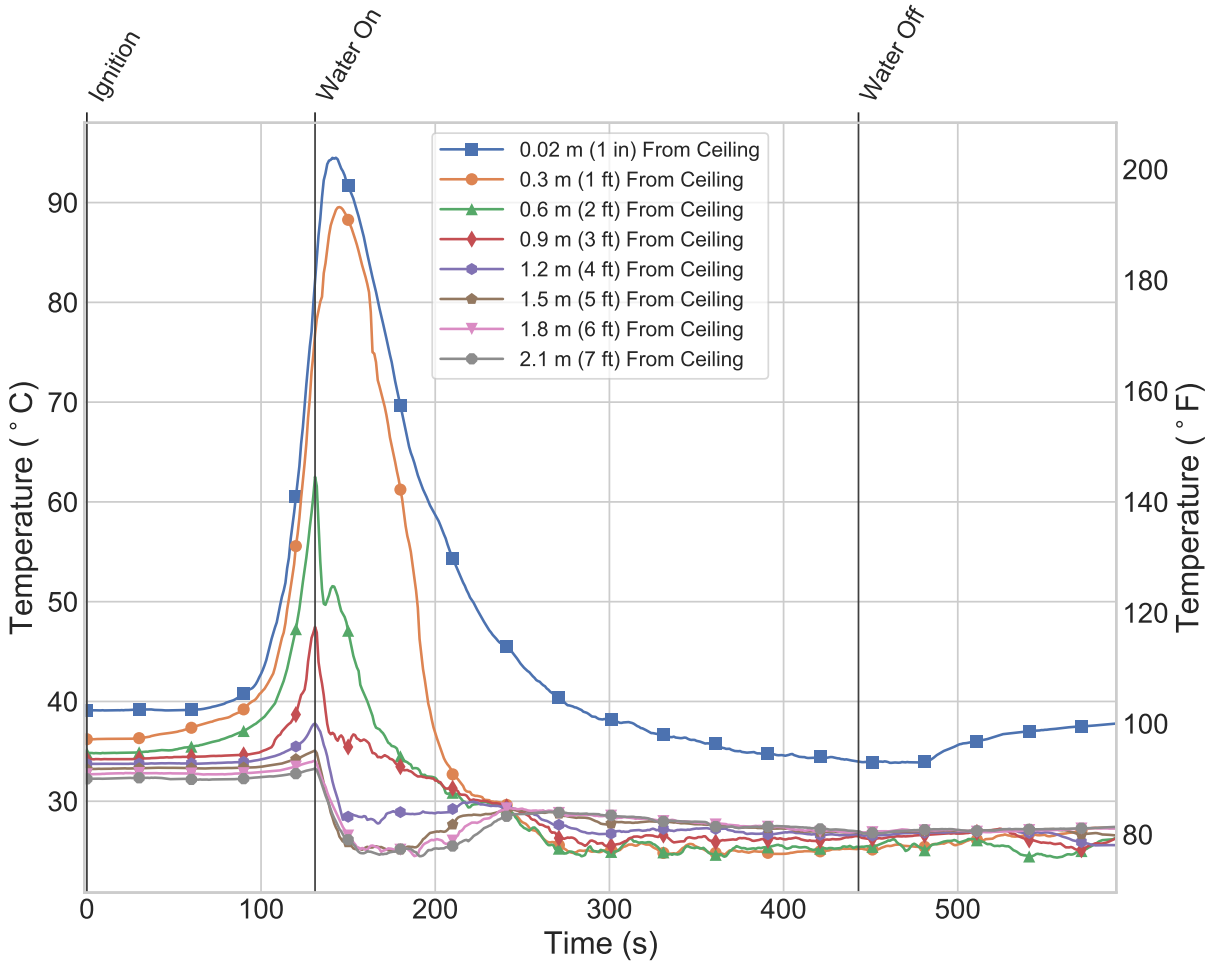

Figure A.25: Fire room (Position 1) temperatures for Experiment 8.

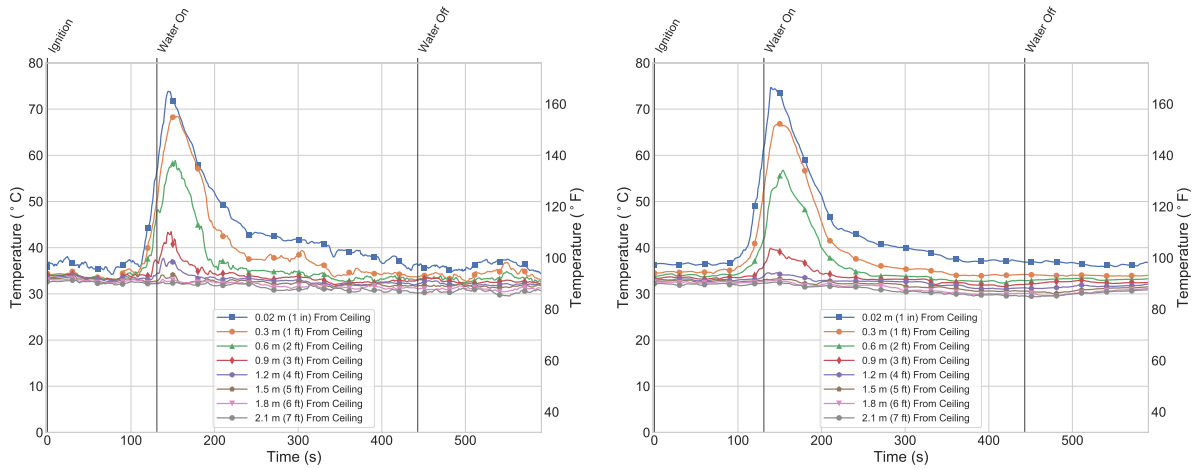

(a) Front Door End of the Hallway (Position 2) (b) Closed End of the Hallway (Position 3)

Figure A.26: Hallway temperatures for Experiment 8.

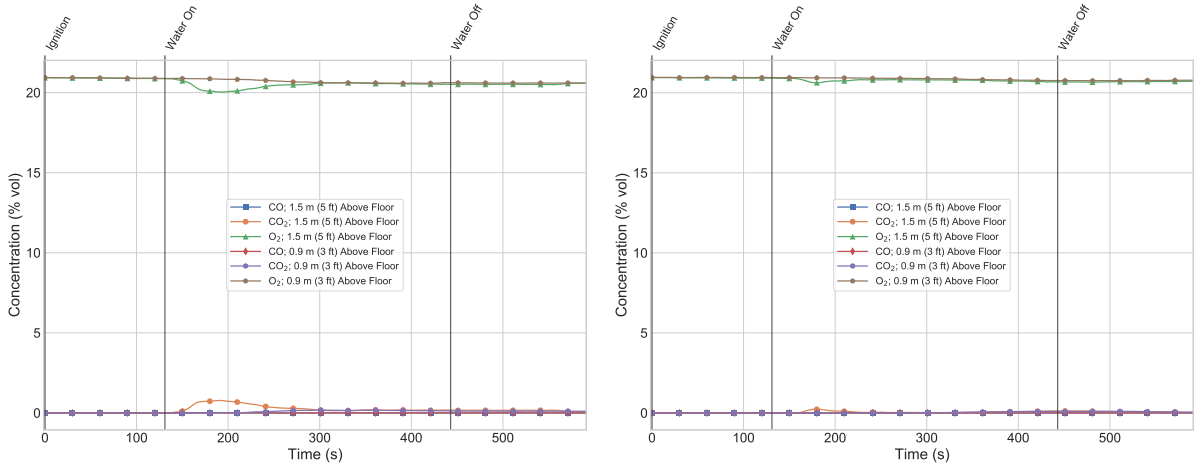

(a) Fire Room (Position 1) (b) Hallway (Position 3)

Figure A.27: Gas concentration measurements for Experiment 8.

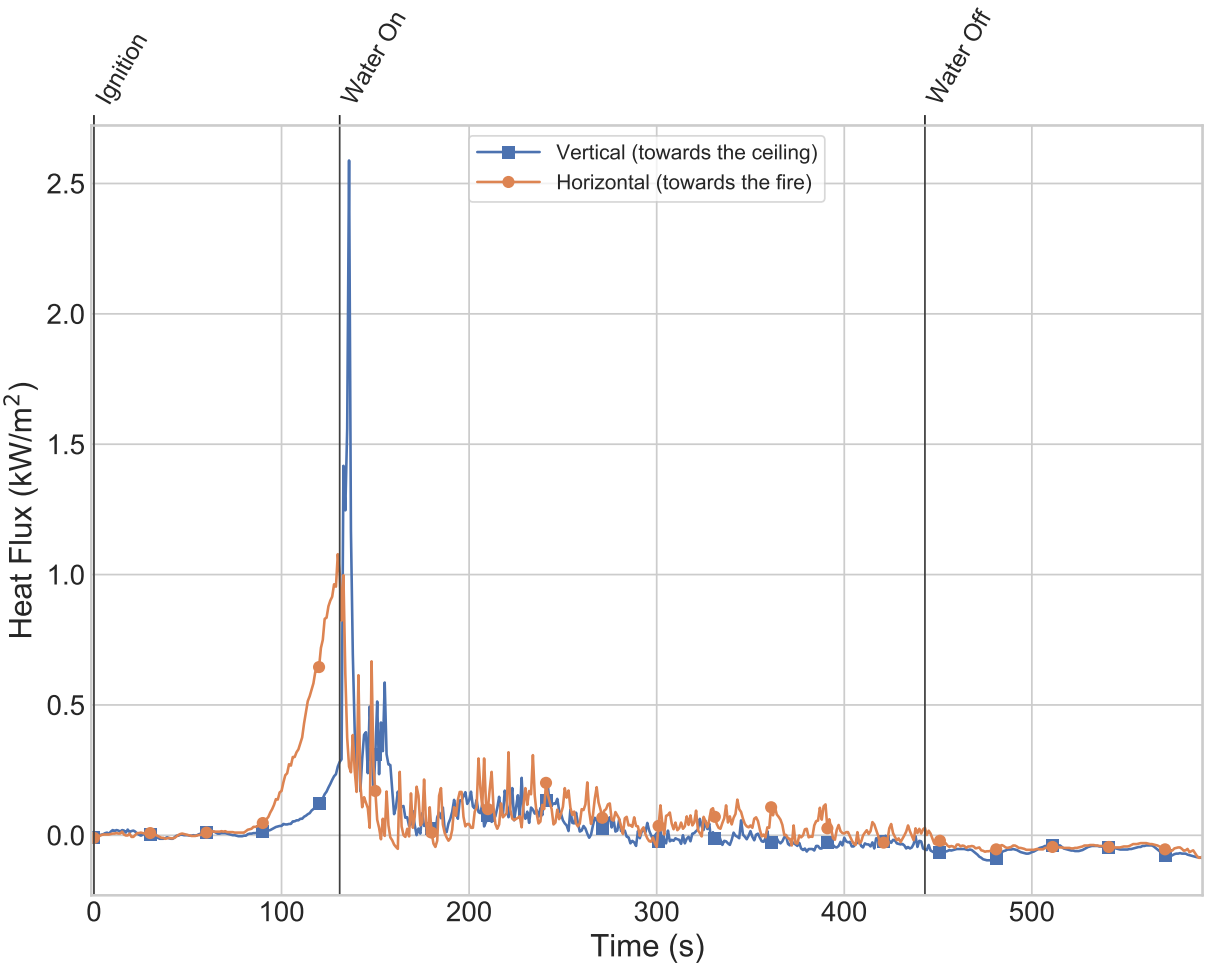

Figure A.28: Heat flux measurements 0.9 m (3 ft) above the floor in the fire room (Position 1) for Experiment 8.